A COMPARISON OF THE METHODS OF ENGINEERING SEISMIC REFRACTION ANALYSIS AND GENERALIZED LINEAR INVERSION FOR DERIVING STATICS AND SHALLOW BEDROCK VELOCITIES

IAN LESLIE

A COMPARISON OF THE METHODS OF ENGINEERING SEISMIC REFRACTION ANALYSIS AND GENERALIZED LINEAR INVERSION FOR DERIVING STATICS AND SHALLOW BEDROCK VELOCITIES

by

Ian Leslie

A thesis submitted to the

School of Graduate Studies

in partial fulfilment of the

requirements for the degree of

Master of Earth Sciences

Department of Earth Sciences
Memorial University of Newfoundland

January, 1994

ISBN 0-612-01880-6

Canada

ABSTRACT

Refracted first arrivals recorded in high resolution seismic surveys contain key information for deriving statics and are important for improving the resolution of reflections. They may also be useful for estimating shallow bedrock velocities as an aid to interpreting bedrock geology below the weathered layer. Two different techniques to estimate near-surface information are described in this thesis : one is a generalized linear inversion (GLI) technique that uses damped least squares to estimate statics and Occam's method to estimate lateral variations in the bedrock layer for interpretation of geology; the other employs the reciprocal method and the smoothing of forward and reverse apparent velocity profiles in the analysis. A comparison is made between the effectiveness of these techniques for a synthetic data set and 3 high resolution data sets collected at two mine sites in central Newfoundland for mining exploration purposes.

For these data there was no discernible difference in the quality of the stacked seismic sections for the data sets processed with statics derived using GLI compared with the reciprocal method. Lateral variations in bedrock seismic velocity are resolved to the same degree by both direct smoothing and Occam's technique, resulting in similar geological interpretations. The resolution of the bedrock velocities in both methods depends on the acquisition parameters, the signal-to-noise ratio in the field, and the amount of smoothing applied to the data. Future work may be to use a more efficient numerical procedure in GLI to handle sparse matrices and to make a comparison of these techniques for the case of diving raypaths.

For my parents.

ACKNOWLEDGEMENTS

I would first like to thank Prof. Cedric Wright for providing financial support and also for his valuable encouragement and assistance throughout my program. I would also like to thank Prof. Chuck Hurich for his useful discussions and assistance with my writing of the thesis. Finally I would like to thank all the members of the geophysics department, all the earth science graduate students I have known and worked with, and the friends I have met during my stay in Newfoundland for their support. Although too numerous to mention them here, I thank them for the advice or encouragement they have given that helped me to complete my Masters program.

TABLE OF CONTENTS

LIST OF TABLES

LIST OF FIGURES

CHAPTER 1

1.0 INTRODUCTION

If it were feasible, a huge mechanical bulldozer could be used prior to land-based seismic surveys to remove the thin veneer of unconsolidated material (soil, sand, glacial till, gravel and other quaternary deposits), weathered bedrock (upper surface of bedrock which has been fractured and/or chemically altered) and undulations in surface topography (hills and valleys) to create a flat, horizontal surface upon which the shots and receivers could be placed for the survey. This would reduce the degradation of the stacked signal caused by time delays associated with this near-surface, low velocity "weathered layer" (overburden and weathered bedrock) and improve the quality of deeper reflections of interest. This would also allow us to interpret the geology that was hidden by the weathered layer. Unfortunately, such an operation in the field would be impractical (and environmentally unfriendly), and therefore procedures are required in the processing of these data to estimate corrections to remove these effects prior to stacking.

The problem can be considered to be two-fold: i) The most serious problem is to correct for rapid variations in the weathered layer velocity and/or thickness that cause time delays which result in signal misalignment in the CMP gather and deterioration in the quality of the stacked signal. The statics effects cause a decrease in the bandwidth of the signal by acting as a high cut filter. ii) A secondary problem is the estimation of longer wavelength components that cause undulations and apparent structure to appear

on reflective horizons. Although less consequential than the first problem, time structure effects may be minimized by using a correct near-surface model. These two problems have important consequences for other processing tools such as acoustic impedance estimation, NMO velocity estimation, two-dimensional filtering techniques, and residual statics which produce far more reliable results when the near-surface effects are taken into account (Farrell and Euwema, 1984).

A velocity model of the near surface used to remove the above effects may be estimated from the travel times of refracted P-wave energy travelling close to the weathered layer/bedrock interface. Time corrections, known as *static* corrections, are estimated from this model and are used to shift the seismic traces so that they appear to be located on a flat, horizontal datum.

The refracted first arrival times can also be used to estimate lateral variations in bedrock seismic velocity to constrain shallow geological interpretation. The estimation of bedrock velocity variations from refracted arrivals on seismic reflection data has rarely been fully exploited in the past apart from a few notable exceptions (Green, 1980; Brocher, 1981; Wright, 1982; Alter, 1985; Mayrand et al., 1987). The most likely reason for this is the large amount of effort required in the past to pick first-break times from the shot gathers. The interpretation of faults, shear zones, and possible changes in lithology in high resolution seismic work may be possible with this type of analysis.

Many different refraction methods have been used previously. Some approaches use standard engineering methods such as the comparable reciprocal and plus minus

methods (Hagedoorn, 1959; Hawkins, 1961) and the generalised reciprocal method (Palmer, 1981) for determining depth to bedrock and static corrections. Others have used a cumulative difference method to estimate statics (Bahorich et al., 1982; Leven and Taylor, 1989) which incorporates more reciprocal paths per shot or receiver than the conventional reciprocal method but has the disadvantage that errors in the weathering terms are cumulative (Wright and Nguuri, 1994).

Refraction tomography has also been used in several different forms to estimate near-surface velocity models. Hampson and Russell (1984) used a multi-layered near-surface model for the inversion of refracted arrivals, and assume that the velocity in the overburden is known. De Amorim, Hubral and Tygel (1987) assume a model where the base of the low velocity layer is held at a fixed depth and the velocities determined within the layer absorb the traveltime variations. Other models solve for a number of weathering cell thicknesses and velocities with only one or two layers (Olsen, 1989; Docherty, 1992).

The GLI and engineering method approaches are both widely used in the oil industry and by crustal-scale surveys (e.g. Lithoprobe) and there is some research indicating that GLI is an improvement on the engineering technique (e.g. De Amorim et al., 1987; Docherty, 1992) although it is unclear why one should be better than the other. Improvements reported by Spencer et al. (1993) in their processing of Lithoprobe seismic data are supposed to result from allowing for vertical velocity gradients in bedrock but experience with the vibroseis data suggests that this may not be a correct inference

because the velocity gradients are so difficult to measure reliably (Per. Comm. Cedric Wright).

The main purpose of this thesis is to compare the results of estimating static corrections and quantifying lateral variations in bedrock seismic velocity for a number of data sets using an engineering and a generalised linear inversion (GLI) technique. The engineering method (as it will be known here) as used by Wright (Wright et al., 1993; Wright, 1994 a,b; Wright and Nguuri, 1994; Wright et al., 1994) combines the reciprocal method with the method of summary values (Bolt, 1978) to estimate statics and shallow bedrock seismic velocities respectively. The GLI technique is a modification of the method used by De Amorim et al. (1987) that assumes a model with a constant weathering layer thickness and horizontal interface with each layer divided up into a number of cells. The simplicity of this approach makes it easy to apply and is appropriate for the data examined here because the approximations made about the raypaths (i.e. headwave model) are reasonable. An important new feature is the use of Occam's method (Constable, Parker and Constable, 1987) to estimate bedrock velocity variations after removal of the weathering times (i.e. travel times through the weathering layer) from the first-break times. Both methods were tested on a synthetic seismic data set and on high resolution seismic data collected at two base metal mines in central Newfoundland (Buchans and Gullbridge) to assist mineral exploration.

In Chapter 2, an outline of the methodology and theory of the GLI and engineering methods is presented with an explanation of the assumptions that each

technique makes about the near-surface model and seismic data. Chapter 3 compares the results of applying the techniques to synthetic data for both a processed seismic section and derivation of shallow bedrock velocities. Chapter 4 compares the results of the same techniques applied to field data collected at Buchans (using an explosive and Vibroseis™ source) and at Gullbridge (using explosives). Chapter 5 and 6 provide an overall discussion and conclusion which summarize the results and significance of the research.

CHAPTER 2

2.0 METHODOLOGY

Introduction

The GLI and engineering seismic refraction techniques can be used to estimate static corrections and lateral variations in shallow bedrock velocities from the same data: the travel times of seismic P- or S-waves that have undergone refraction at the bedrock/weathering layer interface. These travel times are manually (or automatically) picked on a computer from the traces recorded by receivers along a seismic line and are referred to as *first arrival times* or *first-breaks*. In general, only those arrivals that are recorded beyond the *critical distance* (the minimum shot-receiver offset beyond which the waves travel through the higher velocity bedrock refractor beneath the weathering layer) are used by these techniques. Although the two methods attempt to invert the same type of data, there are differences in the assumptions made about the near-surface properties and observational errors.

In Sections 2.1 and 2.2 of this chapter, the GLI and engineering methods are presented, with an explanation of the background theory and the assumptions used in the analysis of these data. In Section 2.3, an overall evaluation of the advantages and disadvantages of these techniques is discussed.

2.1 Generalised Linear Inversion

Terminology

GLI is used in many geophysical problems such as gravity and seismic modelling (e.g. Lines and Treitel, 1984). The usual procedure is to assume a model consisting of *model parameters* representing some physical property of the earth (e.g. seismic P-wave velocity, density, conductivity). These parameters are assumed to be theoretically related to experimental observations by a mathematical function of the parameters. The observations from an experiment (i.e. geophysical survey) are called the *observables* and the values of the function (obtained from a process known as *forward modelling*) are called the *functionals*. The goal of inversion or *reverse modelling* is to find a solution by perturbing the initial model parameters in such a way that the functionals match the observables within some acceptable tolerance. In this case, the model parameters are the slownesses (inverse of velocities) of partitioned regions or *cells* of the near-surface earth and the functionals and observables to be matched are the travel times of refracted P-waves.

Overview of GLI methodology

The first step in the procedure is to solve for a layered model which has weathering and bedrock subdivided into cells of constant slowness. Initially the bedrock cells have a greater dimension (approximately 5-10 times wider) than the weathering

cells. This model is used to obtain the static corrections which are observed to be fairly insensitive to lateral variations in bedrock velocity over 5-10 stations. This is because the relatively higher bedrock velocity adds only a small component of the travel time to the statics solution.

The next stage is to examine the smaller-scale variations in shallow bedrock velocity for geological interpretation; the inversion of a bedrock model is completed after subtraction of the travel times through the weathering layer from the first arrival times. The purpose is to remove the weathering layer parameters to allow a greater number of bedrock cells to be used, increasing the resolution of the model without increasing the computer time required to carry out the inversion.

2.1.1 Description of the Near-Surface Model and its Assumptions

Assumption for vertical velocity gradient in bedrock

An analysis of the first-breaks picked from the seismic data indicates that, in most cases, a simplifying assumption can be made that vertical velocity gradients for bedrock can be neglected. In other words, it is assumed that the P-waves penetrate only a metre or so below the bedrock/weathering layer interface. Based on this assumption, a simple two-layer model was used to invert the first-break times composed of a weathering layer and a single bedrock layer. Unfortunately, there are many cases for other seismic data where this assumption about the shallow bedrock velocity is not a valid one and a

tomographic approach (e.g. White, 1989) involving diving raypaths is required.

Assumption for weathering layer thickness

For the calculation of statics we are only interested in the travel times through the weathering layer, and so either the thickness or the velocity of this layer can be held constant while the other is estimated (De Amorim et al, 1987); for the modelling done here, a constant thickness is assumed for the weathering layer. By assuming a constant thickness, solutions are obtained which do not represent "true" models for the velocity and thickness of the weathering layer, but the vertical travel times through this layer at each station can be obtained by dividing the assumed thickness by the cell velocity at that particular station.

The uncertainty in weathering velocity results in an error in weathering thickness and thus in an error in the travel time between the base of the weathering layer and the datum (Docherty, 1992); it also results in an uncertainty in the critical angle for the refracted ray between the weathering/bedrock layers. Although the weathering velocity may be calculated from uphole data or the arrival of direct waves, this information may not be available to the extent necessary to determine the sometimes rapid variation in the weathering properties (Docherty, 1992). For the case of significant bedrock/weathering layer velocity contrast and smooth to flat bedrock topography, the error for short-wavelength statics should be small.

Description of the GLI near-surface model

Based on the above assumptions, a model was chosen consisting of a weathering layer of constant thickness and a bedrock layer each divided into blocks of constant slowness separated by vertical boundaries. The weathering layer is split up so that each slowness cell is centred on a receiver station. The width of the bedrock cells is flexible and their boundaries can be positioned to incorporate one or more receiver stations per cell depending on the resolution of bedrock velocities required.

Surface consistency

When the static corrections are obtained from inversion it is assumed that, for all reflected raypaths, the correction applied in the processing sequence is identical at a given station. The assumption is that reflected raypaths are essentially vertical when they travel through the weathering layer, commonly known as the *assumption of surface consistency*. This simplification allows a single static correction to be applied to all traces recorded by a receiver at a given station (known as a *receiver static*) and similarly a single correction can be applied to all receivers that record the same shot (known as a *shot static*).

How good is this assumption in high resolution seismic work? It is a good one if refraction occurs in the weathering layer in a way which tends to make the raypaths vertical when they emerge at the surface. However, there may be situations where this approximation may not be a good one. For example, the assumption may not be

satisfactory in a region with thin overburden where high velocity material (e.g. intrusive volcanic dykes) outcrops in a lower velocity, fractured bedrock. Such situations may require migration procedures to resolve (Farrell and Euwema, 1984).

Equivalence of shot and receiver statics

In some cases (e.g. Buchans and Gullbridge explosives field data) it was found that, in addition to the surface consistent assumption, the shot static term could be assumed equivalent to the receiver static term at the nearest receiver. This may be appropriate in cases where the shots are placed at shallow depths close to receiver positions. For example, previous experience with one data set (Buchans explosive data) using the engineering method found no significant differences in the seismic sections processed with separate versus equivalent shot and receiver statics. This assumption results in an increase in the ratio of equations to unknowns (due to a decrease in the number of unknowns), and thus decreases the level of non-uniqueness inherent in the problem improving the statistical reliability of the solutions (Wiggins et al., 1976). Equivalence of shot and receiver statics also reduces the computer time required for inversion of this model because of the reduction in the number of columns in the matrix to be inverted. There may be cases, however, where extremely rapid variations in weathering velocity or thicknesses over short distances make this assumption a poor one even for the case of shallow shot depths.

2.1.2 Problem Formulation

As stated earlier, obtaining a solution for the near-surface model using GLI is a two stage process : initially a 2-layer model is used to obtain the statics, and subsequently the weathering layer is "stripped off" by subtracting the travel times through the weathering layer from the first arrival times. This allows a model with much smaller bedrock cells to be used as an aid to geological interpretation based on lateral variations in seismic velocity of the subsurface bedrock. Both stages require calculating the values of the functionals for the given slowness model. This raytracing procedure calculated the trajectories of the P-waves through the model for each shot/receiver pair and is required in order to obtain *calculated times* (the functionals) for comparison with the *observed times* (the observables). It is assumed that no ray bending occurs for the raypaths travelling across vertical cell boundaries.

Two-layer model

The initial two-layer slowness model defines a slowness parameter S_i for each weathering layer cell and a slowness parameter S'_k for each bedrock cell, so the raytracing through the model can be written as:

$$t_{ij}=(\frac{h}{\cos\theta_i})S_i+(\frac{h}{\cos\theta_j})S_j+\sum_{k=1}^{N_b} L(i,j,k)S'_k \qquad (1)$$

where S_i, S_j are the slownesses ($1/V_i$, $1/V_j$) for the weathering cells at shot and receiver positions i and j respectively, S'_k is the slowness of the k^{th} bedrock cell, N_b is the number of bedrock cells, L(i,j,k) is the length of the portion of the raypath within the k^{th} bedrock cell for given shot i, receiver j (may be zero for non-intersecting raypaths), t_{ij} is the refracted first arrival time for shot i, receiver j, h is the thickness of the weathering cells (assumed constant in this case), and θ_i and θ_j are the critical angles calculated from Snell's law for raypaths travelling between the base of the weathering layer and the surface at shot i and receiver j.

A small survey example to demonstrate residual statics, based on an idea by Wiggins et al. (1976), shows how the set of equations defining the problem is set up in a matrix for solution by GLI in a FORTRAN program. The hypothetical survey is shown in Fig. 1 below:

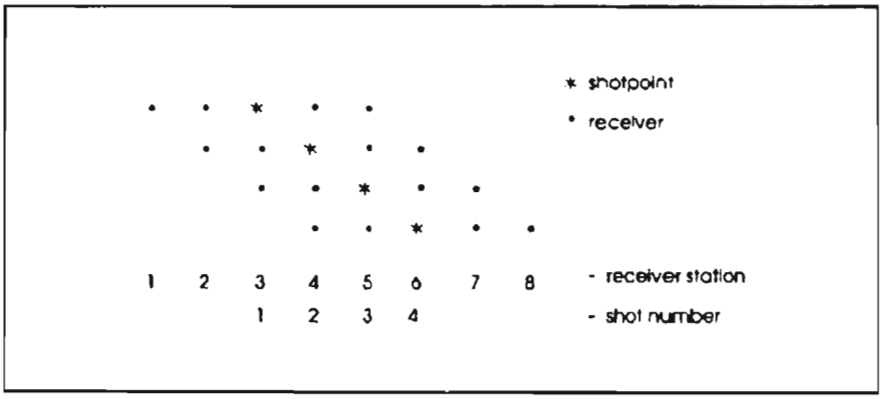

FIG. 1. Example of a small seismic survey.

The survey consists of a *split-spread* geometry of four receivers per shot. The shot and receiver locations are indicated as stars and dots respectively. In this simple case it is assumed that the earth's surface is a horizontal plane upon which the shots and receivers are placed; the shot point interval is equal to the receiver spacing. It is also assumed that the shot points are coincident to the receiver positions, and thus we can assume the equivalence of shot and receiver static terms (Fig. 2).

The number of equations depends on the number of first-break times which is limited by the number of shots and receivers in the survey, the critical distance, and the signal-to-noise ratio (i.e. noisy traces may not be picked). In our survey example we will assume that all four receivers in the spread record identifiable first-arrivals for raypaths travelling through bedrock. Therefore, we will have a total of 16 equations corresponding to a 4-receiver spread recording a total of four shots for the survey.

The number of unknowns depends on the number of slowness cells in the model. It is assumed that all cells are sampled by at least one raypath. In the case of a real survey, a dead channel in the spread may cause undesirable results in the inversion procedure because of the presence of a column of zeros in the matrix of equations. To correct for this problem, the equations corresponding to raypaths arriving at this receiver would be removed from the matrix. For the survey example there are 10 unknowns: the slownesses for 2 bedrock cells and 8 weathering cells.

We can write the system of equations in matrix form for raytracing through the 2-layer model as:

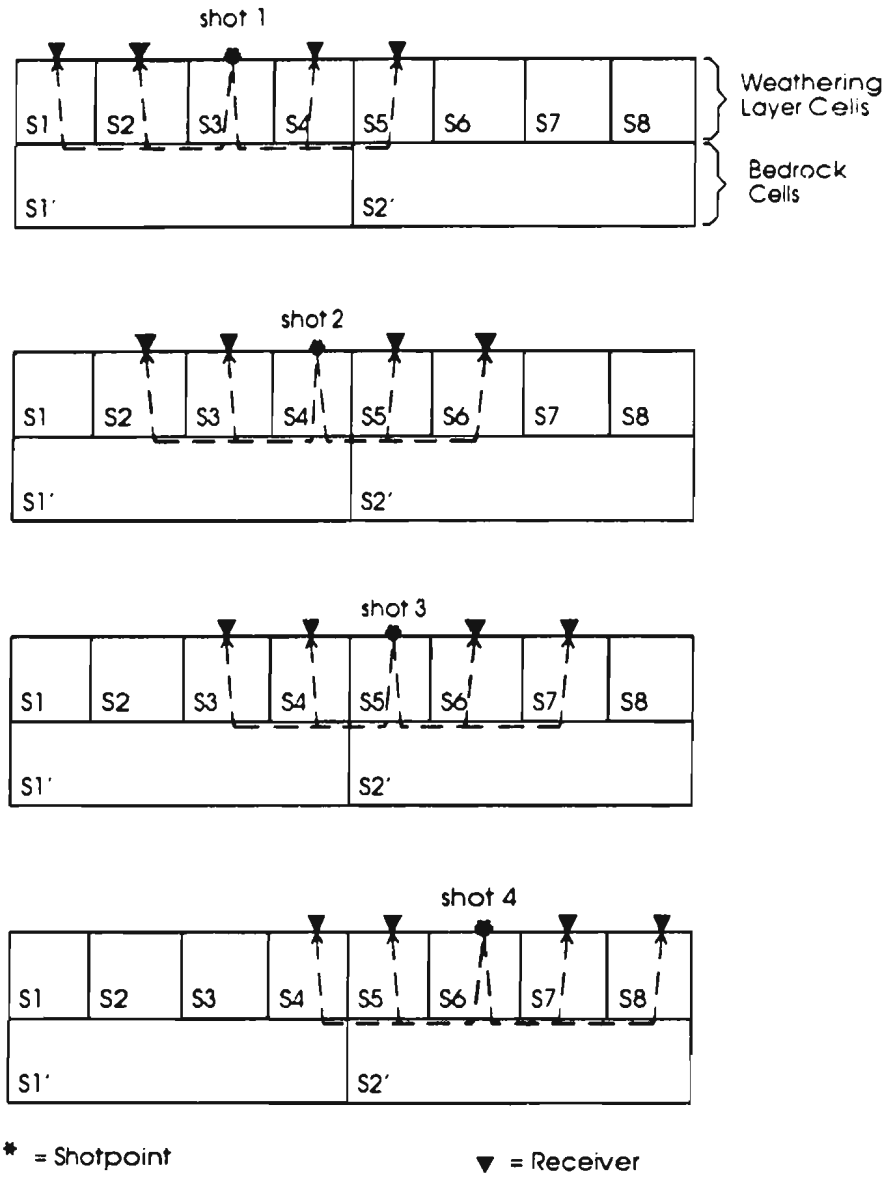

FIG. 2. A cross-sectional view of a hypothetical split-spread 4-channel survey with equivalent shot and receiver spacing above a two layer earth model. Raytracing is shown for refracted arrivals and each cell in the model represents a region of constant slowness; S1 .. S8 represent weathering layer slownesses; S1' .. S2' represent bedrock slownesses. The thickness of the weathering layer is held constant for the inversion (see text for details).

$$\boldsymbol{A}\ \boldsymbol{x} = \boldsymbol{b} \qquad (2)$$

or

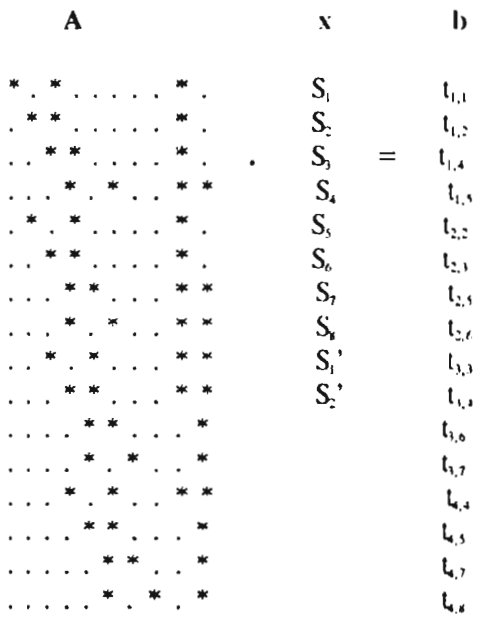

Each element in matrix **A** represents the length of the portion of the raypath contained in a particular slowness cell; the "*" and "." indicate a non-zero and zero value respectively. In tomography problems this matrix has been referred to as the *matrix of partial path lengths* (White, 1989) but we will refer to it here as the *geometry matrix*. Vector **x** contains the slowness values we are trying to solve for and the vector

b contains the observed first-break times. The solution for vector x in Equation 2 will contain the slownesses of the weathering and bedrock cells for this 2-layer model and these are used to calculate the static corrections required for the processing of the reflection seismic sections.

Refining the near-surface model for analyzing detailed bedrock velocity variations

As stated earlier, for analysis of the smaller-scale lateral variations in bedrock velocities, the weathering times are subtracted from the first-break times to simulate placing the survey on bedrock. The main reason for doing this is to reduce computer time by removing the weathering layer cells from the model, thus reducing the number of parameters to solve for. This requires a small time correction to be added to the travel times to make the endpoints of the raypaths in bedrock appear directly below shot i and receiver j. This correction simplifies raytracing procedures by maintaining the survey geometry:

$$\textit{time correction} = \tan\theta_i \sin\theta_i \; h \; s_i + \tan\theta_j \sin\theta_j \; h \; s_j \qquad (3)$$

where Θ_i and Θ_j are the critical angles at shot i and receiver j respectively, h is the thickness of the weathering layer and s_i, s_j are the slownesses of the weathering cells at shot i and receiver j respectively.

The bedrock model defines a slowness parameter S'_i for each cell in the bedrock

layer so that raytracing through this layer can be written as

$$t'_{ij} = \sum_{k=1}^{N_b'} L'(i,j,k) S'_k \qquad (4)$$

where S_k' is the slowness of the k^{th} bedrock cell, N_b' is the number of bedrock cells (in this case one per receiver station), L'(i,j,k) is the length of the portion of the raypath within the k^{th} bedrock cell travelling from shot i to receiver j (may be zero for non-intersecting raypaths), t'_{ij} are the "corrected" first arrivals for shot i, receiver j that assume the raypaths start and end in bedrock directly below the shot and receiver surface positions.

For our survey example (Fig. 1) we will have 16 equations (i.e. same survey geometry as the 2-layer model) and 8 unknowns: the slownesses for 8 bedrock cells (1 cell per station). As before we can write the system of equations in matrix form as:

$$\boldsymbol{A'\,x' = b'} \qquad (5)$$

or

$$
\begin{array}{ccccc}
\mathbf{A'} & & \mathbf{x'} & & \mathbf{b'} \\
\begin{bmatrix}
* & * & * & . & . & . & . & . \\
. & * & * & . & . & . & . & . \\
. & . & * & * & . & . & . & . \\
. & . & . & * & * & * & . & . \\
. & * & * & * & . & . & . & . \\
. & . & * & * & . & . & . & . \\
. & . & . & * & * & . & . & . \\
. & . & . & * & * & * & . & . \\
. & . & * & * & * & . & . & . \\
. & . & . & * & * & . & . & . \\
. & . & . & . & * & * & . & . \\
. & . & . & . & * & * & * & . \\
. & . & . & * & * & * & . & . \\
. & . & . & . & * & * & . & . \\
. & . & . & . & . & * & * & . \\
. & . & . & . & . & * & * & *
\end{bmatrix} & \cdot & \begin{bmatrix} S'_1 \\ S'_2 \\ S'_3 \\ S'_4 \\ S'_5 \\ S'_6 \\ S'_7 \\ S'_8 \end{bmatrix} & = & \begin{bmatrix} t'_{1,1} \\ t'_{1,2} \\ t'_{1,4} \\ t'_{1,5} \\ t'_{2,2} \\ t'_{2,3} \\ t'_{2,5} \\ t'_{2,6} \\ t'_{3,3} \\ t'_{3,4} \\ t'_{3,6} \\ t'_{3,7} \\ t'_{4,4} \\ t'_{4,5} \\ t'_{4,7} \\ t'_{4,8} \end{bmatrix}
\end{array}
$$

The symbols found in the elements of matrix **A'** are as described previously for Equation 2. In this case each element in the geometry matrix **A'** represents the length of the portion of the raypath contained in a particular bedrock slowness cell, vector **x'** contains the bedrock slowness values we are trying to solve for, and the vector **b'** contains the corrected travel times i.e. first-break times with the weathering times removed. The solution for vector **x'** in Equation 5 will contain the bedrock slowness value below each receiver station and thus will provide information on the lateral variations in shallow bedrock velocities that may be used as an aid to geological interpretation.

Formulation for crooked seismic lines

In the case of field data, a three-dimensional model is assumed to account for the crooked geometry of the seismic line. For raytracing, the raypaths may sample each weathering and bedrock cell at a variety of azimuths but it is assumed that the velocities within each cell are constant and isotropic. This assumption is a good one for the data analyzed in this thesis because the range of azimuths is usually less than 10-20 degrees. A horizontal baseline is used to locate the boundaries of the bedrock cells defined as vertical planes perpendicular to this baseline. The width of these bedrock cells can be set as constant or be chosen so that each receiver station along the survey line is midway between the boundaries of a cell.

2.1.3 Inversion Procedure

The above example of a small survey was used to describe the formulation of the problem. In reality, the seismic data will usually consist of many more shotpoints and receivers which will result in a much larger ratio of equations to unknowns. The solution to these sets of equations cannot be solved exactly. The presence of more equations than unknowns (said to be overdetermined) means that the systems will have a unique least-squares solution for a given number of parameters but this solution will imperfectly fit the data i.e. the final model obtained will be an inaccurate and nonunique one. In addition, the first-break times are corrupted by time-picking errors due to noise in the traces. These errors can cause wide variations or instabilities in estimates

of model parameters (Treitel et al., 1994).

The problem is assumed to be non-linear because the inclination of the raypaths in the weathering cells depend on the unknown slowness distribution in the model. An assumption can be made however that, for small velocity perturbations to an initial model, the equations are linear. This assumption will be a good one for the model used here so long as the raypaths through the overburden are close to being vertical (i.e. large velocity contrast between the bedrock and weathering cells). The strategy for solving the non-linear problem is to start with an initial slowness model and arrive at the final solution in small, linear least-squares steps.

An iterative non-linear least-squares technique with Singular Value Decomposition (SVD) is chosen for the inversion of the first-break times because SVD has been observed to be mathematically robust (Lines and Treitel, 1984) and is also simple to invoke in a computer program with standard mathematics software packages (e.g. LINPACK™ developed by Dongarra et al. (1979) was used here). Another feature of this particular method is that the variances of the model parameters can be estimated and therefore some idea of the validity of the solution can be obtained.

One disadvantage of the technique is that least squares, or the L_2 norm as it is also known, may suffer from a lack of robustness when the data contains large errors or *outliers* (Treitel et al., 1994). Some authors suggest the use of an L_p norm where p approaches 1, resulting in a reweighted form of the normal equations (Gersztenkorn et al., 1986). Another disadvantage is that run-time and memory requirements are large

due to SVD not taking advantage of the geometry matrix being sparse i.e. over 80% of this matrix is filled with zeros due to non-intersecting raypaths. Some techniques that work more efficiently on sparse matrices include Preconditioned Conjugate Gradient (Scales, 1987), and LSQR (Paige and Saunders, 1982). ART and SIRT (Herman, 1980) can also be adapted for sparsity but tend to converge more slowly (Scales, 1987).

2.1.4 Least-Squares Theory

A brief summary of the non-linear least-squares technique based on Lines and Treitel (1984) and Constable et al. (1987) will be provided here. Let the vectors $\mathbf{T}_o$ and $\mathbf{T}_c$ represent the observed and calculated times where $\mathbf{T}_o$ represents n observed travel times and $\mathbf{T}_c$ represents n calculated travel times. Let the difference between the observed and calculated times be represented by e:

$$\boldsymbol{e}=\boldsymbol{T}_o-\boldsymbol{T}_c \tag{6}$$

In least-squares problems $\mathbf{e}^T\mathbf{e}$ is the quantity we are attempting to minimize. The model response $\mathbf{T}_c$ may be considered to be a function of m parameters, namely the slowness cells in the model, which can be represented by a vector S of m slowness parameters. The model response function may be written as:

$$\boldsymbol{T}_c = \boldsymbol{F}(\boldsymbol{S}) \tag{7}$$

where F is a given function of the slowness parameters S.

We start the iterative procedure with an initial estimate of the model S^0. When we raytrace through the initial model S^0 we obtain the initial model response T_c^0. As discussed earlier, we can assume that the model response is linear for a small perturbation of the model parameters and therefore S^0 can be represented by the first-order Taylor expansion (Lines and Treitel, 1984):

$$T_c = T_c^0 + \sum_{j=1}^{m} \frac{\partial T_c}{\partial S_j}\Big|_{T_c=T_c^0} (S_j - S^0{}_j) \tag{8}$$

which can be written in matrix form as

$$T_C = T_C^0 + A\ \Delta x \tag{9}$$

where **A** is the n by m Jacobian matrix of partial derivatives of the model response with respect to the slowness parameter and $\Delta\mathbf{x}$ is the parameter change vector which represents the perturbations to the initial model parameters:

$$\Delta x_j = S_j - S^0{}_j \tag{10}$$

It should be noted that the Jacobian matrix **A** in Equation 9 is equivalent to the geometry matrix of Equation 2. This is because the partial derivatives in this matrix are

the coefficients of the slowness terms equivalent to the partial path lengths within each cell of the model.

We can express the residual vector **e** of Equation 6 in terms of this expansion of $\mathbf{T}_c$ shown in Equation 9:

$$\boldsymbol{e}=\boldsymbol{T}_o-\boldsymbol{T}_c=\boldsymbol{T}_o-(\boldsymbol{T}_c^0+\boldsymbol{A}\Delta\boldsymbol{x})=\boldsymbol{g}-\boldsymbol{A}\Delta\boldsymbol{x} \tag{11}$$

where **g** is the *discrepancy vector* or the *residual travel time* between the initial model and the observed travel times $\mathbf{T}_o$.

Since we are trying to find the least-squares solution to our problem, we want to minimize the squared error $\mathbf{e}^T\mathbf{e}$ with respect to the parameter change vector $\Delta\mathbf{x}$. To do this we require the condition:

$$\frac{\partial(\boldsymbol{e}^T\boldsymbol{e})}{\partial(\Delta\boldsymbol{x})}=0 \tag{12}$$

Substituting **e** from Equation 11 and differentiating (Graybill, 1969 describes differentiation with respect to a vector which implies $\partial(\mathbf{e}^T\mathbf{e})/\partial(\Delta x_i) = 0$ for all i.) and solving for $\Delta\mathbf{x}$ gives:

$$\Delta\boldsymbol{x}=(\boldsymbol{A}^T\boldsymbol{A})^{-1}\boldsymbol{A}^T\boldsymbol{g} \tag{13}$$

known as the Gauss-Newton solution (Lines and Treitel, 1984). The solution for the parameter change vector can be used in the iterative procedure to modify the initial

model by updating each initial slowness parameter by rearrangement of Equation 10:

$$S_j = S^0{}_j + \Delta x_j \tag{14}$$

In other words, the new model will be found by perturbing the initial model by the parameter change vector. This new model will become the current model for the next iteration and so on until the conditions for convergence are satisfied (outlined below in Section 2.1.8).

2.1.5 Regularization

There is a problem with the solution shown in Equation 13 when the inverse of $\mathbf{A}^T\mathbf{A}$ does not exist i.e. when $\mathbf{A}^T\mathbf{A}$ is *singular*. If this matrix is close to being singular the result may be a diverging solution where the perturbations may grow and result in the initial model diverging rapidly away from the true solution (Lines and Treitel, 1984).

To compensate for this problem, two different techniques are used for the two different stages of the procedure : i) For inversion of a two-layer model for statics, a least-squares technique with *damping* is used; ii) For refinement of the bedrock velocities after stripping off the weathering layer, a least-squares technique with a constraint on the *roughness* (i.e. the converse of smoothness) of the parameter change vector is used, also known as *Occam's method* (Constable et al., 1987). The reason for using two different techniques is that it was found that the damped least-squares solution for bedrock velocity

is typically scattered and difficult to interpret for a model with many cells compared with a smoothed solution obtained using Occam's method. These two regularization techniques are described in more detail below.

Damped least squares

Damping attempts to smooth the final solution by limiting the energy in the parameter change vector Δx and by preventing singularities or near-singularities from causing the solution to diverge. A constraint is added to the problem which restricts the squares of the parameter change vector to be below a certain tolerance Δx_0^2. Minimizing the squared error subject to this constraint modifies the Gauss-Newton solution:

$$\Delta x = (A^T A + \beta I)^{-1} A^T g \qquad (15)$$

where β represents a damping factor.

This solution in Equation 15 combines the method of *steepest descents* for large values of damping with the method of least squares when the damping parameter is close to zero (see Lines and Treitel, 1984 for details). In general the steepest descents method works best when the sum of the squared residuals is large (i.e. far away from the solution) and the least-squares method works best when the sum of the squared residuals is small (i.e. close to the solution). Since the least-squares method converges more rapidly close to the solution than the steepest descents method, an approach where an

initial large amount of damping is reduced after each iteration was used for fastest convergence and stability (Lines and Treitel, 1984).

Occam's method

Solving the least-squares problem subject to a constraint on roughness by Occam's method (Constable et al., 1987; Docherty, 1992) attempts to produce a smooth solution by again limiting the energy in the parameter change vector. In this case however, absolute bounds are not used but the energy is controlled by the addition of a derivative of the parameter change vector itself; in this case high-frequency components of this vector are penalised by this derivative function. Again, minimizing the squared error subject to this constraint results in a modified form of the Gauss-Newton solution (Constable et al., 1987; Scales et al., 1990):

$$\Delta x=(A^TA+\mu D^TD)^{-1}A^Tg \qquad (16)$$

where μ, hereafter known as the *smoothing parameter*, controls the amount of smoothing and **D** is a first difference matrix. First difference smoothing is used here because it produces bedrock velocity curves that resemble the solutions using engineering refraction analysis. However, Scales et al. (1990 p. 120) recommend the use of second rather than first difference smoothing because it doesn't penalise solutions which are smooth and have a large slope.

It can be seen how similar damping and Occam's method are by replacing the first difference operator in Equation 16 with the identity matrix **I** and comparing this to Equation 15. We can think of the process described by Equation 15 (damping) as analogous to pre-whitening (Lines and Treitel, 1984) in seismic deconvolution of a time series and Equation 16 (Occam's) as analogous to low pass filtering where we reduce the effects of the higher frequency components of the parameter change vector. Both processes are attempting to reduce the high frequency noise present in the solution.

2.1.6 Singular Value Decomposition

Since the formation of $\mathbf{A}^T\mathbf{A}$ and $\mathbf{A}^T\mathbf{g}$ in Equations 15 and 16 involve numerical inaccuracies Golub and Reinsch (1970) have proposed that it is better to attempt a solution of the rectangular system

$$\boldsymbol{A}\ \Delta\boldsymbol{x} = \boldsymbol{g} \tag{17}$$

where the solution is

$$\Delta\boldsymbol{x} = \boldsymbol{A}^{-1}\ \boldsymbol{g} \tag{18}$$

For geophysical problems where the number of equations n is much greater than the number of unknowns m, the inverse $\mathbf{A}^{-1}$ must be considered to be the so-called *generalized* inverse (Lanczos, 1961).

One technique to find the generalized inverse of matrix A was developed by Golub and Reinsch (1970) and involves the singular value decomposition (SVD) of this matrix. A is factored into a product of three matrices:

$$A = U \Lambda V^T \tag{19}$$

where U is a matrix containing m of the total n observation eigenvectors of length m, V is a matrix of the m parameter eigenvectors of length n, and Λ is a diagonal m by m matrix which contains the eigenvalues λ_j arranged in order of decreasing size (see details on p. 169, Lines and Treitel, 1984).

Either damping or Occam's method can be incorporated into the SVD. In the case of damping we add a "D.C shift" (Lines and Treitel, 1984) to the eigenvalues so that very small eigenvalues will not have such a strong influence on the parameter change vector:

$$\Delta x = V \, diag\left(\frac{\lambda_j}{\lambda_j^2 + \beta}\right) \, U^T g \tag{20}$$

(see details in Lines and Treitel, 1984) where *diag* indicates a diagonal matrix with diagonal elements indicated in the parenthesis, V is the m by m matrix containing the m parameter eigenvectors, U is the n by m matrix containing m of the n observational eigenvectors, g is the discrepancy vector, Δx is the parameter change vector, β is a

damping parameter, and λ_j are the singular values.

When we combine Occam's method with SVD the result is:

$$\begin{aligned} \Delta \boldsymbol{x} &= \boldsymbol{V}[\boldsymbol{\Lambda}^2 + \mu(\boldsymbol{DV})^T(\boldsymbol{DV})]^{-1}\boldsymbol{\Lambda}\boldsymbol{U}^T\boldsymbol{g} \\ &\approx \boldsymbol{V}\ diag\left(\frac{\lambda_j}{\lambda_j^2 + \mu(\boldsymbol{DV})^T(\boldsymbol{DV})}\right)\boldsymbol{U}^T\boldsymbol{g} \end{aligned} \tag{21}$$

(see Scales et al., 1990 for details) where μ is the smoothing parameter, **D** is the first difference matrix, and the remaining variables are as in Equation 20.

In Equation 21 a rough eigenvector in the j^{th} column of **v** results in a large entry in the j^{th} diagonal element in the matrix $(\mathbf{DV})^T(\mathbf{DV})$. This reduces the contributions from the high-frequency eigenvectors to the solution and essentially smooths the solution (Docherty, 1992).

The main difference between damping and Occam's method used in combination with SVD is that damping assumes that the high frequency eigenvectors that contribute to the high frequency variations of the parameter change vector are associated with the small eigenvalues when attempting to generate a smooth solution whereas Occam's method does not. There are examples where the assumption that damping makes is a bad one; Occam's method sometimes works much better than damping when used to solve seismic inversion problems (see Docherty, 1992).

2.1.7 Estimating Errors In Model Parameters

The measured first arrival times, surveyed elevations and shot/receiver locations all have errors associated with them. It is assumed, however, for the inversion procedure that the largest source of error in the statics and bedrock velocity estimates is due to errors in travel times from picking traces corrupted by some level of noise.

For the inversion of the 2-layer model using damped least squares, it is assumed that the errors in the travel times are statistically independent. This assumption will be better for times picked from traces with high rather than low signal-to-noise ratios because the picker will sometimes interpolate across noisy traces using adjacent less noisy traces as a guide. If this assumption of statistical independence is assumed to be valid we can use the equation (Aki and Richards, 1980)

$$\sigma_{pj}^2 = \sigma_d^2 \sum_{i=1}^{k} v_{ji}^2 \frac{1}{\lambda_i} \tag{22}$$

to estimate the variance of the j^{th} parameter in the solution where:

v_{ji} is the j^{th} component of eigenvector $\mathbf{v}_i$, λ_i is the i^{th} singular value, and

σ_d^2 is the variance of the travel-time residuals estimated by:

$$\sigma_d^2 = \sum_{i=1}^{n} \frac{(T_{i_{obs}} - T_{i_{calc}})^2}{n-m} = \sum_{i=1}^{n} \frac{g_i^2}{n-m} \tag{23}$$

where $g_i = (T_{i\,obs} - T_{i\,calc})$ is the i^{th} component of the travel-time residual or discrepancy vector.

For the inversion of the bedrock layer after removal of the weathering times, velocity error estimation is more difficult. When attempting to use all the model eigenvectors from the inversion to estimate variance, it is found that the error estimates were unrealistically large due to the presence of small eigenvalues in the solution. If the roughness constraint is included to reduce the effects of these very small eigenvalues, the error estimates are unrealistically small. Therefore it was decided to use the errors obtained from the damped least-squares method for the wider bedrock cells, which gave intermediate values between these extremes. In general, this is a good assumption if the smoothed solution appeared to be follow the general pattern of the wide cell solution.

An additional refinement of this technique includes using a method termed here the *midpoint method* on the smooth solution to determine the standard deviations for the data assuming dependence on the cell centred on all raypaths; in other words, a standard deviation for the data is estimated for each station. This is useful for indicating regions of bad first-break picks which are identified by a relatively large estimated standard deviation.

2.1.8 Iterative Procedure and Termination Conditions

The flowchart shown in Fig. 3 illustrates the general iterative procedure to obtain the final solution from the initial model and observations. For the damped least-squares

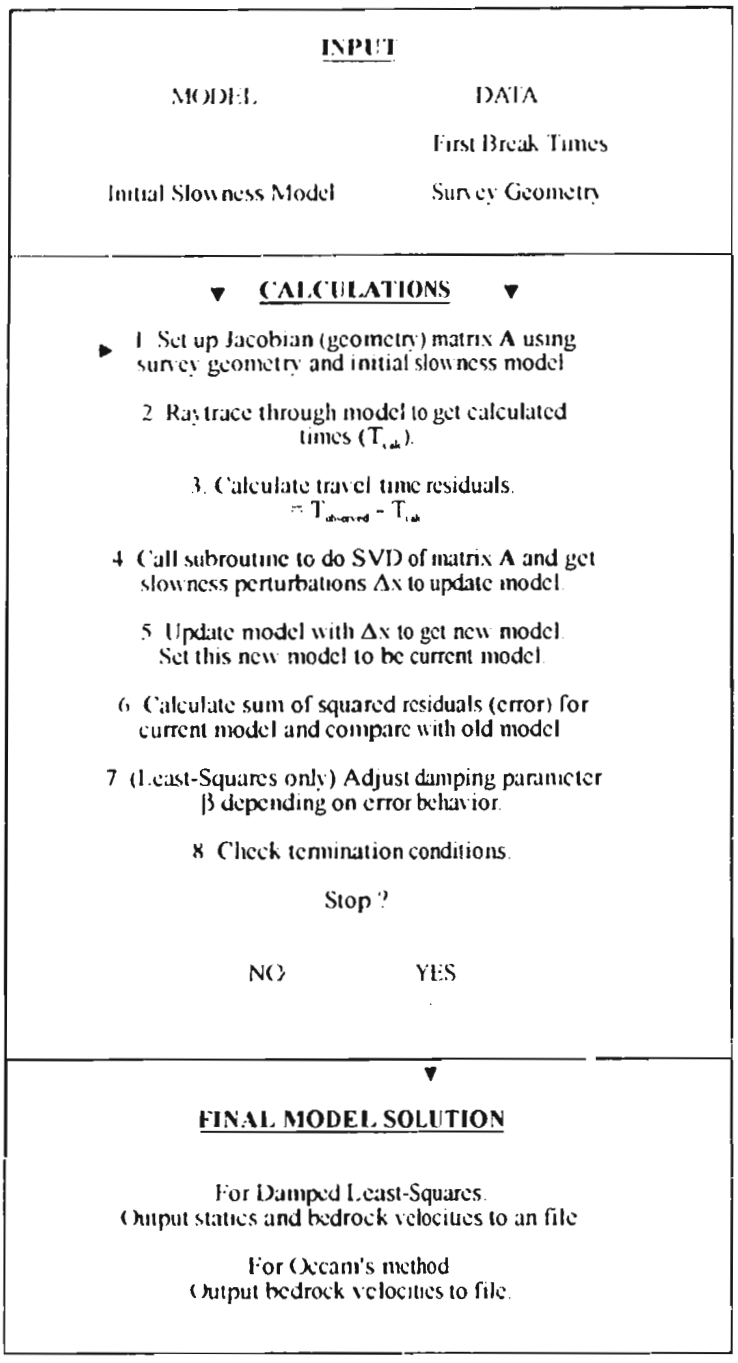

FIG. 3 Flowchart illustrating the general inversion procedure.

solution of the 2-layer model (from which statics corrections are obtained) the initial damping parameter β is reduced after each iteration to increase the rate of convergence of the procedure, but when Occam's method is used to refine the bedrock layer of the model, the smoothing parameter μ remains constant over the entire iterative procedure.

The termination conditions for the iterative procedure are:

1. the slowness perturbations fall below a certain tolerance level (i.e. the model was not changing significantly);
2. the residual errors fall below a certain tolerance level (i.e. the fit of the model to the data is acceptable);
3. a specified number of iterations is reached.

2.2 Engineering Seismic Refraction Analysis

Introduction

The methods of deriving refraction static corrections for seismic reflection processing described here are based on the reciprocal method (Hawkins, 1961), the similar plus-minus method (Hagedoorn, 1959) and the cumulative difference method (Bahorich et al, 1982; Leven and Taylor, 1989). The overall procedure for application to refraction statics and bedrock velocity analysis has been described previously and was programmed in FORTRAN routines and implemented by Wright (Wright, 1994a,b; Wright and Nguuri, 1994) on a number of high resolution seismic data sets.

The first step in the procedure is to estimate bedrock velocities by smoothing the first-break times for use in correcting the travel times for situations of crooked-line recording. The statics are estimated and then the weathering times subtracted from the first-break times so that a more refined bedrock velocity model can be obtained. In this section, a summary of the engineering seismic refraction method is presented. Wherever possible the assumptions of the method and the possible sources of errors are stated and compared with the GLI method.

2.2.1 Estimating Shallow Bedrock Velocities

The reciprocal method assumes that, for the combinations of shots and receivers used to derive travel times through the weathering layer, the raypaths are in the same vertical plane; therefore a small time correction is required to correct for off-line shots and receivers in situations of crooked-line recording; the estimation of bedrock velocities is required initially to estimate these corrections.

The initial estimation of bedrock velocities is accomplished by smoothing the first-break times without removing any static corrections using the *method of summary values* (Bolt, 1978). As with the GLI near-surface model it is assumed that the vertical component of the velocity gradient can be neglected for the data sets analyzed for this thesis; as stated earlier, this assumption is appropriate for the data in this thesis but is not always applicable. Apparent velocity curves are obtained in both the forward and reverse directions and used to calculated bedrock velocities using the method of Wright (1994b).

The method of summary value smoothing (Bolt, 1978) uses a window for the first-break data over which a least-squares method is used to fit a line and a quadratic to the times. The points of intersection of these two lines are called the "summary value" points and the velocity estimate (inverse slope of the least-squares line) is plotted at their midpoint rather than at the midpoint of the window. This method of smoothing allows for any curvature in the data within the range of the window. This window may be of fixed length as it slides along the entire line or preferably it can be varied based on an

empirical selection rule or trade-off parameter to ensure comparable smoothing between different data sets (Bolt, 1978; Wright, Muirhead and Dixon, 1985; Wright, 1994a). For the data sets analyzed here a window of fixed width is used to avoid making the numerical procedures too cumbersome. A cubic spline is fitted through the summary points (with a small amount of smoothing) to give velocities at regular intervals.

For both Occam's method and the method of summary values, there is some ambiguity in deciding how smooth the solution for bedrock velocity should be. For the method of summary values, this is controlled by the length of the smoothing window that runs over the data; for Occam's method it is controlled by the smoothing parameter μ. In both cases a simplifying assumption is made (fixed length window for smoothing; a constant μ for Occam's method) to avoid excessive computational procedures. The length of window or smoothing parameter are chosen subjectively based on experience and on the appearance of the velocity profiles.

2.2.2 Reciprocal Time-Depth Terms

The reciprocal time-depth is the time delay of the critical ray in travelling between the refractor and the surface (Hawkins, 1961). In the practical situation of a seismic survey, corrections must be made when deriving the time-depths to account for the differences in the surface positions for shots and receivers at a given station. These corrections allow for the differences in elevation due to burial of shots and for displacement of shots and receivers horizontally from the line. If we let $T_{A'c}$ represent

the measured travel time (i.e. first-break pick) of a raypath travelling from shot A' to a receiver at C (Fig. 4(a),(b)) the corrected travel path for a raypath assumed to go from receiver A to receiver C would be:

$$T_{AC} = T_{A'C} + S_{A'} + e_{A'C} \qquad (24)$$

where $S_{A'}$ is a small time correction to allow for differences in position for receiver A and shot A', and $e_{A'B}$ is the error in measuring the first-break time of a refracted P wave travelling from shot A' to receiver B.

If we denote shot locations as A', B', and C' and receiver locations as A,B and C, we can estimate a time-depth term r_B by incorporating the errors and corrections:

$$\begin{aligned} r_B &= {}^1/_2\,[T_{AB} + T_{CB} - {}^1/_2\,(T_{AC} + T_{CA})] \\ &= {}^1/_2\,[(T_{A'B} + S_{A'} + e_{A'B} + T_{C'B} + S_{C'} + e_{C'B}) - \\ &\quad {}^1/_2\,(T_{A'C} + S_{A'} + e_{A'C} + T_{C'A} + S_{C'} + e_{C'A}) - \\ &\quad \Delta/V_2\,] \end{aligned} \qquad (25)$$

where Δ/V_2 is a time correction for horizontal displacement of shots and receivers causing different raypath lengths in bedrock, V_2 is the bedrock velocity derived from smoothing the first-breaks, and Δ is the distance correction.

If we assume the general case of a receiver at location k we can search over all possible reversed shot/receiver paths which bracket this receiver to get a reliable estimate

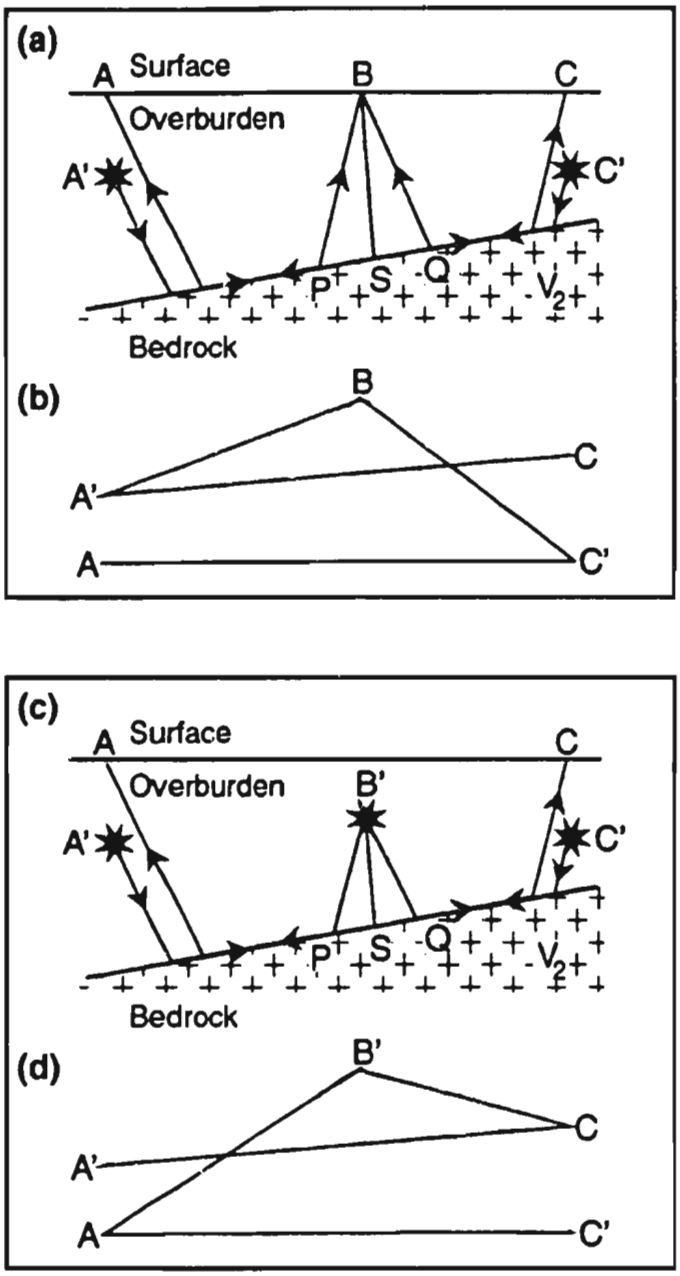

FIG. 4. (After Wright and Nguuri, 1994) Illustration of the reciprocal method used for deriving shot and receiver static terms for split spread recording: (a) receiver terms, vertical section; (b) receiver terms, map view; (c) shot terms, vertical section; (d) shot terms, map view.

of time-depth r_k. Similarly if receiver k is replaced by shot k (as in the case of shot B' in Fig. 4(c) and (d)) we can estimate a time-depth s_k by searching over all possible reversed shot/receiver paths which bracket this shot and take the median value. To minimize the effects of time measurements with large systematic errors without having to search for and remove such data, the median of the r_k (or s_k) values should be used. This may have advantages over the damped least-squares technique in situations where the data contain large errors or outliers due to picking errors. As stated in section 2.1.3, the L_1 norm may theoretically perform better than least squares in these situations.

A short note on the Generalized Reciprocal Method

For the comparisons done in this thesis, all travel times through the weathering layer are estimated by the reciprocal method since the optimum XY distance of the generalized reciprocal method (Palmer, 1981) is always less than one receiver spacing (Wright, 1994 a,b). For adequate determination of XY values for use by this method, at least three geophone intervals per optimum XY spacing are required (Palmer, 1981) and therefore no advantage in using this technique instead of the reciprocal method.

Cumulative Difference (CD) Method

An alternative approach to estimating reciprocal terms is the cumulative difference or CD method (Bahorich et al, 1982; Leven and Taylor, 1989). This method has the advantage of having more reciprocal paths per shot than the conventional reciprocal

method (for a reasonably complete data set) but also has the disadvantage that the errors are cumulative (Wright and Nguuri, 1994). The CD approach estimates reciprocal terms by using times to adjacent shots (or receivers) from receivers (or shots) on opposite sides of the adjacent locations (Figs. 5(a) and (b)). As with the reciprocal method, a correction is made for the geometry of the shots and receivers and incorporates the bedrock velocities estimated from smoothing the first-breaks times. From the CD analysis a set of time terms r'_k and s'_k are estimated for receiver k and shot k respectively. For the data sets used in this thesis, static corrections computed by this method are not significantly different from those computed by the reciprocal method (Wright and Nguuri, 1994).

Derivation of the static terms

The static corrections δt_r (receiver static term) and δt_s (shot static term) corresponding to reciprocal time terms r_k and s_k respectively are given by :

$$\delta t_r \approx r_k + \frac{1}{2}(\cos i_+ + \cos i_-) \approx r_k \frac{V_2}{\sqrt{V_2^2 - V_1^2}} \tag{26}$$

$$\delta t_s \approx s_k + \frac{1}{2}(\cos i_+ + \cos i_-) \approx s_k \frac{V_2}{\sqrt{V_2^2 - V_1^2}} \tag{27}$$

The geometry of the raypaths is assumed to be as shown in Fig. 6.

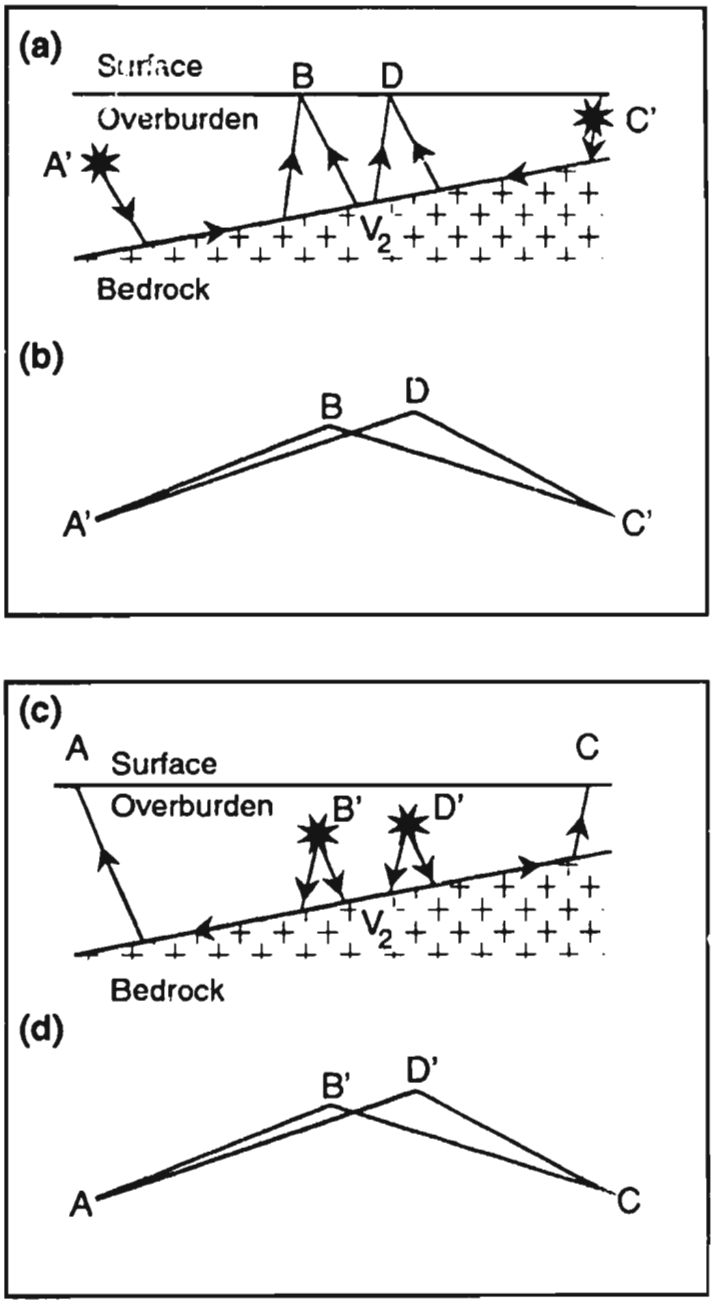

FIG. 5. (After Wright and Nguuri, 1994) Illustration of the cumulative difference method used for deriving shot and receiver static terms for split spread recording (a) receiver terms, vertical section; (b) receiver terms, map view; (c) shot terms, vertical section; (d) shot terms, map view.

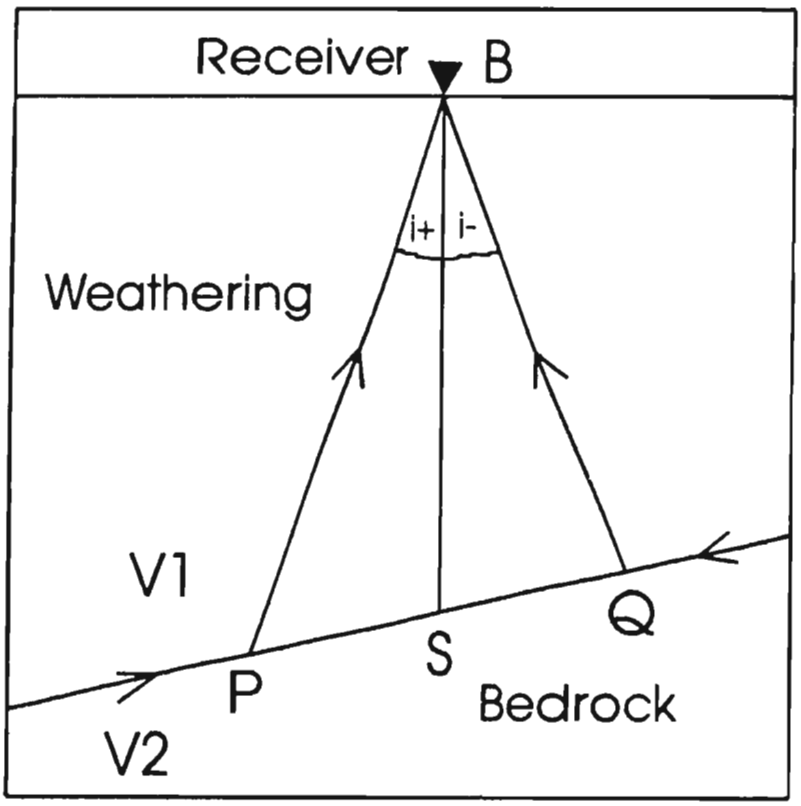

FIG 6 (After Wright and Nguuri, 1994) Ray diagram illustrating the estimation of static corrections from reciprocal times. The reciprocal term is estimated from paths PB and QB. SB is vertical (see Equations 26 and 27 in text)

2.3 Overall Comparison of the GLI and Engineering Methodology

Similarities

There are many similarities between the assumptions that the two techniques make in modelling the first-break data:

i) The assumption that the vertical velocity gradient in bedrock is insignificant results in a simplification of the data analysis in both cases (i.e. two-layer problem).

ii) The assumption of surface consistency simplifies the procedure for processing (i.e. constant static shift at each shot/receiver position) and also decreases the non-uniqueness of the problem in both cases.

iii) The subtraction of the weathering times from the first-break data allows a more refined solution for the bedrock velocities to be obtained for both techniques. In the case of the engineering method, smoothing the first-break times without this correction appears to produce good results but with larger errors.

Differences

The main difference between the techniques is in the assumptions that are made about the distribution of errors in the data. The engineering technique as used here takes

the median values of the time-depths for the estimation of statics in contrast to the GLI technique, which solves the problem by a least-squares technique that, theoretically, may not perform as well as the engineering technique on data with large outliers (i.e. data containing occasional bad first-break picks). An improvement in the GLI technique may have been to use an L_p norm with p close to 1 instead of least squares (p=2).

Another important difference in the methods is the way that the bedrock velocities are calculated. The engineering method combines forward and reverse apparent velocities in a formula that accounts for local bedrock dip. In contrast, the GLI method assumes a simple, horizontal refractor. The differences in these assumptions was tested by synthetic modelling and the results are discussed in the next chapter.

There is a significant difference in the efficiency of the techniques, specifically with respect to computer memory and runtime requirements. The GLI is at a disadvantage due to the inefficiency of the SVD technique when applied to the sparse geometry matrix. However, there are more efficient, approximate methods that may be faster than SVD.

Finally, it is difficult to compare the advantages or disadvantages of the summary value smoothing technique and Occam's method. The relationship between μ for Occam's method and the length of the smoothing window for summary value smoothing was not established here in a strict mathematical sense. Both techniques however appear to produce bedrock velocity profiles that are similar in appearance and so lead to equivalent geological interpretations; this will be shown for the field data in Chapter 4.

CHAPTER 3

3.0 SYNTHETIC DATA RESULTS

Introduction

The following chapter describes some of the synthetic modelling that was done as part of the research for the thesis. The main purpose was to compare the effectiveness of the GLI and engineering techniques applied to seismic data containing reflected signals, noisy first-breaks and statics of similar magnitude to those observed in high resolution data recorded in volcanic settings in eastern Canada. In Section 3.1, the forward modelling that was done to create the synthetic data is described. Section 3.2 explains what assumptions and initial parameters were used by both techniques in the calculation of the static corrections and bedrock velocities from the first-break data. Section 3.3 compares the quality of stacked CMP seismic sections processed after application of refraction static corrections and the resolution of lateral variations of seismic velocity in uppermost bedrock derived from both the GLI and engineering techniques. Finally, Section 3.4 provides a brief summary and conclusions for the work done on the synthetic data set.

3.1 Generating the Synthetic Data

Earth Model

The synthetic reflection data were created by Wright and Nguuri (1994) and were

generated using the AIMS™ modelling software for a velocity model presented in Table 1 and shown schematically in Fig. 7. The model consisted of two reflectors placed at depths of 500 m and 1350 m in a bedrock with a velocity that varied laterally from 3.0 km/s at x=0 to 5.0 km/s at x=2500 m as a linear function of x. The bedrock was assumed to have no vertical velocity gradient. Synthetic seismograms were generated by placing the sources on the surface of bedrock. A weathering layer of constant thickness and random velocity variations between specified limits provided a source of surface-consistent static anomalies shown in Fig. 8. Each constant velocity weathering cell had a width equal to the receiver spacing, and each shot and receiver was placed mid-way between the cell boundaries. The range of random velocities assigned to each cell was changed at several locations along the profile (see Table 1).

Survey Parameters

A 48 channel split-spread recording configuration with the source at channel 25 was used (see Table 1). The sources were fired at every second receiver station and thus simulated a 12-fold survey. Two sources of different frequency content were used: a zero phase (Ricker) wavelet with a dominant frequency of 80 Hz and the same wavelet subjected to a high-pass filter in which the low cut was greater than 80 Hz, thus producing higher frequency, more complex signals. White noise was added in both cases to create traces that resembled real seismograms. The first-break times were calculated by raytracing through the velocity model for 60 shots of the hypothetical survey.

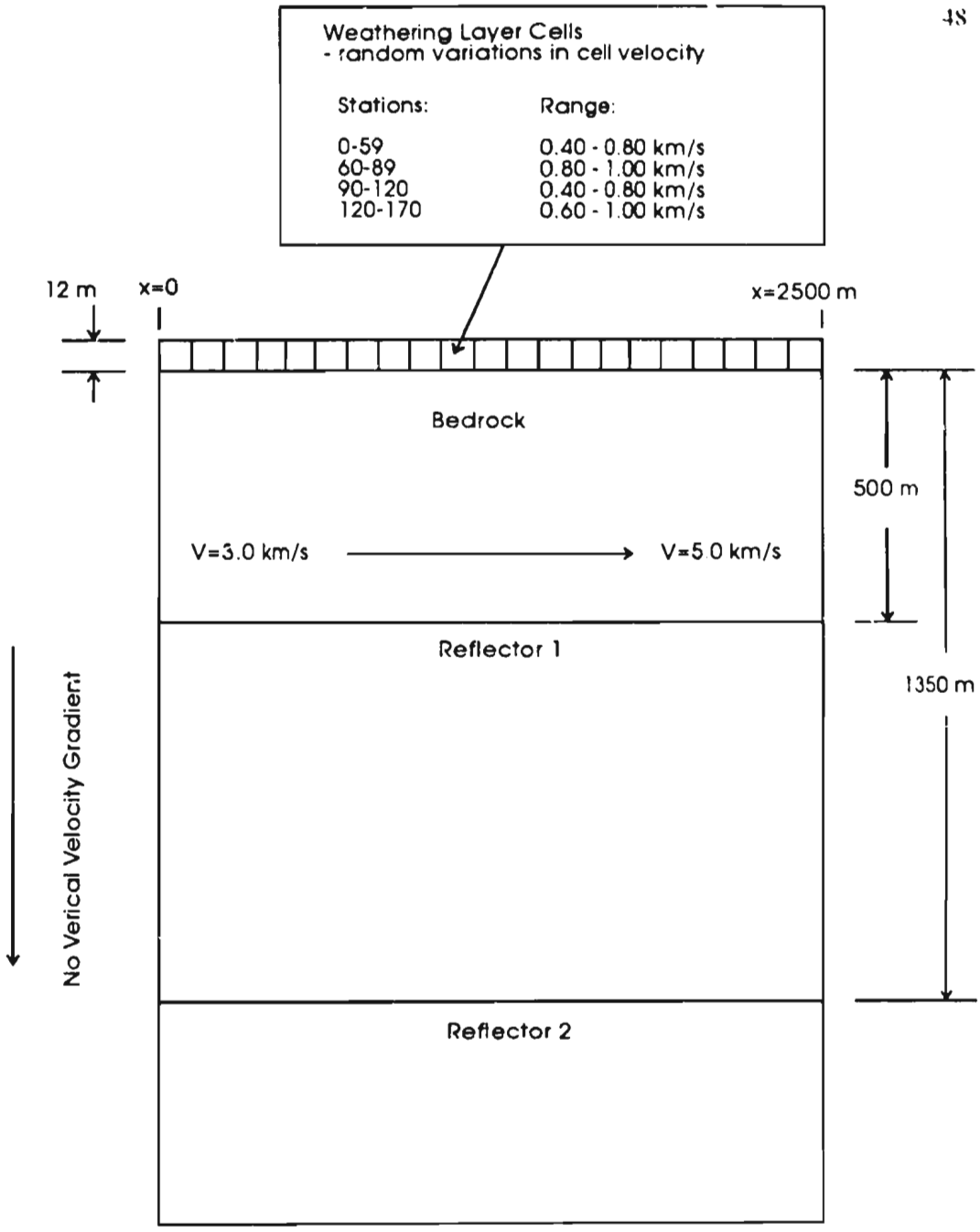

FIG. 7. Cartoon representing the synthetic model used to create the synthetic data analysed by the GLI and engineering methods.

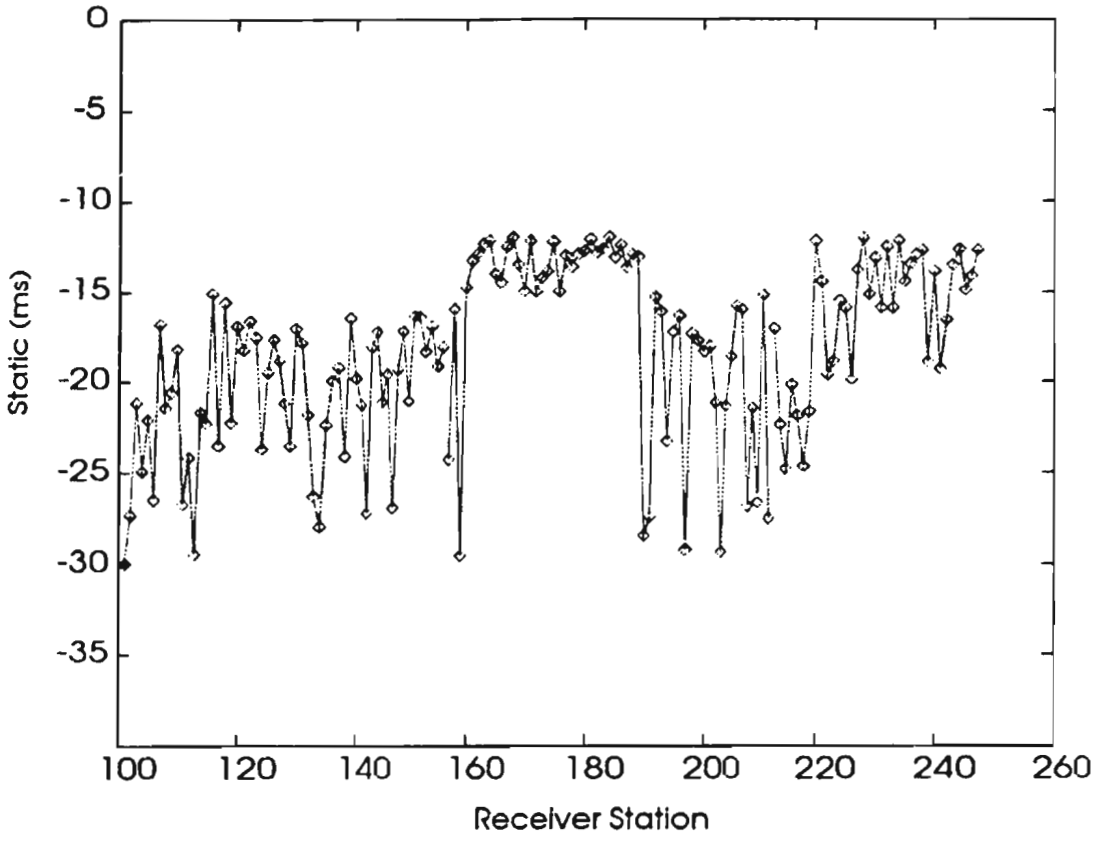

FIG. 8. Forward model statics derived from model shown in Fig. 7 and Table 1. Note that the higher, more restrictive range of random velocities between stations 160-189 and higher velocities between stations 220-250 result in a lower, more restrictive range of statics for these portions of the line.

TABLE 1. (After Wright and Nguuri, 1994) Source-receiver parameters used in generating synthetic shot reflection gathers and velocity model.

SOURCE-RECEIVER PARAMETERS:	
No. of recording channels:	48
Shot-receiver configuration:	Symmetric split spread; shot at trace 25
Receiver spacing:	10 m
Source (on surface):	80 Hz wavelet (zero phase)
Shot spacing:	20 m
Recording fold:	12
No. of shots:	60 for refraction statics calculations; 50 for processing
VELOCITY MODEL:	
Depth to bedrock:	12 m
Overburden velocities: (randomly varied between specified limits)	0.40-0.80 km/s; locations 101-159 0.80-1.00 km/s; locations 160-189 0.40-0.80 km/s; locations 190-219 0.60-1.00 km/s; locations 220-270
Bedrock velocities:	3.0 km/s at x = 0 m to 5.0 km/s at x = 2500 m; linear increase as a functopm of x; no depth variation

Error models for first-break times

Two models of timing errors were used to add errors to the first-break times and simulate a data set derived from picking first-breaks on noisy seismic traces: i) a model with Gaussian errors of mean zero and standard deviation σ of 3.0 ms, and ii) a model with the same Gaussian distribution contaminated by relatively low probability (0.083) Gaussian errors of mean zero and standard deviation 7.5 ms. This latter case gave a more realistic simulation of real time picks containing occasional large errors due to picking the wrong peak or trough on noisy traces (also known as *cycle skipping*). The use of $\sigma = 3.0$ ms is larger than one expects in high resolution surveys (per. comm. Wright, 1994); for example, the GLI results for real data from surveys at Buchans and Gullbridge (see Section 4.0) had a σ computed from residuals of around 2 ms.

3.2 Procedures

GLI initial models and procedure

The GLI procedure used to solve these synthetic data was slightly different from that described in the methodology section (Section 2.0); the bedrock velocities were determined from the initial damped least-squares inversion of the two-layer model and were not refined by stripping off the weathering layer and solving for the bedrock velocities using Occam's method. This was because the purpose of the synthetic modelling was to test the limits of resolution for bedrock velocity using damped least

squares. The evolution of Occam's technique as applied to further refining the bedrock velocities came about later, based on the results from both synthetic and real data.

A number of models with different bedrock cell widths were tested with 20, 40, 80 and 160 m cell widths (A model with a cell width of 20 m was only tested for the inversion of data with contaminated Gaussian errors due to the relatively greater computational time involved i.e. more parameters (bedrock cells) in this model).The initial two-layer models for GLI assumed, in all cases, a constant weathering and bedrock cell velocity of 1.0 km/s and 4.0 km/s respectively. The purpose of testing these models was to observe the sensitivity of the velocity error estimates and static solutions to the bedrock cell width.

The weathering layer thickness was assumed to be 12 m for the near-surface model, equal to the thickness of the true forward model thickness. Tests done on a smaller data set indicated that, for a relatively horizontal refractor and high weathering/bedrock velocity contrast, large errors in thickness can still give reasonable estimates of statics and bedrock velocities. This is similar to observations made by De Amorim et al. (1987) where they tested a number of initial models and found that good results could be obtained even with moderate errors in thickness.

The number of unknowns (Table 2) depended only on the number of bedrock cells since the number of weathering cells remained constant (one per station):

TABLE 2. Number and type of parameters in slowness models used for the damped least-squares inversion of the synthetic data.

Width (m) of Bedrock Cells	No. of Bedrock Cells	No. of Weathering Cells	Total No. of Parameters (M)
20	83	166	249
40	43	166	209
80	22	166	188
160	11	166	177

In general there was a direct relationship between the number of bedrock cells in the model and the amount of computer time required to obtain a solution. The average run time for the inversion was approximately 5-7 hours for 10-15 iterations. By far the most time consuming step in the iteration was the call to the LINPACK™ subroutine to compute the SVD of the geometry matrix **Z**.

The selection of the initial damping parameter β and the reduction factor for each iteration was important for the efficiency of the inversion but in most cases did not affect the final solution obtained from the procedure. Through trial and error the best values were found to be $\beta = 4.0$ with a reduction factor of 0.6 per iteration.

Engineering method - procedure and assumptions

For comparison with the GLI method, the engineering method assumed a model

for the weathering layer velocity with the correct weathering velocity at each shot or receiver location in converting time-depth terms to static corrections. The inclination of the modelled raypaths through the weathering layer was affected by the assumption of weathering velocity and thus the statics and bedrock velocity solutions were sensitive to the model assumed for this layer. The assumption of correct weathering layer thickness for the GLI model resulted in weathering velocities that were close to the true weathering velocities.

Separate shot and receiver statics were calculated for the engineering technique, in contrast to the GLI technique which assumed equivalent shot and receiver statics. Because of this, the static terms at stations with coincident shot and receiver points may have been better resolved by the GLI technique due to the relatively higher redundancy at these locations. For the comparison of the results, the equivalent statics from the GLI technique were compared with the receiver statics from the engineering technique; the differences between the shot and receiver statics for the latter technique were not significant.

3.3 Comparison of Results

Static corrections

The statics derived using the GLI and engineering techniques for the best resolved stations along the line (stations 130-240) are very similar in magnitude. This is shown in the graphs comparing the residuals ("true" statics minus estimated statics) for both

techniques applied to the data with a Gaussian (Fig. 9) and contaminated Gaussian (Fig. 10) distribution of errors added to the arrival times. An interesting result was that the least-squares technique appears to have performed as well if not slightly better than the reciprocal method (e.g. stations 200-240) for the inversion of the data contaminated with occasional outliers (Fig. 10(a) and (b)). This slight but perceptible improvement may be related to the relatively higher redundancy of the GLI method resulting from the assumption of equivalent shot and receiver statics. Theoretically, the reciprocal method may have been expected to perform better because it uses the median values of the time-depth terms to estimate a static value at a station.

The GLI solutions for statics were relatively insensitive to the width of the bedrock cells for the best resolved portion of the seismic line. This was because the true bedrock velocity increases smoothly as a linear function of x, and the averaging of the velocities in the cells of the GLI solution provided a good approximation of the true, smooth velocity function. Small errors in the bedrock velocity will contribute very little to the error in the statics. This is why some authors assume an average constant velocity for the bedrock when solving for statics because the errors introduced by such a simplification are usually small (e.g. Docherty, 1992). However, the bedrock velocity variations in some cases may be important for fine-tuning the statics solution in order to reduce the degredation of higher frequency signal in the stack.

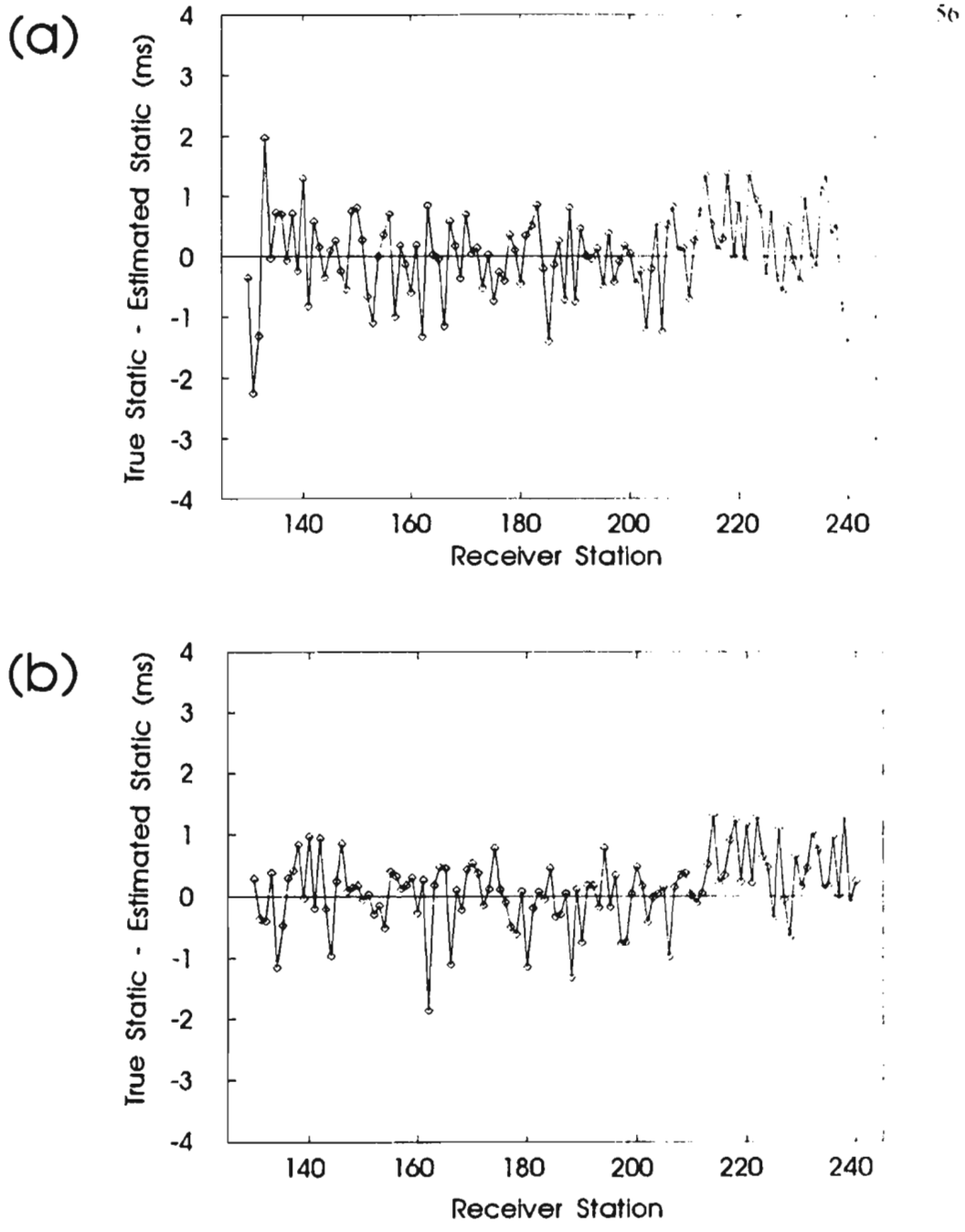

FIG. 9. Graphs showing differences between true static times from the synthetic forward model and the static times estimated using the (a) reciprocal method and (b) GLI technique. These were applied to first arrival times with a Gaussian distribution of timing errors with mean 0.0 ms and s.d. 3.0 ms.

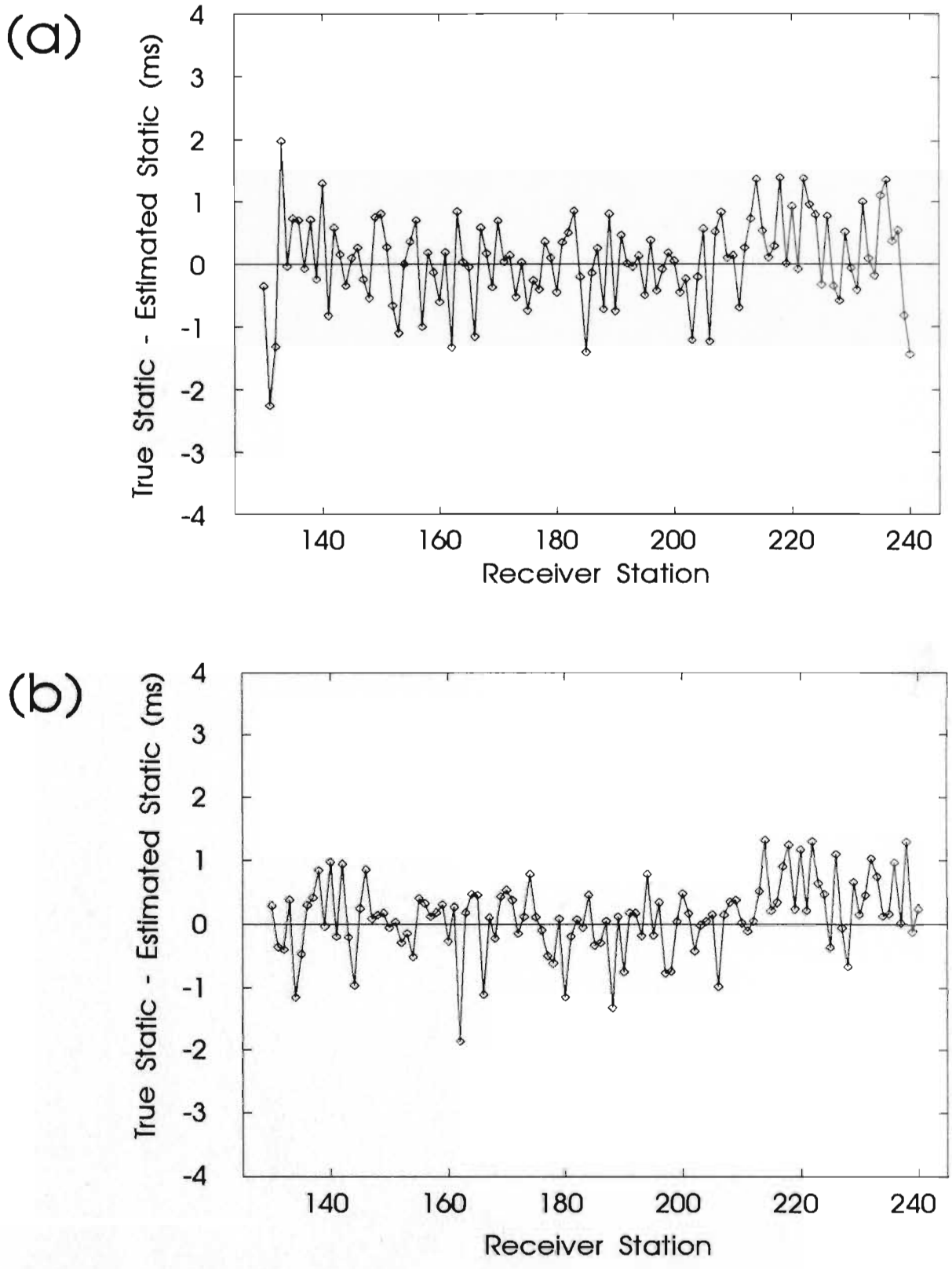

FIG. 9. Graphs showing differences between true static times from the synthetic forward model and the static times estimated using the (a) reciprocal method and (b) GLI technique. These were applied to first arrival times with a Gaussian distribution of timing errors with mean 0.0 ms and s.d. 3.0 ms.

Stacked reflection CMP sections

The procedure that was used in processing the stacked seismic reflection sections is shown in Table 3. Initially the processing was done with no corrections for statics (i.e. without step 1 in Table 3) in order to simulate processing with field statics (elevation corrections) to compare with the sections processed with refraction statics. This section (Fig. 11) shows the deterioration of the reflected signal due to statics effects. This deterioration is mainly due to the systematic change in the range of random overburden velocities from 0.40-0.80 km/s to 0.80-1.00 km/s in the forward model which resulted in misalignment of the NMO-corrected gather across this step in weathering velocity ranges. This effect seems to predominate over the counteracting tendency of the lower range of static variations to produce better aligned reflected signals in this region.

The relatively greater deterioration of the reflected signal for higher frequencies

TABLE 3. (After Wright and Nguuri, 1994) Processing sequence for synthetic shot gathers.

1. Apply refraction static corrections to shot gathers.
2. Sort into CMP gathers.
3. Apply automatic gain control.
(3A. Apply high-pass filter to simulate higher frequency, more complicated signals.)
4. Add more noise to traces.
5. Apply normal moveout corrections computed from correct velocity model.
6. Stack traces and display output.

can also be seen in the stacked section produced using a wavelet of dominant frequency

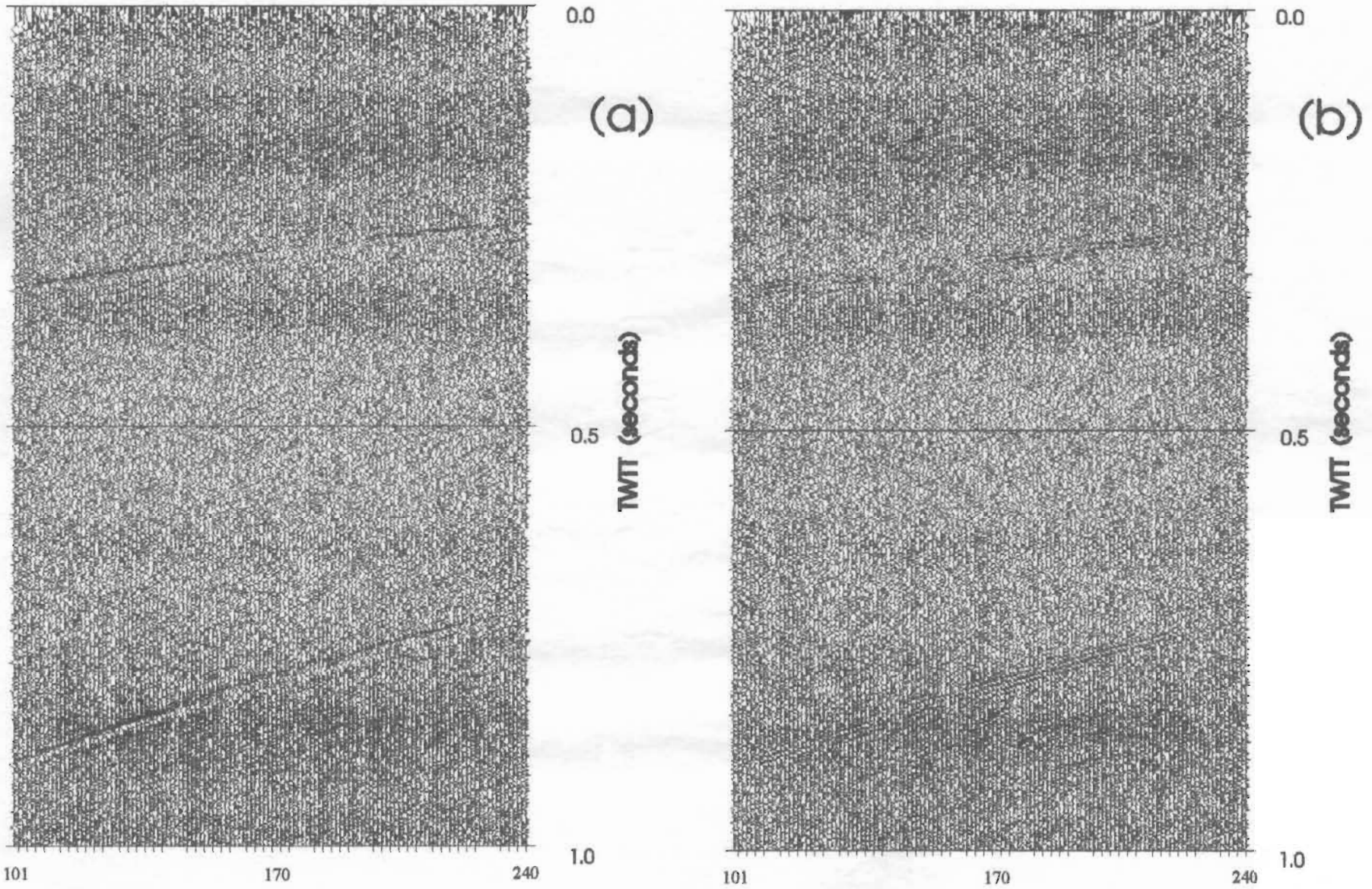

FIG. 11. Results of processing synthetic data for overburden model with no statics corrections: (a) signal with dominant frequency of 80 Hz; (b) signal with dominant frequency of 150 Hz.

of 150 Hz (Fig. 11(b)). This is due to a given static shift causing a greater misalignment between traces for higher frequency than lower frequency signals, and thus a relative decrease in the quality of the section.

Application of refraction static corrections

The next step was to apply the static corrections described in the previous section to the processing sequence. The sections processed with corrections derived from the GLI (Fig. 12) and engineering (Fig. 13) methods applied to data with a Gaussian distribution of errors display a number of important characteristics. There is a significant improvement in these sections compared with the sections processed with no statics. The two techniques appear to have produced results that are essentially identical for the best resolved portion of the line (i.e. stations 130-240) as expected from the magnitudes of the statics shown in the previous section. The only difference in the quality is that the reciprocal method (Fig. 13) appears to have performed better than GLI (Fig. 12) at the beginning of the (i.e. stations 101-130 on the left hand side of the seismic sections) and enhanced a stronger, continuous reflection in this region. This is only an apparent improvement, however, because the poorly resolved statics of the reciprocal method were replaced by a constant value between stations 101 and 130 corresponding to the value at station 131. The rapid variations in the statics derived by GLI in this region due to instability resulted in a relatively greater deterioration of the signal compared with the reciprocal method. The solution in this region is unstable for both techniques due to

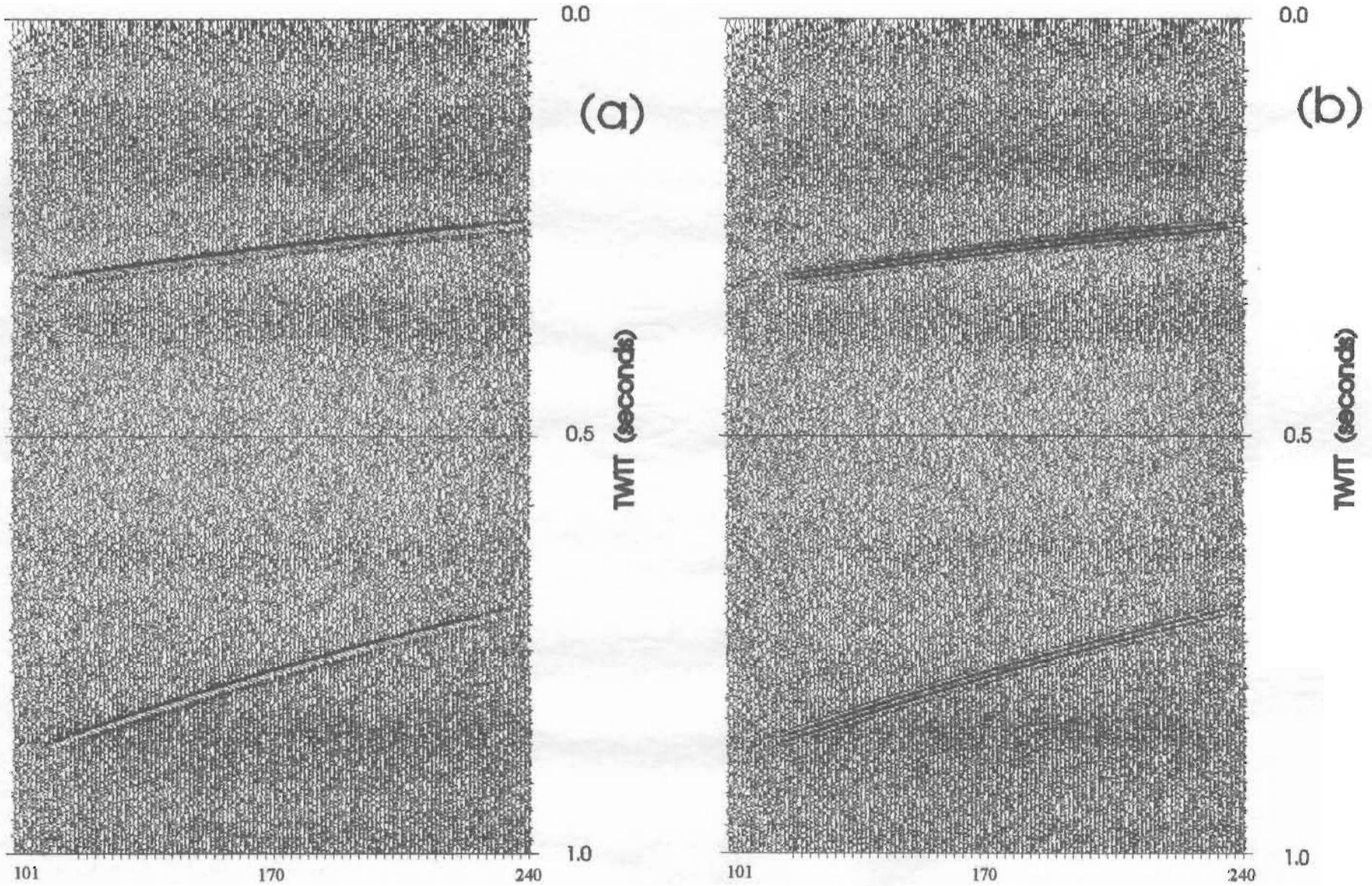

FIG. 12. Results of processing synthetic data with Gaussian time-picking errors of standard deviation 3.0 ms and static corrections computed by the GLI method. (a) signal with dominant frequency of 80 Hz; (b) signal with dominant frequency of 150 Hz.

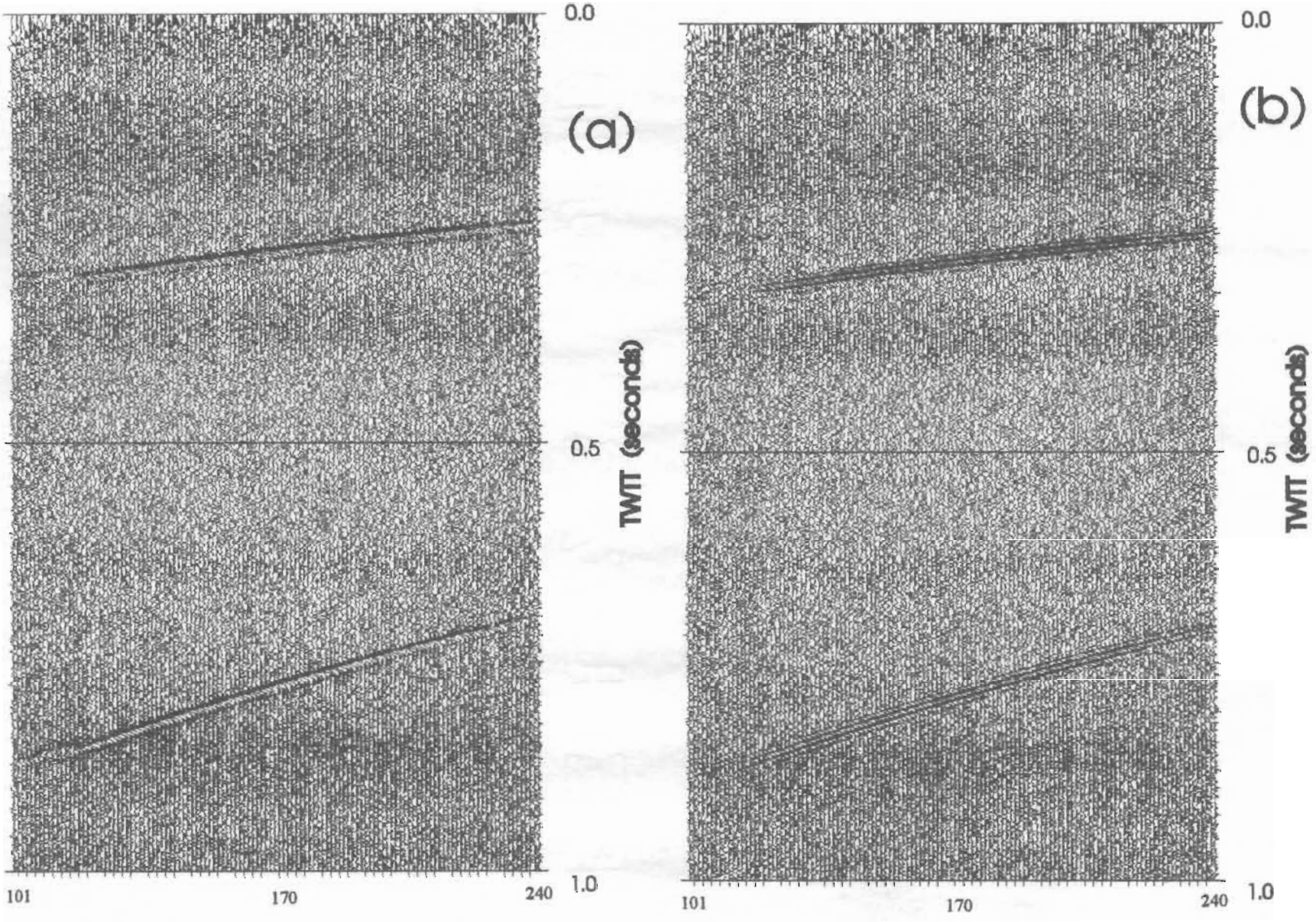

FIG. 14. Results of processing synthetic data with contaminated Gaussian time-picking errors and statics corrections computed by the GLI method. (a) signal with dominant frequency of 80 Hz; (b) signal with dominant frequency of 150 Hz.

poorer resolution of the weathering cells compared with the middle of the line. Superimposed on this effect for both techniques is the decrease in the quality of the reflections at the ends of the line due to a reduction in the CMP fold resulting in a decrease in the effectiveness of the stack.

There is no significant difference between the sections processed with statics derived using GLI on first-break data with the Gaussian distribution of errors added (Fig. 12) versus the data with a contaminated Gaussian distribution of errors added (Fig. 14). The results for the reciprocal method applied to the data with contaminated Gaussian errors, not shown here, are similar (Wright and Nguuri, 1994)).

Bedrock velocity estimation

As described previously, GLI models with different bedrock cell widths of 20, 40, 80 and 160 m were used for the inversion. The model with 20 m wide bedrock cells was used only for the data with "contaminated" Gaussian errors because the larger number of parameters involved in the inversion resulted in a much larger computational time. The results for GLI along the best resolved part of the line are shown in Figs. 15 through 17 for the Gaussian error model and in Figs. 18 through 21 for the contaminated Gaussian model. The error bars indicate the 95 % confidence limits derived with a constant standard deviation estimated from the travel times residuals using the technique outlined in Section 2.1.7. Part (b) in each figure indicates the raypath coverage within the model and thus gives some indication where the bedrock velocity is well determined.

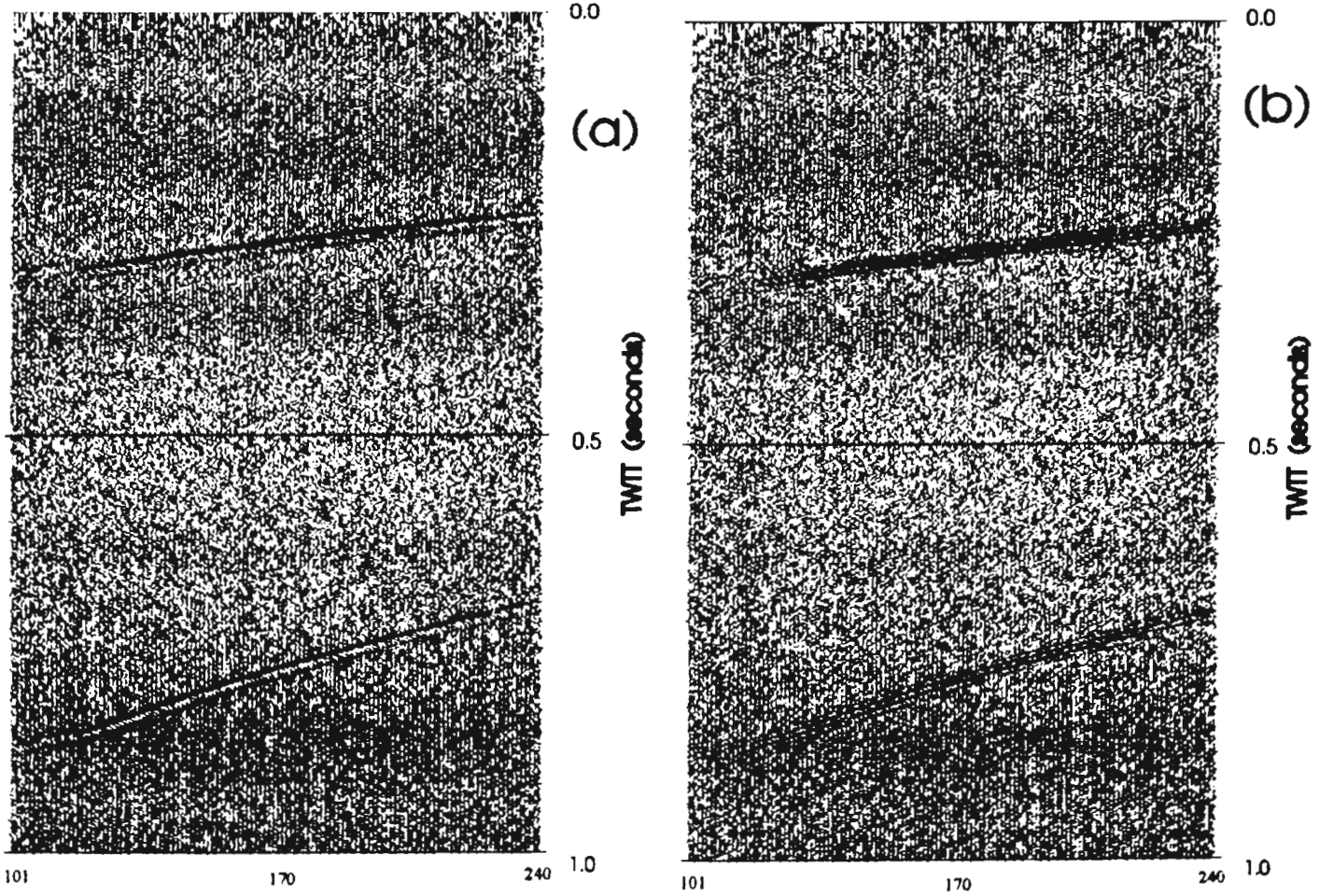

FIG 14. Results of processing synthetic data with contaminated Gaussian time-picking errors and statics corrections computed by the GLI method (a) signal with dominant frequency of 80 Hz, (b) signal with dominant frequency of 150 Hz

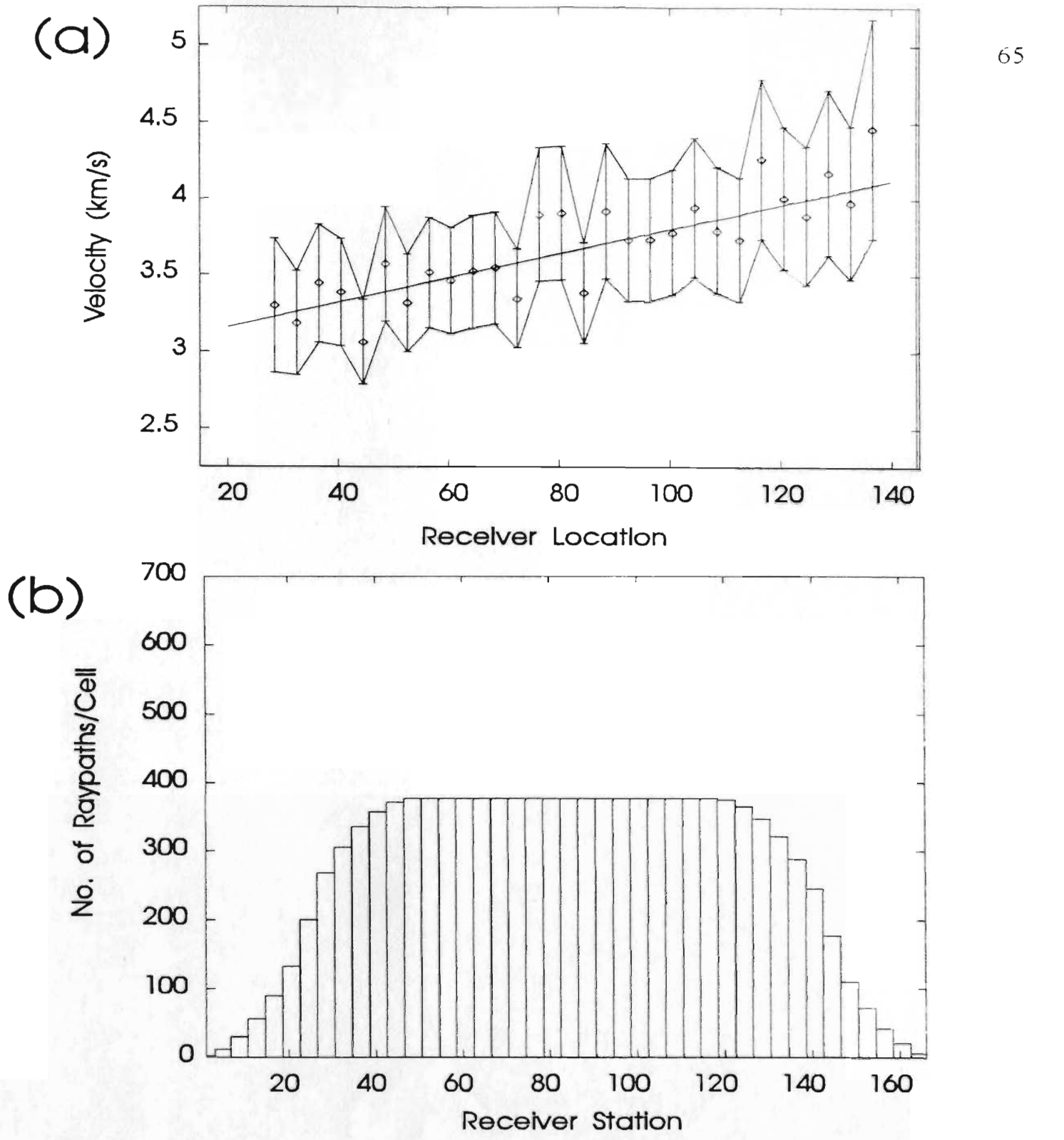

FIG. 15. (a) Bedrock velocity estimated from synthetic seismic data (refracted first arrivals) using an iterative damped least-squares technique and a model with 20 m wide bedrock cells. Random errors with a Gaussian distribution (σ = 3.0 ms) were introduced to the first-break times. 95 % confidence limits on the velocity estimates and the true synthetic model velocity (sloping solid line) are also indicated; (b) Number of refracted raypaths that intersect each bedrock cell in the model. Note that the most poorly sampled cells at the ends of the line have been left off the upper part of the diagram.

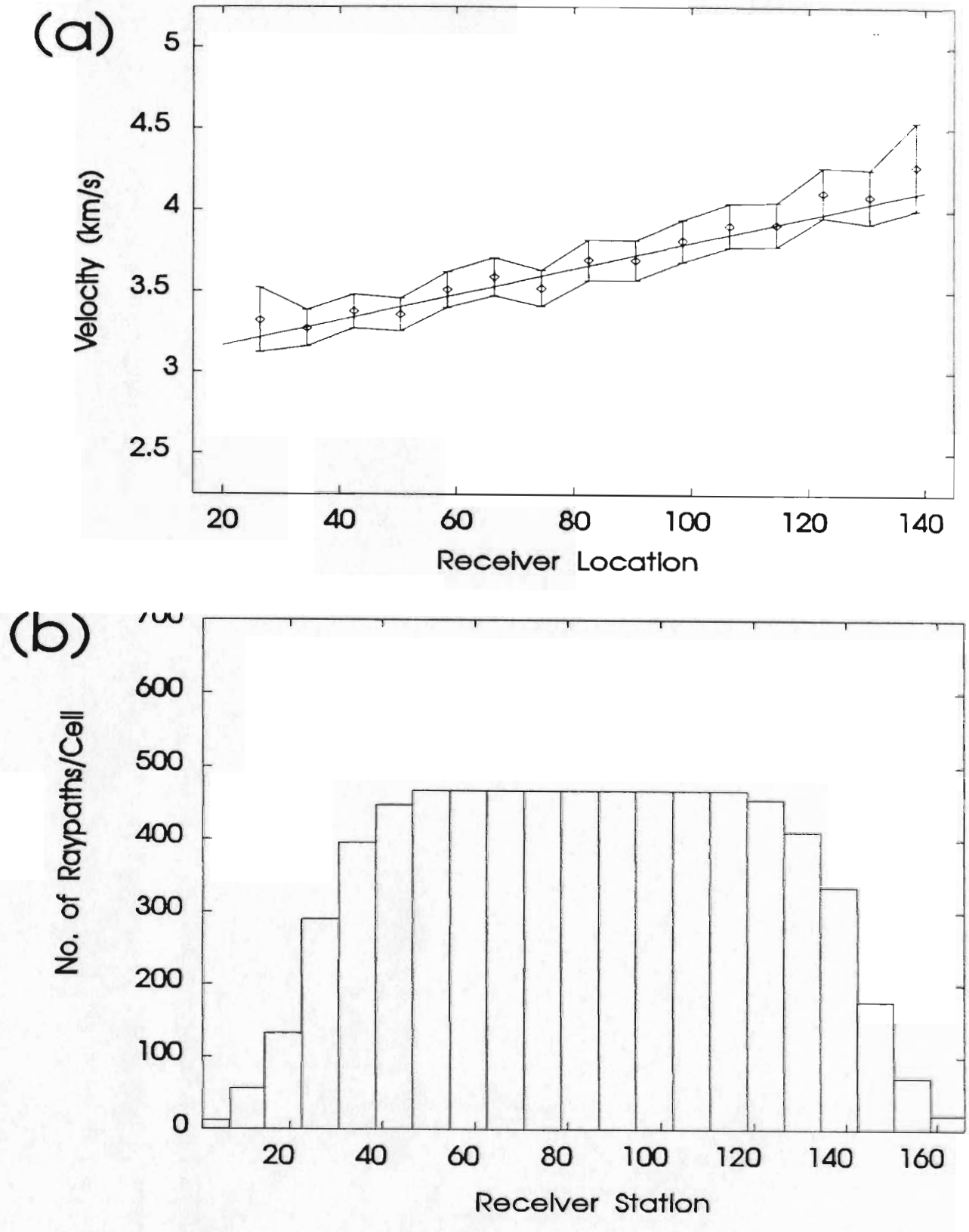

FIG. 16. As with Fig. 15 for a model with 80 m wide bedrock cells.

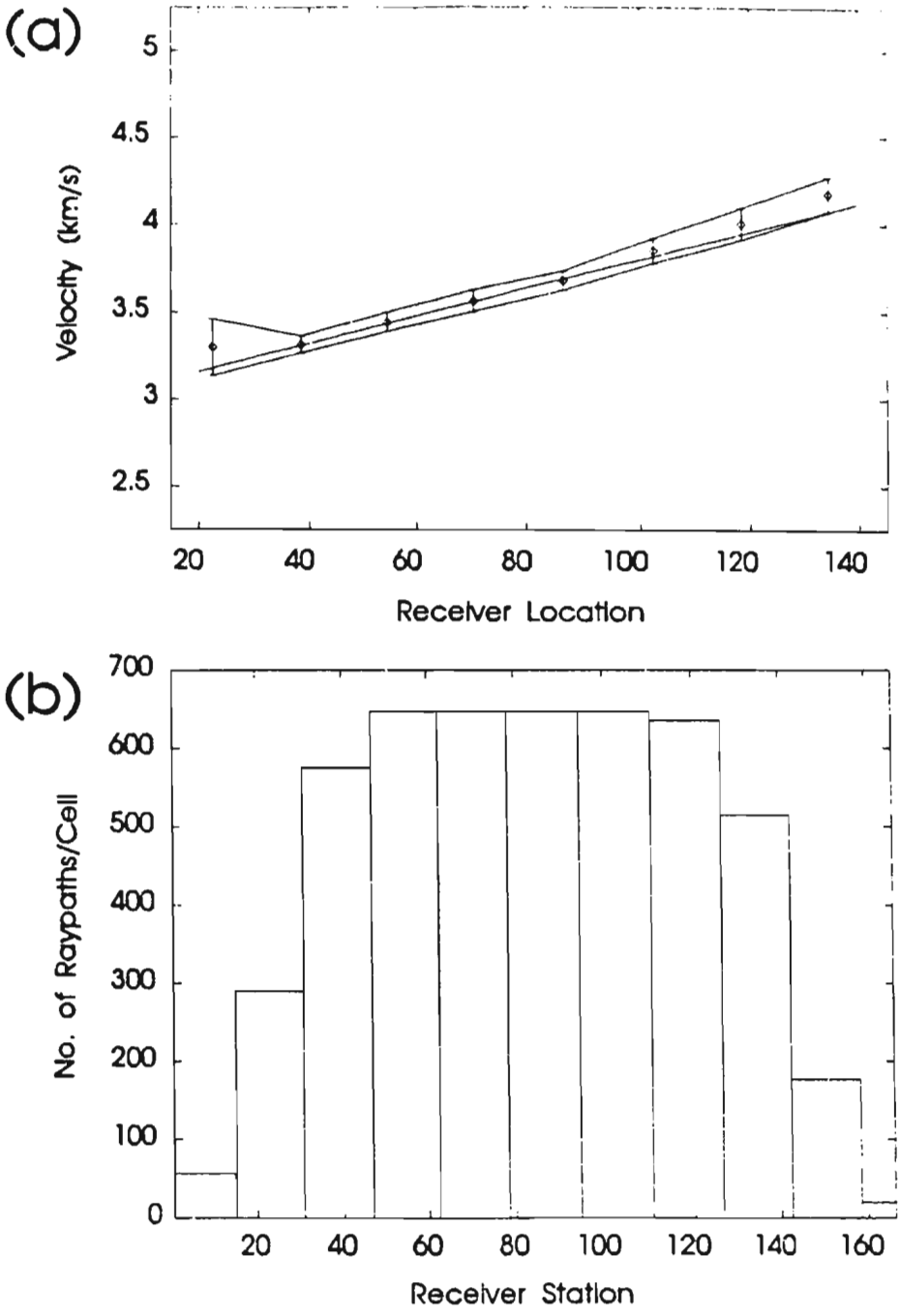

FIG. 17. As with Fig. 15 for a model with 160 m wide bedrock cells.

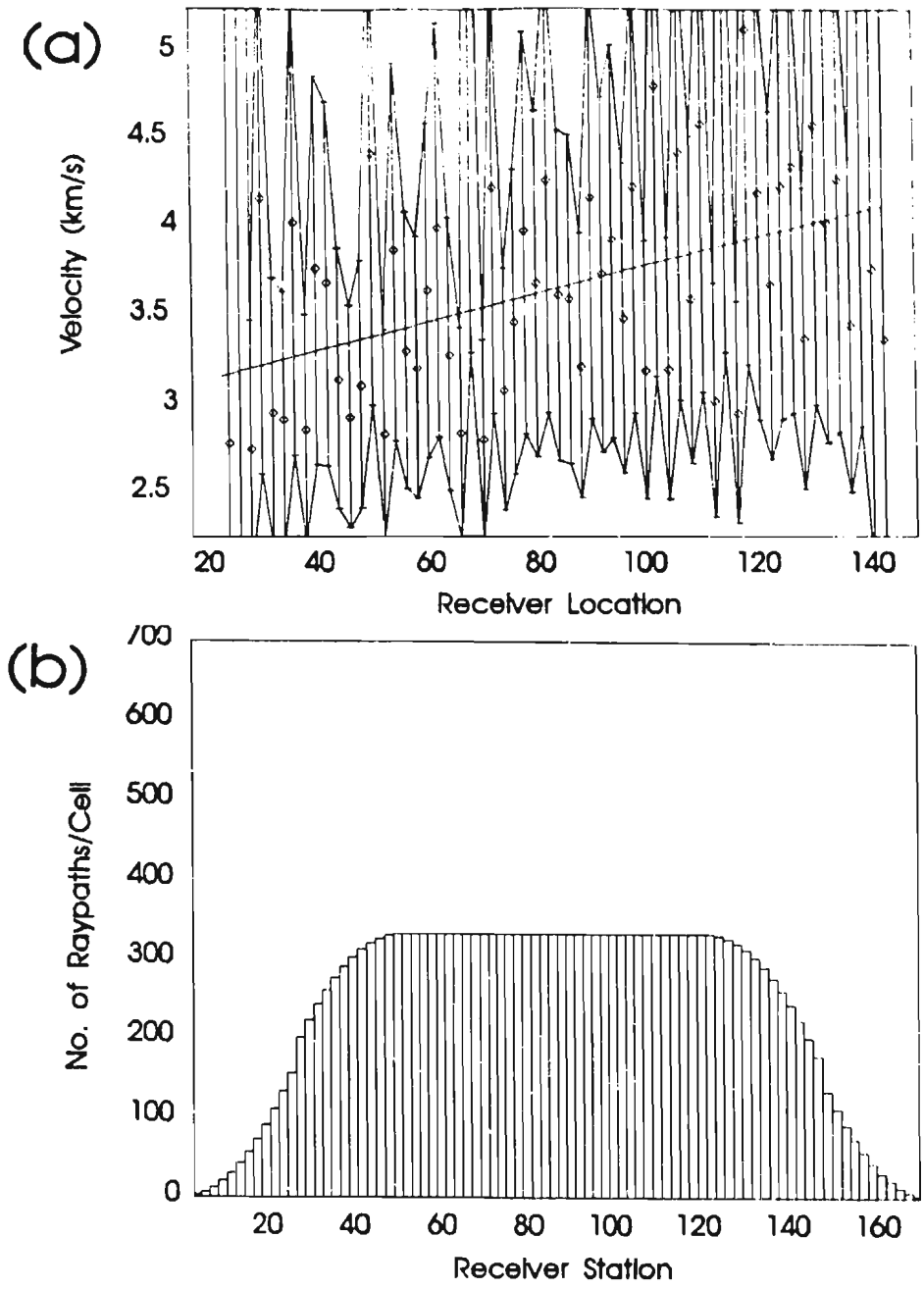

FIG. 18. (a) Bedrock velocity estimated from synthetic seismic data (refracted first arrivals) using an iterative damped least-squares technique and a model with 20 m wide bedrock cells. Random errors with a Gaussian distribution (σ = 3.0 ms) contaminated by occasional large errors (σ = 7.5 ms) were introduced to the first-break times. 95 % confidence limits on the velocity estimates and the true synthetic model velocity (sloping solid line) are also indicated; (b) Number of refracted raypaths that intersect each bedrock cell in the model. Note that the poorest sampled cells at the ends of the line have been left off the upper diagram.

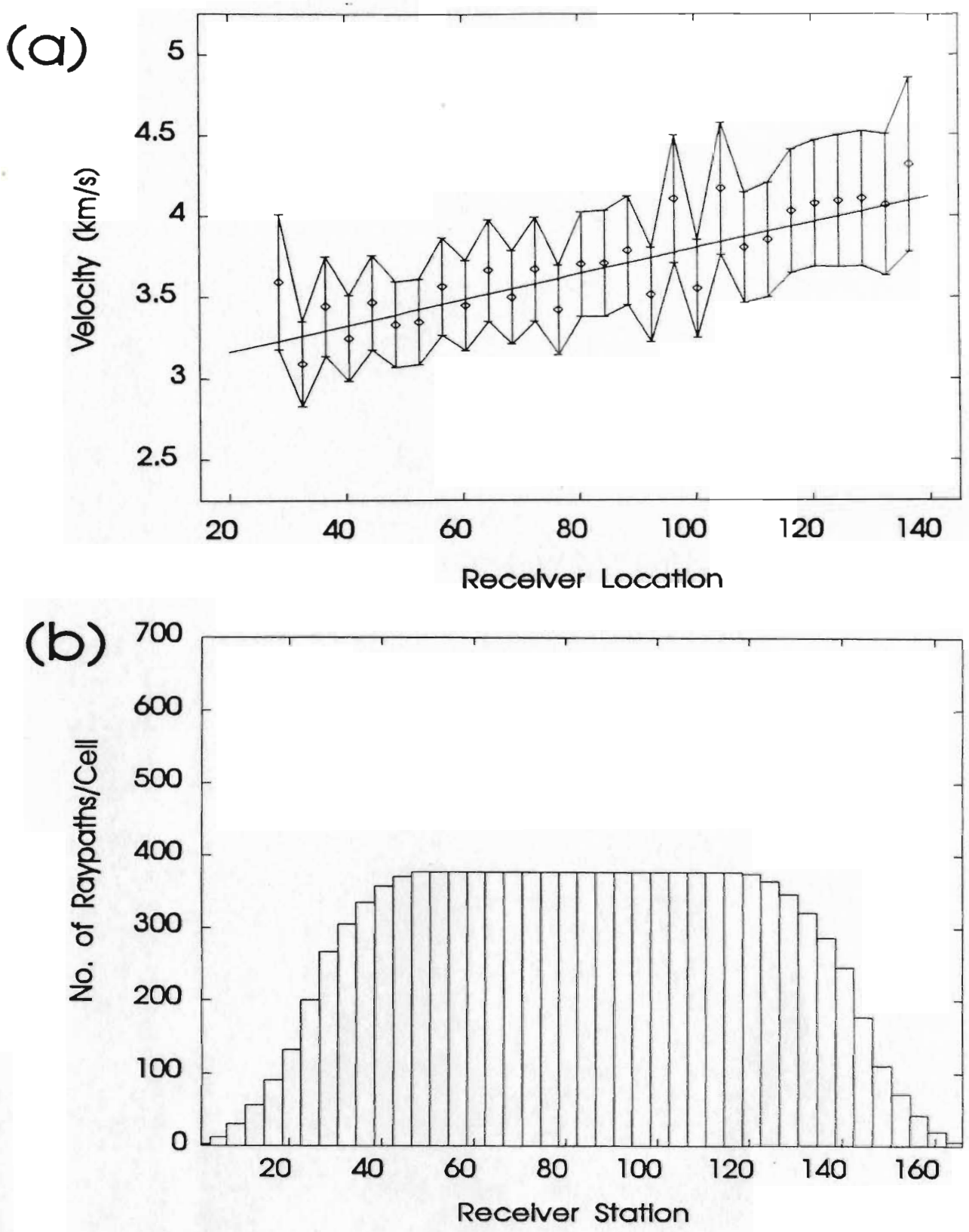

FIG. 19. As with Fig. 18 for a model with 40 m wide bedrock cells.

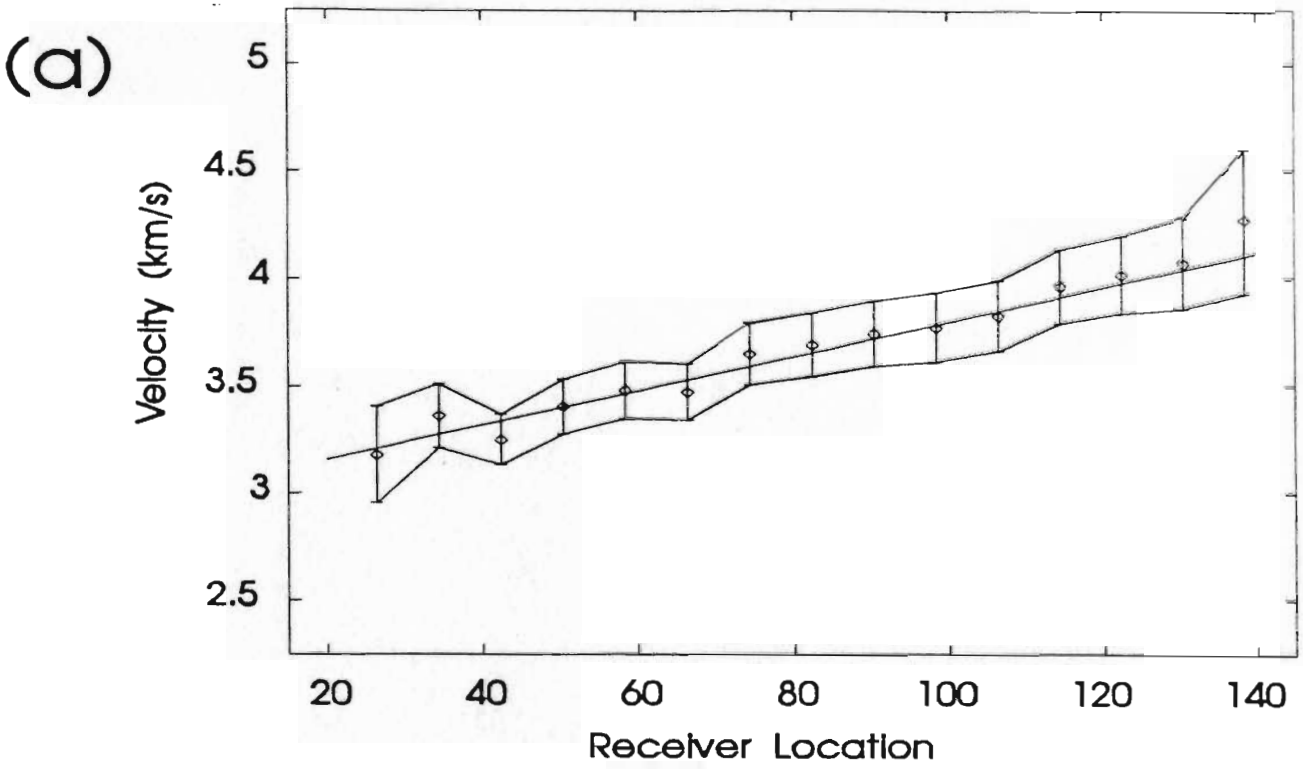

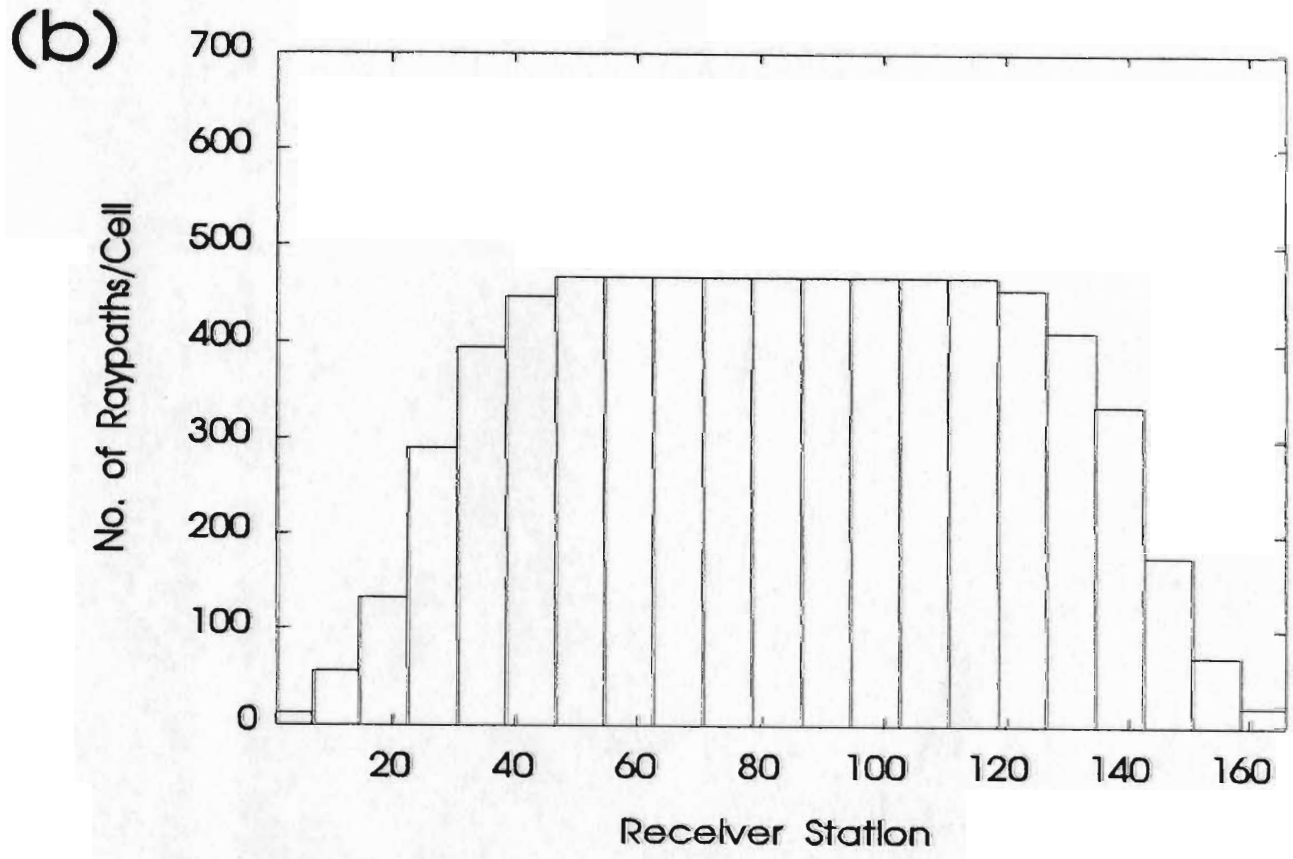

FIG. 20. As with Fig. 18 for a model with 80 m wide bedrock cells.

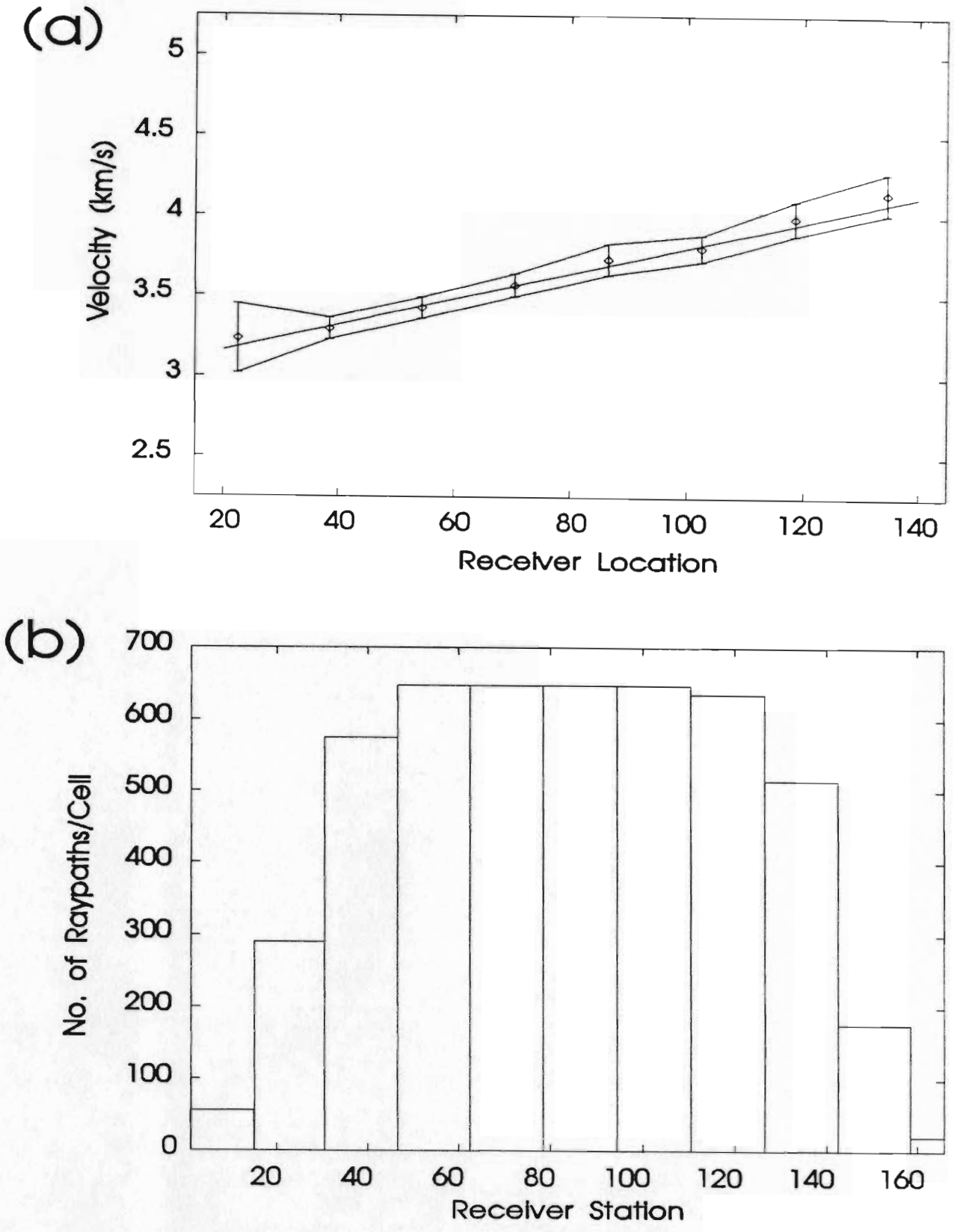

FIG. 21. As with Fig. 18 for a model with 160 m wide bedrock cells.

The main difference between the results of the GLI and engineering techniques (shown in Fig. 22) applied to the data is in the degree to which the bedrock velocities can be resolved. The engineering technique employed summary value smoothing over a window of first-break times to estimate a velocity value at each receiver station. In comparison, the cells for estimating bedrock velocities in the GLI technique essentially averaged the velocities over a range of stations. An attempt to obtain a better resolved solution using damped least squares on a model with 20 m wide bedrock cells (Fig. 18) resulted in a solution with a large amount of scatter around the true velocity and very large error estimates. From this inversion result it was deduced that unconstrained damped least squares would not be able to resolve the short-wavelength trends in velocity to the same degree as the summary value smoothing technique.

By inverting these data using GLI for a number of different cell widths, the trade-off between parameter error and resolution (defined, in this case, by the width of the cell) was demonstrated. For example, the error estimates were reduced from an average of approximately +/- 0.40 km/s for the 40 m wide cells (Fig. 15) to less than +/- 0.10 km/s for the 160 m cells (Fig. 17) or roughly a 75 % reduction in the errors. The scatter of the values about the true velocity also decreases with increasing cell width. These two effects are due to the increasing path length and increasing number of raypaths sampling each cell (compare Figs. 18 and 21).

There is little difference between the solutions for the GLI technique applied to data assuming different error models (i.e. Gaussian and contaminated Gaussian

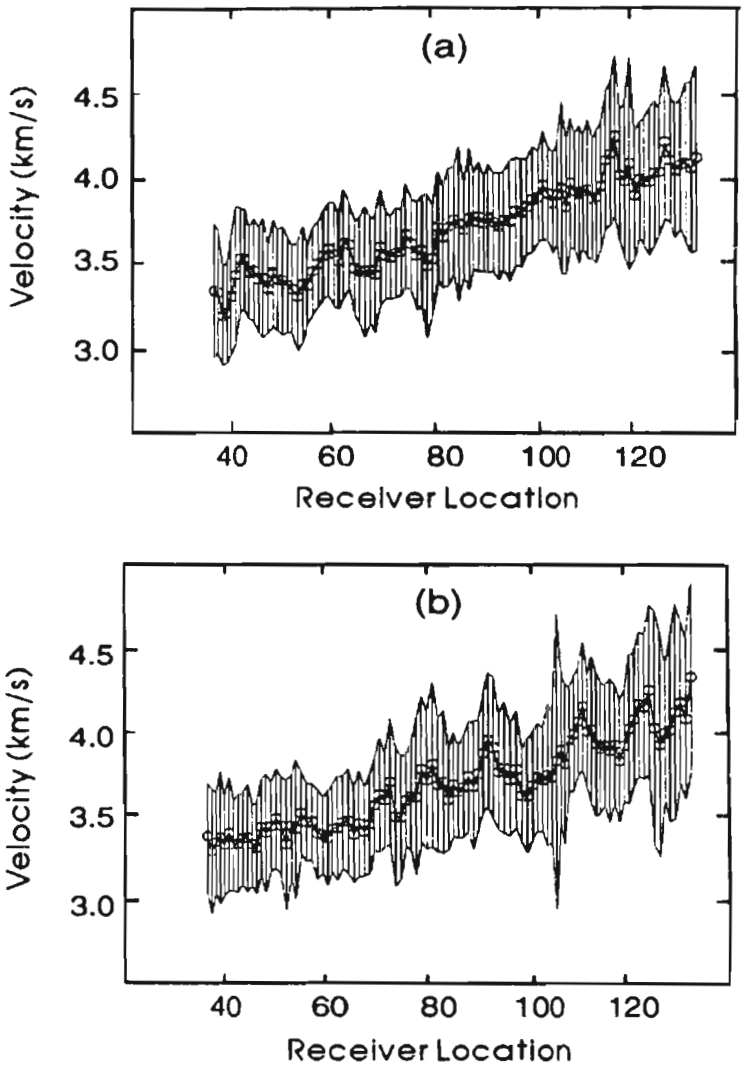

FIG. 22. (After Wright and Nguuri, 1994) Bedrock velocity estimates along the synthetic data profile estimated using summary value smoothing after subtraction of reciprocal time corrections: (a) Gaussian timing errors; (b) contaminated Gaussian errors.

distribution of errors) maintaining a constant cell width (i.e. compare Figs. 15 and 19, Figs. 16 and 20, Figs. 17 and 21) but there are differences for the engineering technique solution (Fig. 22) depending on the error model used. The latter solution appears to have velocities with slightly more scatter about the true solution and increased errors for the case of contaminated Gaussian distribution of errors on the first-breaks (Fig. 22 (a))compared with the Gaussian distributed error model. The most likely reason why this was not observed for the GLI solutions was that the averaging over 4 to 16 stations reduces the scatter and errors on the cell velocities to a greater degree than the engineering technique.

The overall conclusion from this modelling for determining bedrock velocities was that unconstrained, damped least squares under conditions of noise and fold similar to these data would result in a lower resolution of bedrock velocities than the engineering method. Therefore, some constraint would have to be used in order to obtain the same degree of resolution of bedrock velocities for reliable geological interpretation.

Dependence of solutions on refractor dip

An important difference between the two models is the assumption each method makes about the dip of the weathering layer/bedrock interface in the subsurface. The engineering technique assumes a near-horizontal refracting interface for the calculation of statics, but combines the apparent slownesses calculated in the forward and reverse directions in a formula which takes into account the local bedrock dip (Wright, 1994b).

The GLI technique as used here, however, assumes a horizontal interface for both the calculation of statics and bedrock velocities. Because of the differences in the assumption of dip it was thought necessary to try to understand the effect that large dips may have on the final solutions obtained by each method. To this end, some synthetic first-break data from a small model with an apparent interface dip in the plane of the profile between 0 and 20 degrees were created. The raytracing was done assuming a headwave travelling along the interface. The results indicated that the engineering technique may have some advantages over the GLI technique in regions where there is a large dip in the bedrock (i.e. greater than 15 degrees).

The field data analyzed in this thesis were collected in regions where the dip of the bedrock/weathering interface is probably less than 10 degrees in most instances. For example, analysis of the Gullbridge data using the engineering technique indicated that the maximum dip was around 8 degrees (Wright, 1994 b). In these cases the assumption of a horizontal interface for the GLI technique should not produce significantly different results than the engineering technique.

3.4 Summary of Results and Conclusions for the Synthetic Data

The synthetic modelling provided useful guidelines for analysing field data, and allowed some aspects of the methodology to be tested. The main results and conclusions were:

i) The GLI and engineering methods produced nearly identical results for the determination of static corrections, even for the case of first-break data with errors added that had a contaminated Gaussian distribution. This was somewhat unexpected as, theoretically, the reciprocal method might have been expected to perform better on these data with large outliers. The reason for this may be because the GLI model assumed the equivalence of shot and receiver statics which increased the redundancy at some stations. The seismic sections demonstrated the improvement in applying the static corrections derived using both methods, especially for the case of a higher frequency wavelet.

ii) The static corrections appeared to be fairly insensitive to the width of the bedrock cell chosen for the best resolved portion of the line (i.e. away from the ends).

iii) For the GLI solutions there was an increase in the errors and scatter about the true solution for the velocities with decreasing cell width. This was best demonstrated from attempting to invert a model with a cell width of 20 m, where the errors were much larger than those observed by the engineering technique.

iv) The GLI technique appeared to give poor results for forward models that had an interface with a dip of 15 degrees or more.

The main conclusion of this work was that future work on field data would

require some other constraint than damping to be applied for GLI in order to reduce the instability of the solutions for models which have many bedrock cells. This was deemed necessary in order to compare the GLI technique with the engineering technique with respect to the resolution of bedrock velocities. It was from this work on the synthetic data that the use of Occam's method for deriving more refined bedrock velocity solutions evolved for the analyses of the field data.

CHAPTER 4

4.0 FIELD DATA RESULTS

Introduction

High resolution seismic data were collected for base metal mining purposes in two regions containing rocks of mainly volcanic origin: Buchans (in 1991) and Gullbridge (in 1992) in central Newfoundland, Canada. Statics and shallow bedrock velocities were calculated with the GLI and engineering techniques using first-breaks picked from these data sets. In this chapter, a comparison of the results of these analysis is made.

In Section 4.1, the geology of the two areas is briefly described and Section 4.2 summarizes the field procedures for the seismic surveys at Buchans and Gullbridge. Section 4.3 compares the results for the Buchans data (explosive sources, 48-channel) including the bedrock velocity profiles and the results of processing the seismic section with statics derived from the two techniques. Section 4.4 is also concerned with data collected at Buchans, but using a Vibroseis™ technique (120-channel) and no re-processing of the seismic section with statics derived from the GLI. Section 4.5 makes a similar comparison for data recorded at Gullbridge using explosive sources (120-channel), again with no re-processing of the seismic sections with GLI-derived statics due to the high noise content of these data. Finally, Section 4.6 summarizes the results and concludes by making an overall comparison of the techniques and their effectiveness in deriving statics and bedrock velocities from these data.

4.1 Geology of the Buchans and Gullbridge Regions

Two mining regions in north central Newfoundland (Buchans and Gullbridge) have been sites for seismic investigations to assist exploration for new base metal deposits (Fig. 23). The Buchans area has produced 17.5 million tons of concentrate from four main ore bodies between 1928 and 1979 (Neary, 1981) while the smaller Gullbridge copper deposit produced about 3 million tons of concentrate between 1967 and 1972 (Upadhyay and Smitheringale, 1972).

The Buchans and Gullbridge mines lie in the Notre Dame Subzone of the Dunnage tectonic-stratigraphic zone (Williams and Piasecki, 1990). Volcanogenic sulphides at Buchans and Gullbridge are hosted within the Buchans-Roberts Arm volcanic belt of early Ordovician age. The Buchans and Roberts Arm Groups are both marine volcanic and volcaniclastic successions associated with an island arc.

4.2 Description of the Seismic Surveys

Buchans

In June 1991, a high resolution seismic reflection profile was recorded in the vicinity of the Buchans mine site in central Newfoundland (Fig. 24). The 24-fold line using explosive sources was recorded by the Memorial University of Newfoundland Centre for Earth Resources Research (CERR) coincident with the Lithoprobe line 14 recorded using a Vibroseis source and 60-fold geometry. The purpose of the CERR

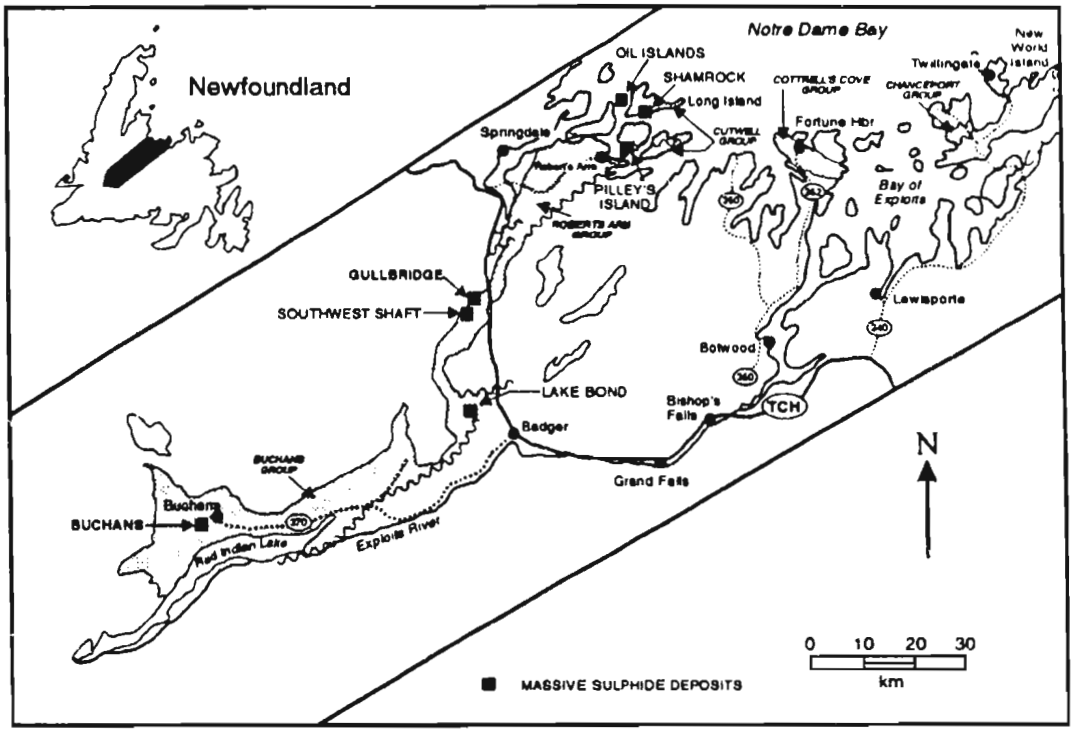

FIG. 23. Location of Gulbridge and Buchans mines in central Newfoundland.

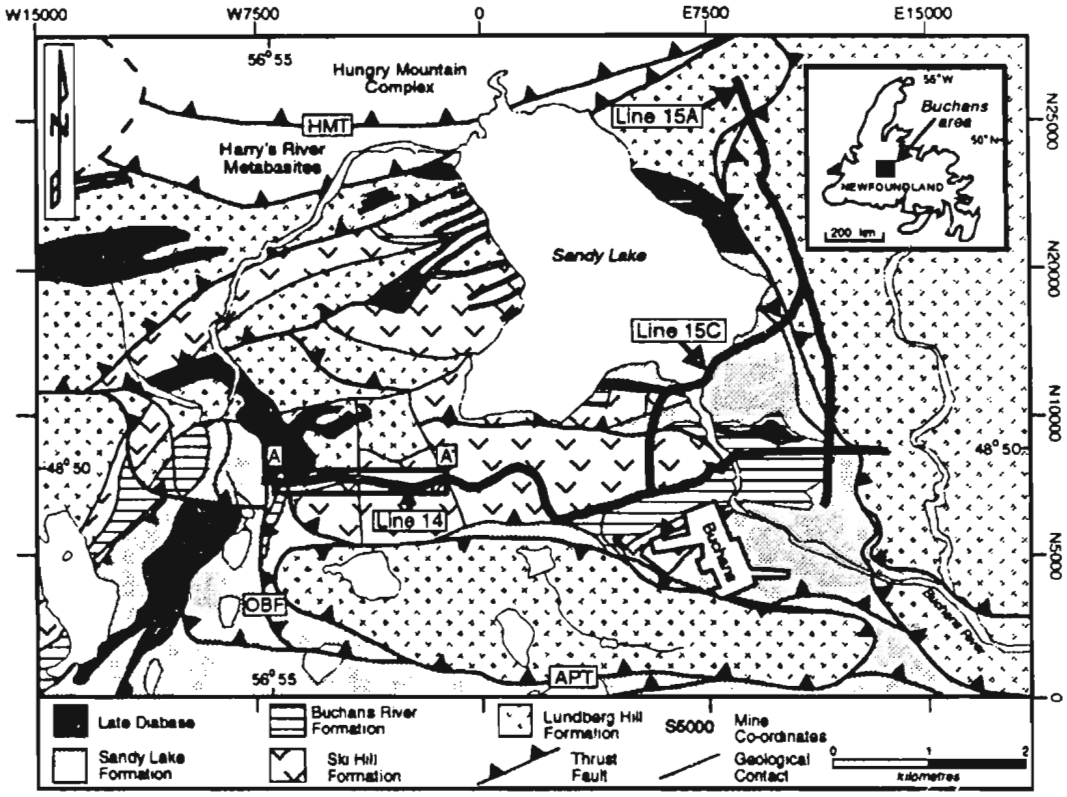

FIG. 24. Location and generalised geology of the Buchans area adapted from Thurlow and others (1992) with the grid of the Lithoprobe high resolution seismic reflection lines shown. The coincident CERR line is marked AA'.

survey was to compare the resolution of shallow structures of economic importance with that obtained using Vibroseis. It was found that the application of refraction statics was one of the key steps in the processing of these seismic data to clearly resolve fault zone reflectivity (Spencer et al., 1993; Wright et al. 1994).

The principal targets for the high resolution surveys were the Old Buchans Fault at a relatively shallow depth (< 500 m) and the deeper Powerline Fault (approximately 1000 m depth). Both of these faults were imaged on the CERR explosives survey as well as on the Lithoprobe East Vibroseis seismic survey. The CERR seismic survey line lies roughly along the strike of these structures so the apparent dips are much less than true.

The field parameters used by CERR and Lithoprobe along Line 14 are shown in Table 4 (Wright, 1994a; Wright et al., 1994).

Gullbridge

In 1992 three 30-fold high resolution seismic reflection lines were recorded in the vicinity of the Gullbridge copper mine in north central Newfoundland (Fig. 25). The main objectives of the seismic work were to map the faults of the Gullbridge Imbricate System (Pope and Calon, 1990) down to about 1 km depth to obtain a better understanding of the structural control on mineralization, to correlate any observed reflections with lithological changes or shear zones observed in borehole cores, and finally to use variations in seismic velocity in shallow bedrock to map changes in lithology and faults in areas of poor surface exposure (Wright et al., 1993; Wright,

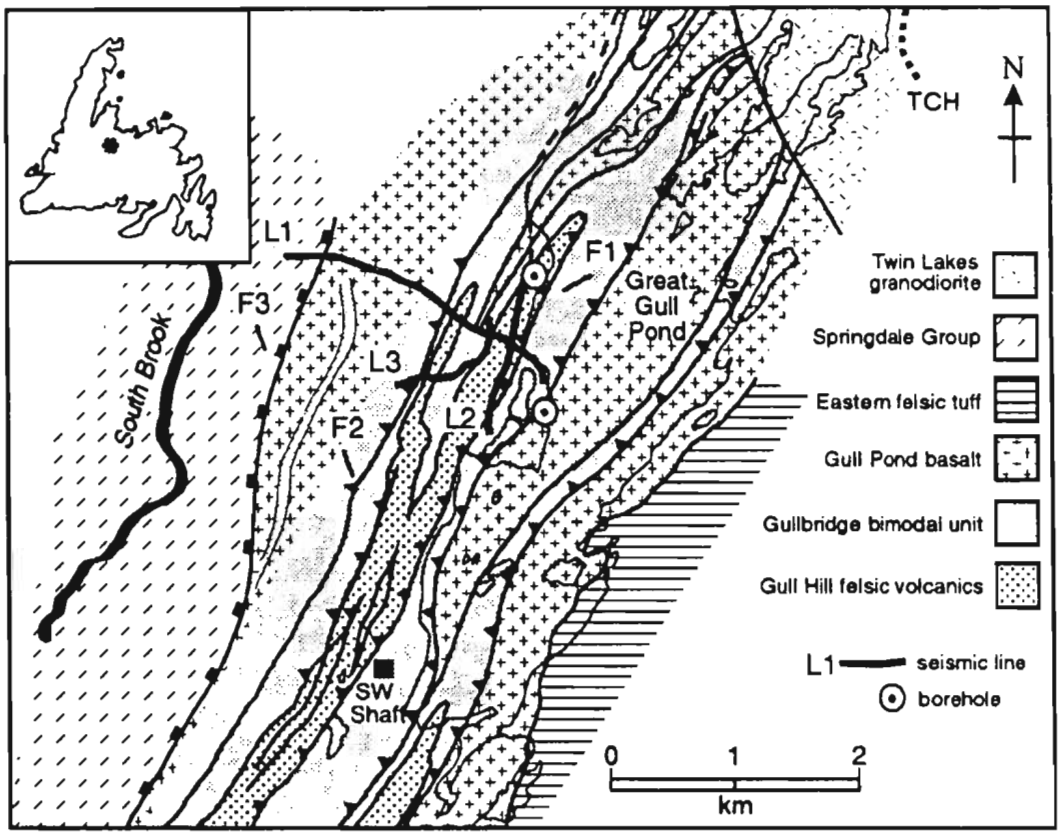

FIG. 25. Geological map of Gullbridge (from Pope and Calon, 1990) with seismic reflection lines superimposed. F1, F2 and F3 mark the faults identified in the seismic work.

1994a).

The field parameters used for the seismic surveys are shown in Table 4.

TABLE 4. Recording parameters of seismic surveys at Buchans and Gullbridge (After Wright, 1994 a).

Survey	Buchans Vibroseis	Buchans Explosives	Gullbridge Explosives
Recording instruments	240 channel twin DFS V Calder	48 channel DFS V	120 channel DFS V
Geophone spacing	10 m	9.8 m	7.5 m
Recording geometry	Asymmetric split spread: 78-shot-162.	Off-end: one station offset	Symmetric split spread
Geophones at each takeout	Arrays of twelve 14 Hz geophones spread over 1 m^2	Single 14 Hz geophones	Single 40 Hz geophones
Source interval	20 m	9.8 m	15 m
Recording fold	60	24	30
Source type	Vibroseis: two vibrators, nose-to-tail	Primaflex: about 40 g of explosive per shot	Primaflex: about 100 g of explosive per shot
Sample rate	2 ms	1 ms	2 ms
Record length	6 s	1 s	2 s

4.3 Buchans Explosive Data

4.3.1 Procedures

GLI models and procedure

The overall procedure was similar to that outlined in the methodology section

(Section 2.0). The input data were the first-break times from source-receiver offsets greater than 30 m, and were assumed to be raypaths that penetrated bedrock below weathering. Initially, these first-break times were inverted using a damped least-squares technique and a two-layer model to obtain the static corrections. Subsequently, Occam's method was used to invert the corrected first-break times from which the weathering times (derived from the previous damped least-squares procedure) had been subtracted. A bedrock model with relatively smaller cell widths compared with the initial two-layer model was used. Crooked line geometry was accounted for in both cases.

The initial two-layer model was set up as follows:

WEATHERING LAYER	
NO. OF CELLS	ONE PER RECEIVER STATION
INITIAL VELOCITY	0.5 km/s
THICKNESS (constant)	2.0 m
BEDROCK LAYER	
CELL WIDTH	120 m (average width)
INITIAL VELOCITY	5.2 km/s

Some explanation of the reasons for choosing these particular initial model parameters for the Buchans explosives data is necessary. The (constant) thickness of the weathering layer was chosen so that the raypaths would remain in these cells and would thereby simplify the raytracing procedure and increase the likelihood of convergence for the iterative procedure. The model also assumed equivalent shot and receiver statics because previous work using the reciprocal method found little differences in the processed seismic sections that used separate versus equivalent shot and receiver static assumptions (Wright et al., 1994). It also assumed that the bedrock had no increasing velocity with depth (i.e. headwave approach used for raytracing) consistent with numerical tests done by Wright (1994 a).

In calculating the static corrections, the weathering times were combined with the elevation data and, based on an average value estimated from the shot times to nearest geophone (Wright et al., 1994), a weathering velocity of 1.6 km/s was used. The datum corrected to was 290 m A.S.L. The fine-tuning of these statics was accomplished with a bedrock model derived using Occam's method and a smoothing parameter of $\mu = 100$.

The damped least-squares procedure used the following parameters which were chosen by trial and error based on the combination that resulted in the most rapid convergence. A damping parameter $\beta = 150$ and a reduction factor of 0.5 per iteration were used. The procedure was terminated after 10 iterations or when the magnitude of the slowness perturbations was less than 0.001 s/km; a solution was assumed to have converged when either of these conditions was met and when the standard deviation for

the residuals was at or below 2 ms.

Bedrock velocity analysis using Occam's method

Occam's method was applied to the first-break times corrected by subtraction of weathering times, thus simulating the placement of shots and receivers on bedrock. This refined model assumed an initial bedrock velocity of 5.2 km/s but the cell width was smaller than the damped least-squares model, assuming one receiver station per bedrock cell i.e. the cell boundaries were located halfway between each pair of receiver stations.

Three different smoothing parameters were tested for the procedure (μ = 10, 100, 1000) in order to see how the solution was affected by applying different amounts of smoothing. Each solution was derived using a constant smoothing parameter.

Engineering procedure and assumptions

The following is a summary of the details of the procedure used by Wright et al. (1994) in their analysis of the data.

The apparent bedrock velocities at each station were computed by summary value smoothing of the first-break times for each shot gather using window lengths of 120-140 m with a weighted mean calculated for all shots contributing values at a particular shot location. These were used to estimate the small time corrections required in the reciprocal method to accommodate deviations from straight line geometry. Equivalent

shot and receiver statics were assumed and a single average value of 1.6 km/s estimated from shot times to the nearest geophones was used for calculating statics (as for the GLI technique).

Estimating bedrock velocities using summary value smoothing

To estimate lateral variations in bedrock velocities, the shot and receiver weathering times (estimated by the reciprocal method) were subtracted, a distance window of 100-120 m was used in the smoothing, and a weighted mean was taken to estimate a velocity value at each station. Numerical tests indicated no increase in seismic velocity with depth, and the vertical velocity gradient was therefore neglected in the procedure. Fixed window length smoothing was used to avoid making the numerical procedures too cumbersome.

4.3.2 Comparison of Results for Buchans Explosives Data

Static corrections

In general, the statics vary along the line from around 17 ms in the west to 1 ms in the east with a gradual decrease in magnitude from west to east for the solutions derived using GLI and the engineering technique (Fig. 26). The main difference between the two solutions is that the GLI-derived statics are consistently smaller in magnitude, on average approximately 0.5 ms less than the engineering statics (Fig. 27). The larger

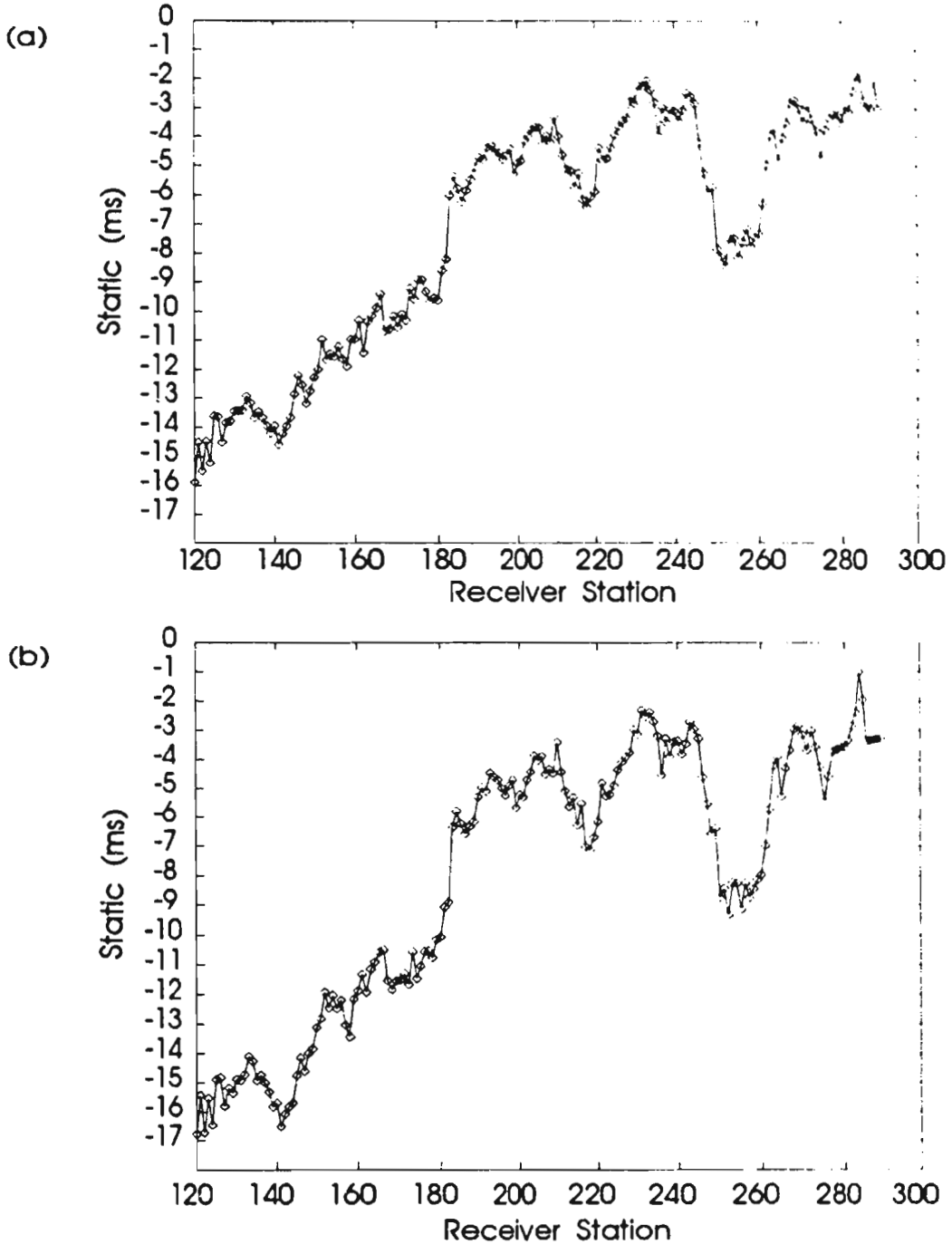

FIG. 26. Statics corrections derived from the (a) GLI and (b) reciprocal methods for Buchans line 14 which were used to correct stacked CDP section to a datum of 290 m A.S.L. Shot and receiver statics were assumed equivalent. These refraction statics include contributions from lateral changes in both weathering and bedrock seismic velocities, as well as changes in station elevation along the line.

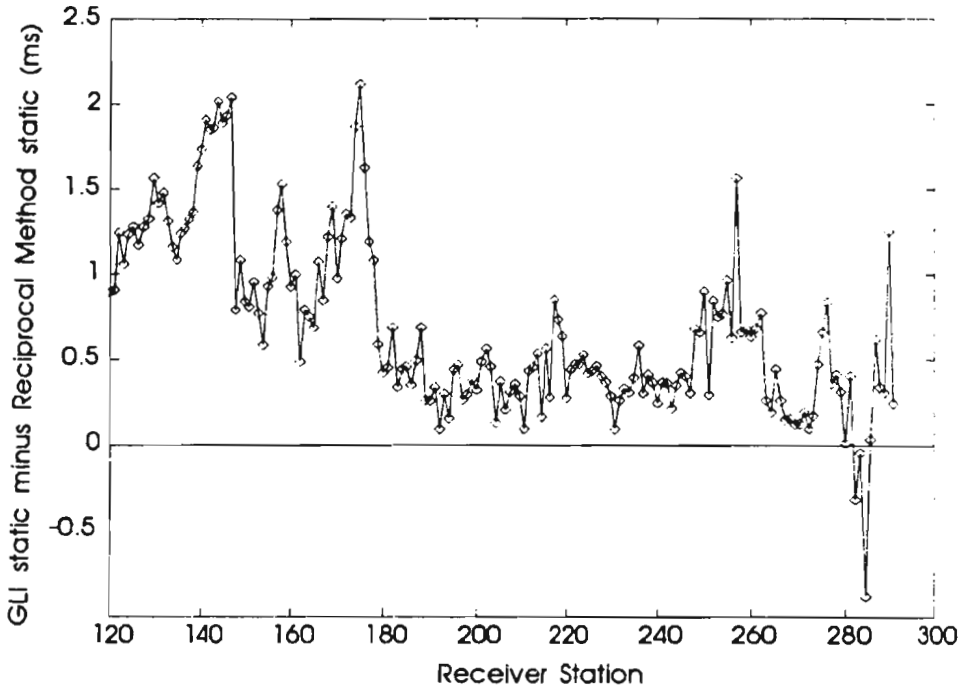

FIG. 27. Difference in statics corrections derived from GLI and reciprocal methods (i.e. difference between solutions shown in Figs. 27 (a) and 27 (b)).

differences at the beginning of the line are due to differences in the bedrock velocities; the resolution of the velocities is poorer for the GLI model along this part of the line. The lower values for statics from the GLI technique are probably due to some of the static time being absorbed by the bedrock cells in the model. This is caused by the modelled raypaths in the bedrock cells being longer than the true raypaths in the earth due to the raypaths in the weathering layer model being inclined at a steeper angle than the true raypaths.

Bedrock velocities

Occam's inversion results for $\mu = 10$, $\mu = 100$, and $\mu = 1000$ are shown in Fig. 28 where the error bars correspond to the 95 % confidence limits on the damped least-squares solution and the standard deviation estimated using the midpoint method (see Chapter 2.0). The relatively larger error bars around receiver station 230 indicate that some of the first-breaks contain large, systematic errors in this region. The main feature of these solutions is that, as expected, the range and frequency of velocity variations decreases with increasing smoothing parameter magnitude (e.g. from 4.5-6.5 km/s for $\mu = 10$ (Fig. 28 (a)) to 5-6 km/s for $\mu = 1000$ (Fig. 28 (c)).

The velocity profile derived by the engineering technique is shown in Fig. 29 (After Wright et al., 1994). By plotting the differences between the solutions derived using Occam's method and the engineering technique (Fig. 30), it can be concluded that using GLI with smoothing parameter $\mu = 100$ results in a solution that, of the three

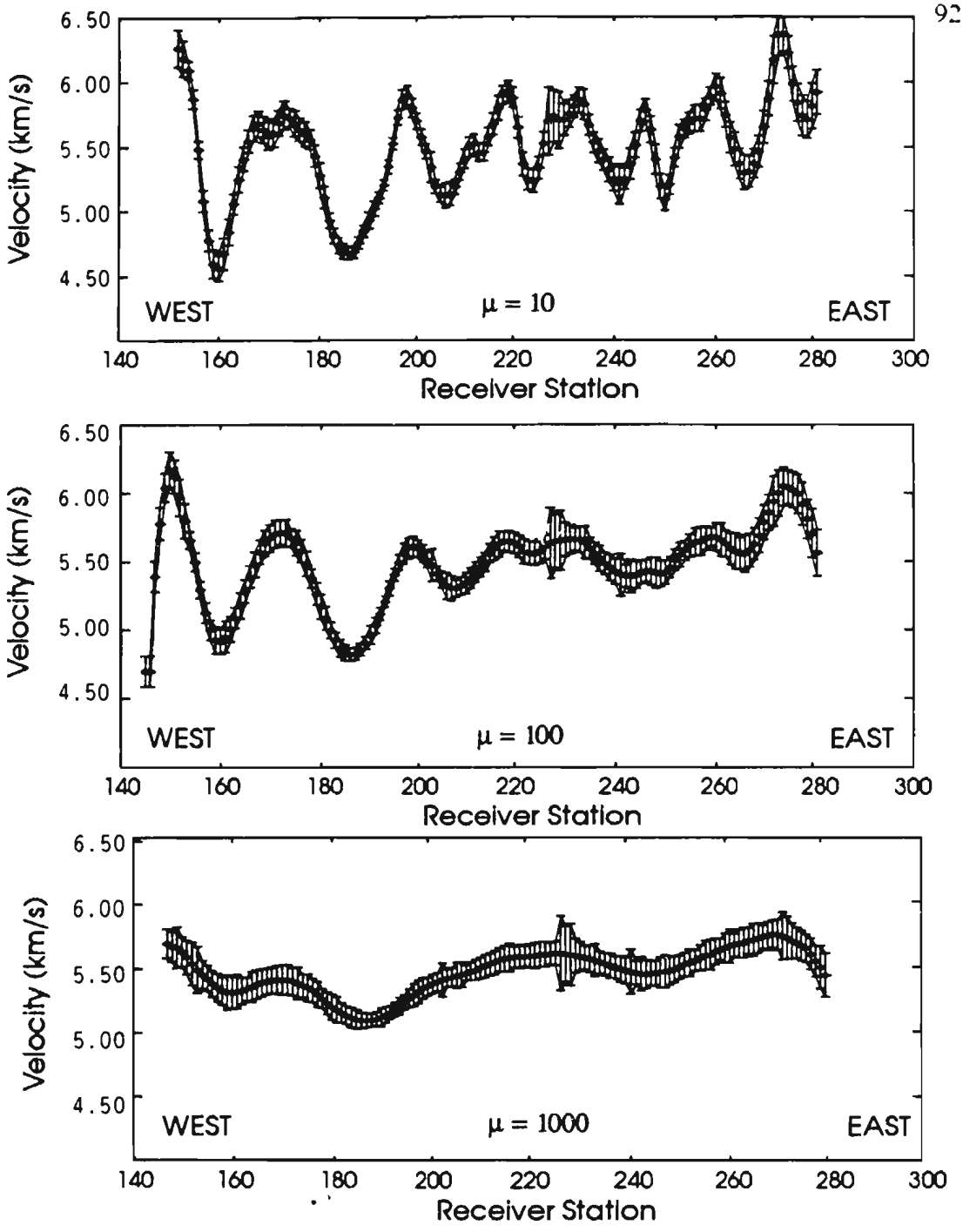

FIG. 28. Estimate of seismic velocity in bedrock along Buchans line 14 using Occam's technique and a smoothing parameter of: (a) 10; (b) 100; (c) 1000. The error bars were calculated for each velocity value using the 95 % confidence limits from the damped least-squares solution with a standard deviation on the residuals estimated using the midpoint method.

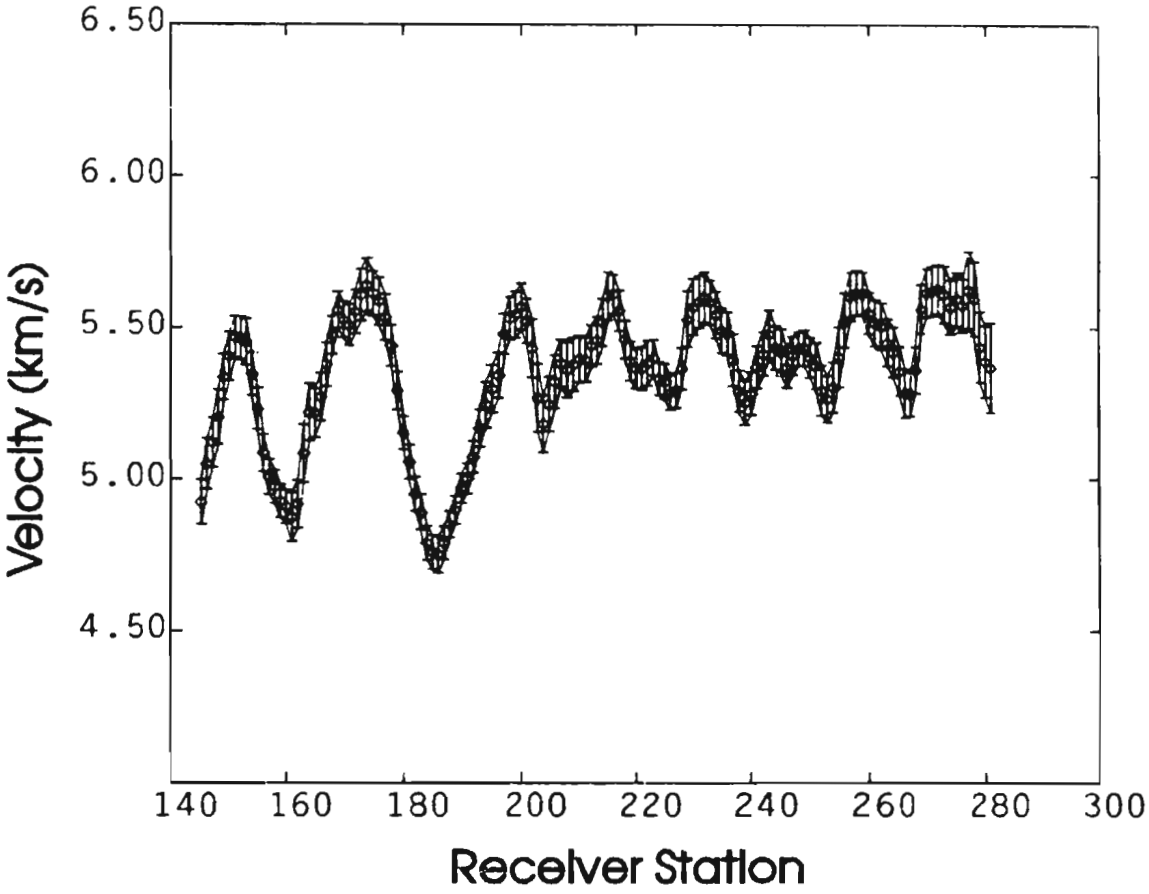

FIG. 29. (After Wright et al , 1994) Engineering method solution for the seismic velocity of bedrock along Buchans line 14 obtained by summary value smoothing the first break times after subtraction of the shot and receiver reciprocal time terms. 95 % confidence limits are shown.

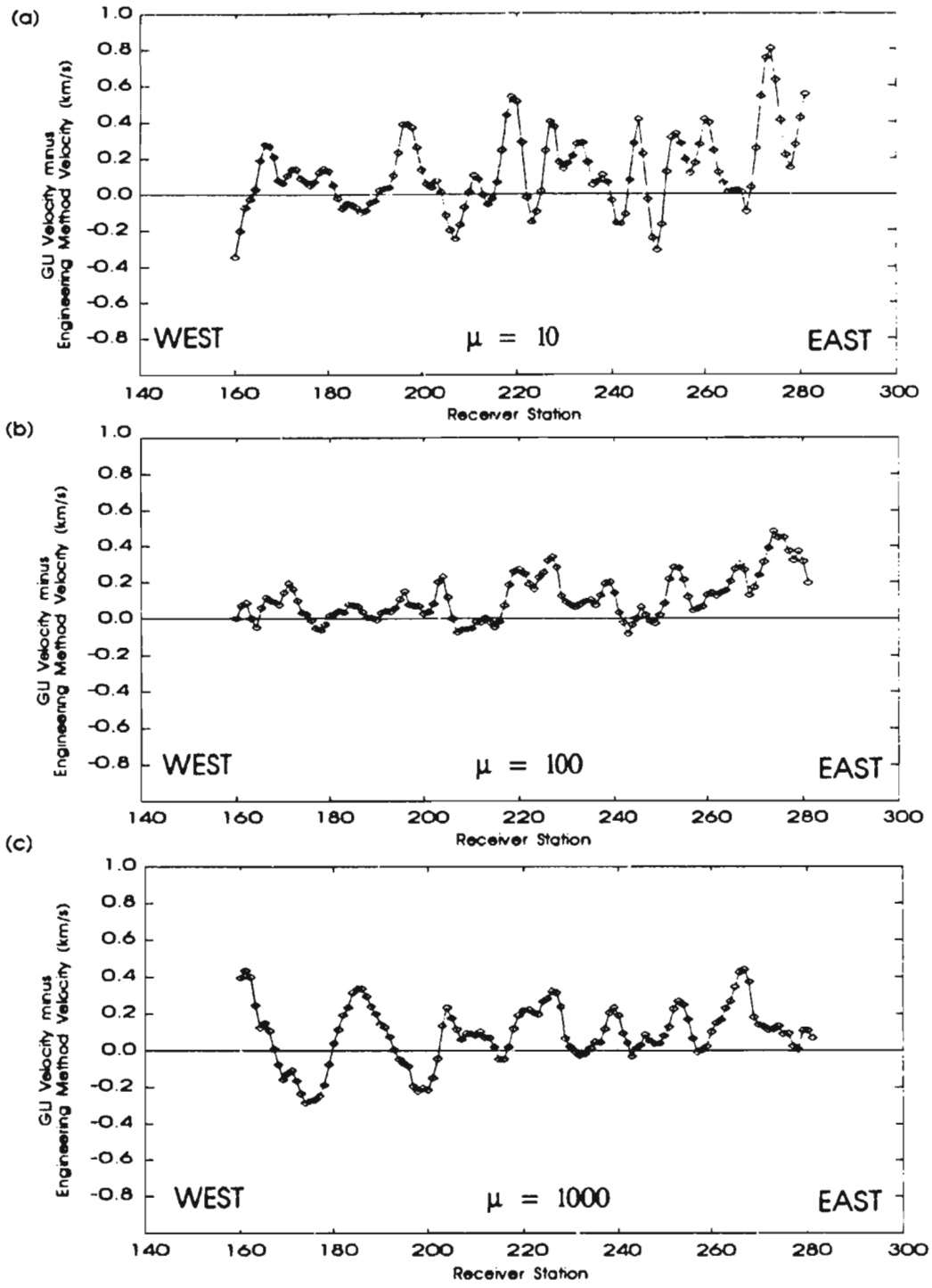

FIG. 30. Difference between estimates in seismic velocity in bedrock along Buchans line 14 using the engineering method (Fig. 29) and Occam's technique using a smoothing parameter of: (a) 10; (b) 100; (c) 1000.

solutions obtained using $\mu=10$, $\mu=100$, and $\mu=1000$, most closely resembles the engineering solution. From plotting these differences it can be seen that there appears to be a small bias (about 0.1 km/s) which results in a higher velocity for Occam's method versus the engineering method. This is most likely due to the same effect described for statics; the raypaths in the weathering layer model are inclined more vertically than in the true earth. The effect however is small, approximately the same magnitude as the errors on the velocity estimates, and much smaller than the observed anomalies.

The Occam's method solution with $\mu=100$ was used for fine-tuning the statics corrections shown in Fig. 26(a). The higher velocity of this solution relative to the reciprocal method solution may have also contributed to the relatively smaller magnitude of the GLI corrections versus the reciprocal method but this contribution would have been very small (approximately 0.1-0.2 ms maximum difference in statics).

There are a number of important aspects of these bedrock velocity profiles that should be explained. To the west (left) of receiver 148 for the engineering method solution (Fig. 29), the values are apparent velocities because the shot-receiver paths are not reversed. In addition, the GLI solutions shown in Fig. 28 do not display velocities at the beginning of the line (i.e. less than station 160) which are more poorly resolved than the rest of the model due to the geometry of the survey. Therefore, a comparison between the two solutions was made only between stations 160 and 280, not including the most poorly resolved stations at the beginning of the line.

For both the Occam's method profile using $\mu = 100$ (Fig. 28(b)) and the engineering method bedrock velocity profile (Fig. 29), there are two distinct minima at locations 163 and 186. The first of these has no clear geological interpretation, and for the GLI solution, occurs close to the part of the line where the model is poorly resolved. The second minimum is coincident with the boundary (probably faulted) between the Lundberg Hill Formation and the Ski Hill Formation (Wright, 1994a). The minimum at 186 can also be observed on the other Occam's method solutions (Fig. 28 (a) and (c)) but are either smaller in amplitude for the solution with $\mu = 1000$ (more smoothed than $\mu = 100$) or larger in amplitude for the solution with $\mu = 10$ (less smoothed than $\mu = 100$). Wright (1994a) interprets the lower seismic velocities in the Lundberg Hill Formation as a consequence of the felsic lithologies compared with the intermediate to basic lithologies of the Ski Hill Formation.

Processing of the seismic sections

The static corrections were calculated by combining the weathering times and bedrock velocity solutions with elevation data for the survey. These corrections (Fig. 26) have short wavelength variations of up to 7 ms corresponding to one complete cycle for a signal of dominant frequency around 140 Hz. If these corrections were not included in the processing sequence (Table 5) the effectiveness of the stack would be greatly reduced. This can be seen clearly from comparing the sections processed with field statics only (Fig. 31 (a)) verses the one processed with the GLI-derived statics (Fig.

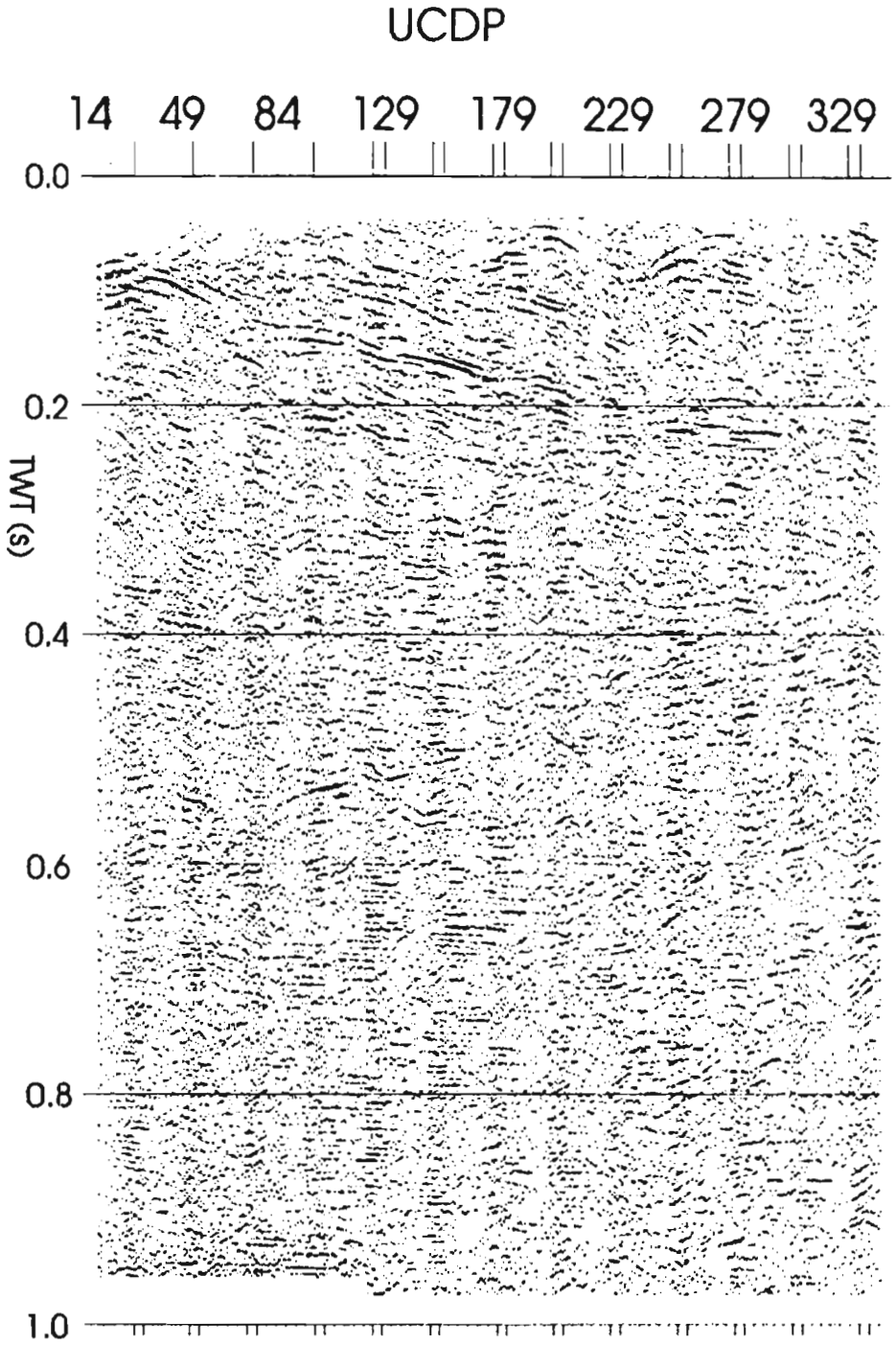

FIG. 31 (a). CDP stacked seismic section from CERR primaflex survey along Buchans line 14 processed with field statics (elevation corrections) only Processing details can be found in Table 6

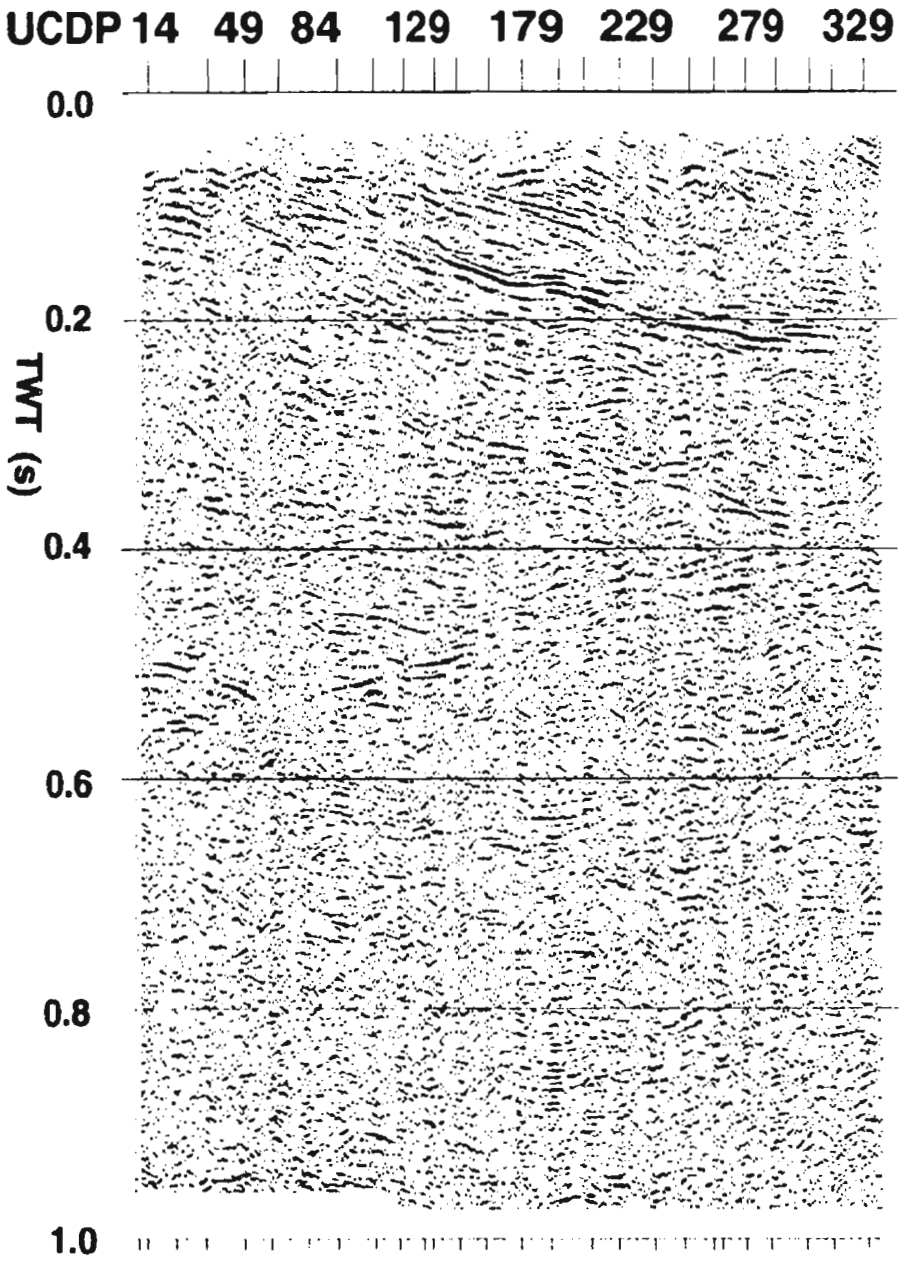

FIG 31 (b) CDP stacked seismic section from CERR Primaflex survey along Buchans line 14 processed with statics derived from GLI method. Processing details can be found in Table 6

31 (b)).

The section processed using static corrections derived by the reciprocal method (Fig. 31 (c)) shows no significant differences compared with the section processed using GLI-derived statics (Fig. 31 (b)) (all other processing parameters are held the same). It was concluded that the interpretation of Wright et al. (1994) (Fig. 32) would not be changed in any way by using the GLI method rather than the reciprocal method for calculating the static corrections for these seismic data.

TABLE 5. (After Wright et al., 1994) Optimal processing sequence for CERR seismic reflection survey (Primaflex sources) at Buchans, NF, 1991.

1. Pick first-breaks and delete bad traces.
2. Compute elevation and refraction statics. Apply to shot gathers.
3. Velocity analysis (velocity spectra and constant velocity stacks) on high-pass filtered or spectrally-balanced shot gathers.
4. Estimate laterally varying stacking velocity model by linear regression on many separate velocity estimates.
5. Apply NMO correction using stacking velocity model on unfiltered CMP gathers.
6. Spectrally balance NMO corrected gathers over 2 octaves (60-240 Hz).
7. Apply mutes to remove refracted P arrivals.
8. Apply mutes to remove high frequency air wave.
9. Stack using some pseudo-coherence weighting.
10. Apply noise attenuation and coherency filtering.
11. Apply amplitude balancing and plot output.

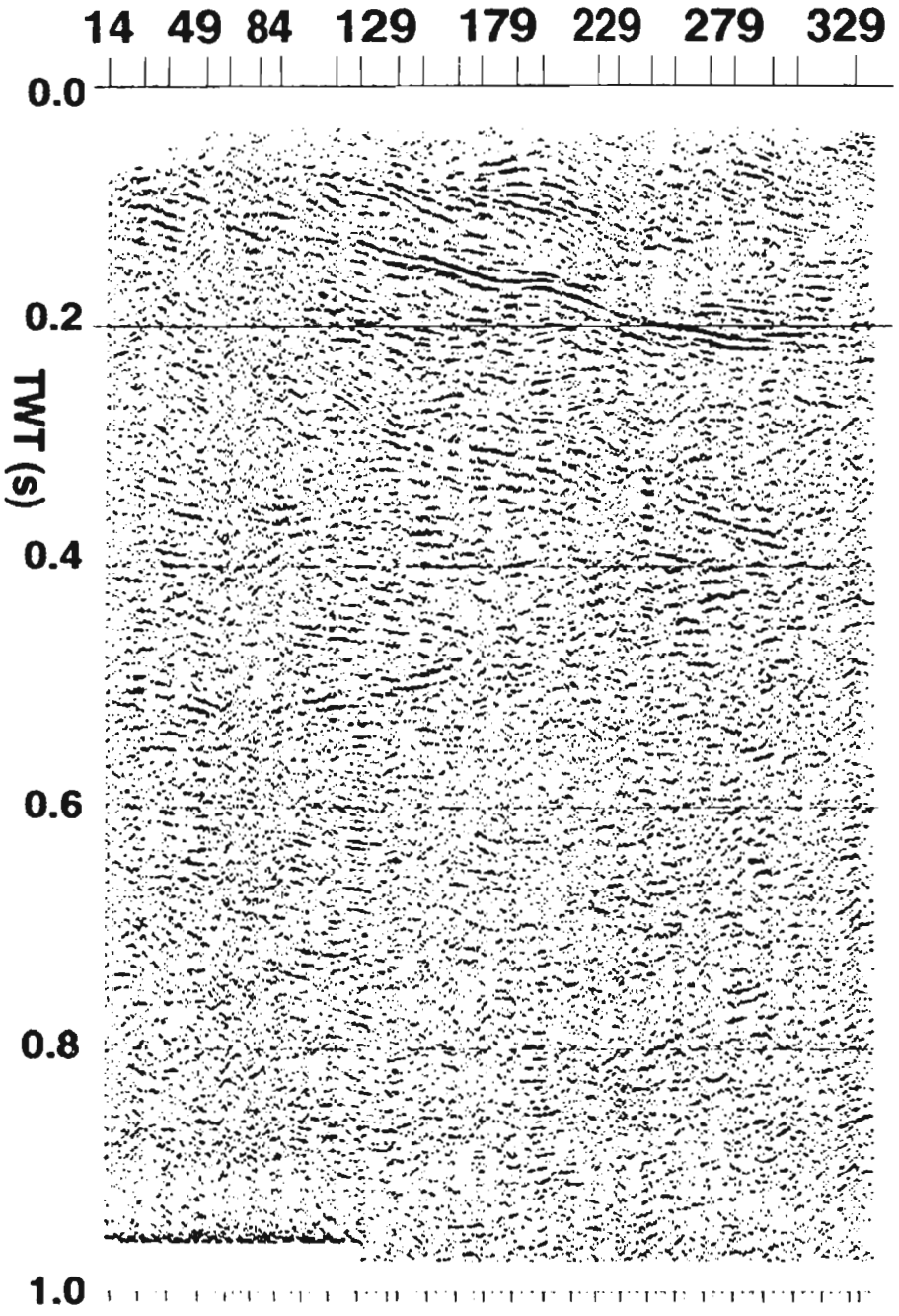

FIG. 31 (c) (After Wright et al., 1994) CMP stacked seismic section from CERR primaflex survey along Buchans line 14 processed with statics derived from the reciprocal method Processing details can be found in Table 6.

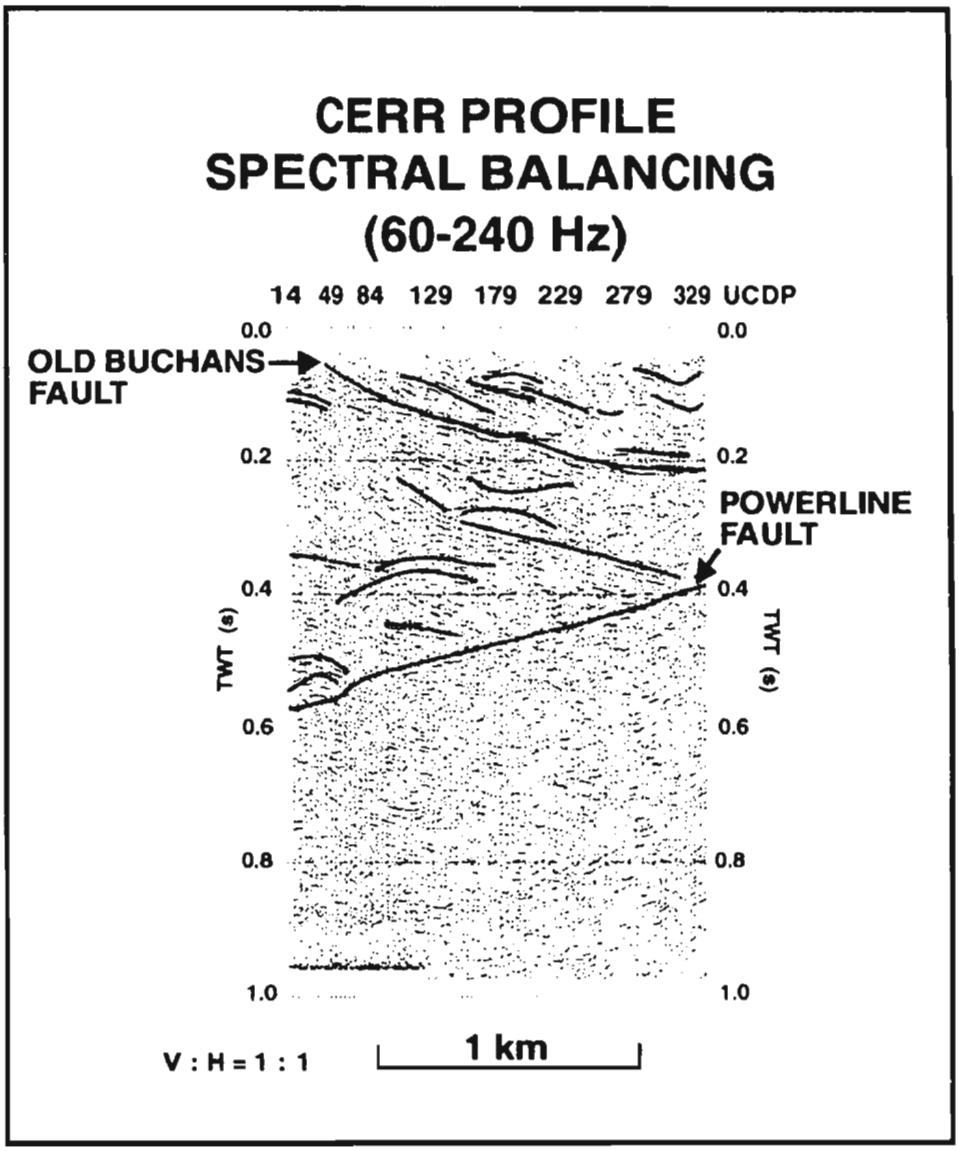

FIG. 32. (After Wright et al. 1994) Seismic section for Buchans as shown in Fig. 31 (c) with geological interpretation superimposed

4.4 Buchans Vibroseis™ Data

These data from Line 14 (Fig. 24) were inverted for the purpose of comparing the GLI and the engineering techniques in resolving bedrock velocities for Vibroseis data. No reprocessing of the seismic sections was done because the interest was in the resolution of velocities for bedrock only. A comparison was also made between the interpretations of these velocities and those of the explosives data collected along the same line.

4.4.1 Procedures

GLI model and procedure

The initial two-layer model used to determine the weathering times for the next stage of refined bedrock velocity analysis using Occam's method is shown below:

WEATHERING LAYER	
NO. OF CELLS	ONE PER RECEIVER STATION
INITIAL VELOCITY	0.5 km/s
THICKNESS (constant)	0.5 m
BEDROCK LAYER	
CELL WIDTH	120 m
INITIAL VELOCITY	5.2 km/s

An important difference with the explosives data was that separate shot and receiver statics were assumed for the procedure. This was done to reduce some of the problems with the first-break data due to cycle skipping. The main reason for these problems was the presence of a powerline along the survey line which resulted in contamination of some of the traces from 60 Hz noise, making them difficult to pick. Some of the shot gathers were picked incorrectly, and in some cases apparently indicated a shot going off before time zero. It was hoped that, by assuming separate statics, this effect could be absorbed into the shot static terms.

A damping parameter of $\beta=50$ with a reduction factor of 0.5 per iteration was used for the damped least-squares procedure. The procedure was terminated if i) 10

iterations were exceeded or ii) the model perturbations were all less than 0.001 s/km. The first-break data used in the inversion was limited to offsets between 200 and 400 m. This was done to reduce the number of equations and also because of evidence from offsets greater than 400 m that a second bedrock layer was present; the two-layer model would not have been suitable for modelling these larger offset arrivals.

Bedrock velocity analysis using Occam's method

Occam's procedure was used for the inversion of a model with one bedrock cell per receiver station. The initial velocity for the bedrock was 5.2 km/s and a weathering velocity of 1.6 km/s was assumed (as with the Buchans explosives data) when removing the weathering times from the first arrival times. The termination conditions were identical to those used for the damped least-squares inversion. The smoothing parameter ($\mu = 100$) was chosen based on the results for the inversion of the explosives data with an identical amount of smoothing.

Engineering procedure

An identical procedure as described in Section 4.3.1 for the Buchans explosives data (summarized from Wright et al., 1994) was used except that the final bedrock velocities were obtained by smoothing the raw first-break times only. No refined velocities were calculated by removing the weathering times from the first-break times and re-smoothing the data.

4.4.2 Comparison of Results for Buchans Vibroseis Data

For the velocity profiles derived using the engineering (Fig. 33 (a)) and GLI techniques (Fig. 33 (b)), the velocities vary from approximately 4.8 to 5.5 km/s and an important result for both profiles is that the local velocity minima present around Vibroseis station 60 corresponds to the minima found at survey station 190 for the explosives survey. Although the trough in velocity is of smaller amplitude (Wright, 1994a), it provides further evidence for the presence of an important geological transition at this point (i.e. between the Lundberg Hill and Ski Hill Formations).

In both profiles the 95 % confidence limits shown increase dramatically beyond station 130. This is due to a larger number of bad picks in the data due to electromagnetic noise from a powerline, corrupting many of the traces along this part of the line.

The magnitude of the difference between the two solutions (Fig. 34) reaches a maximum of about 0.35 km/s around station 120. This feature appears to be the result of more smoothing in the solution obtained using Occam's method that removed this higher-frequency spike, probably an artifact of the noise in the data, from the velocity solution. There is also a difference in the width of the 95 % confidence limits on these solutions beyond station 140 which appear to be wider for Occam's method, increasing to a maximum of +/- 0.4 km/s. Occam's method used a more restrictive range of first-break times than the method of summary values to estimate velocities and resulted in a higher standard deviation for the data residuals and thus relatively higher error estimates.

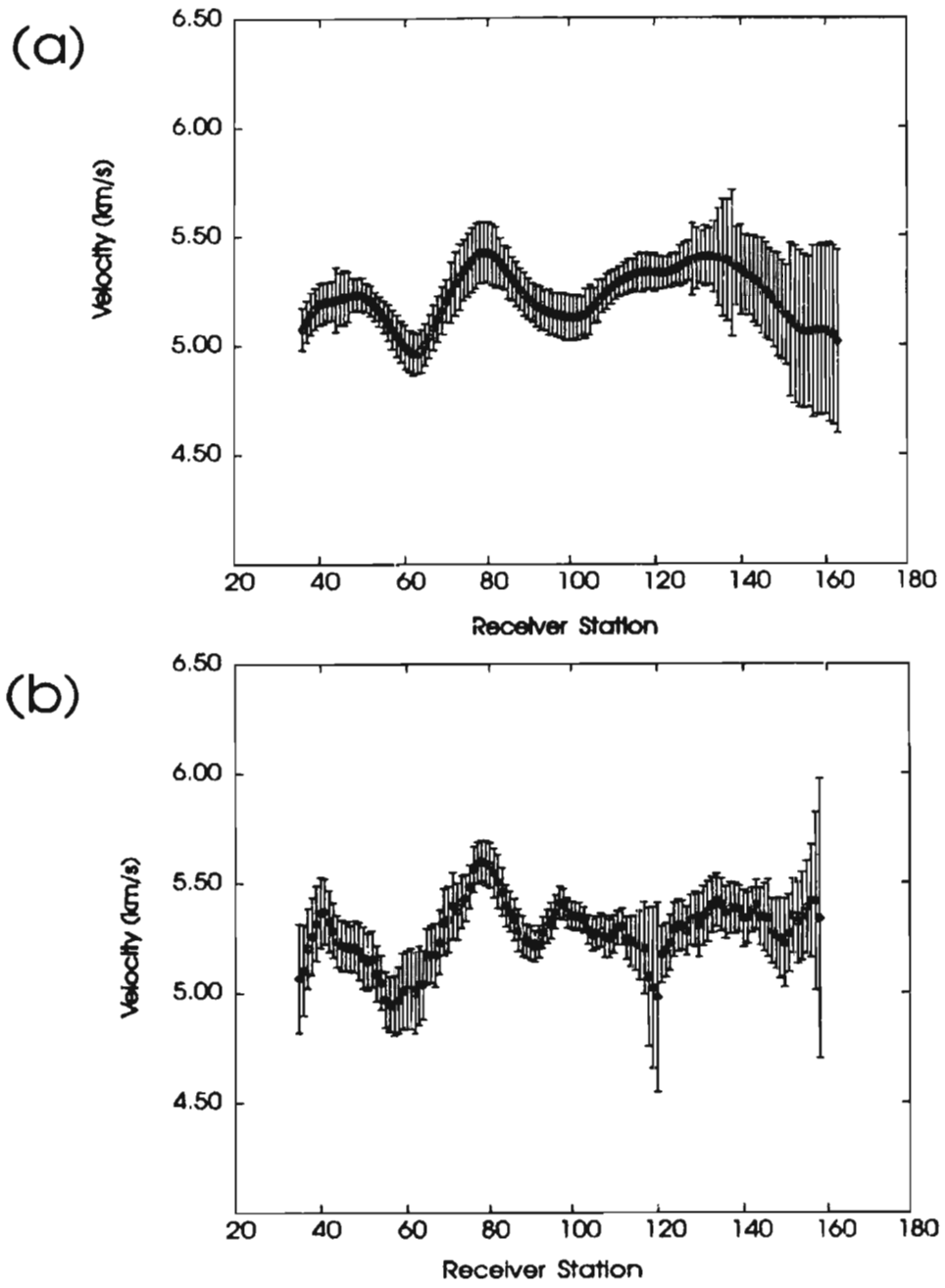

FIG 33 Bedrock seismic velocity estimates for a portion of the Lithoprobe line 14 derived using (a) Occams method with lambda = 100 and (b) using summary value smoothing on raw first break times picked from Vibroseis data..

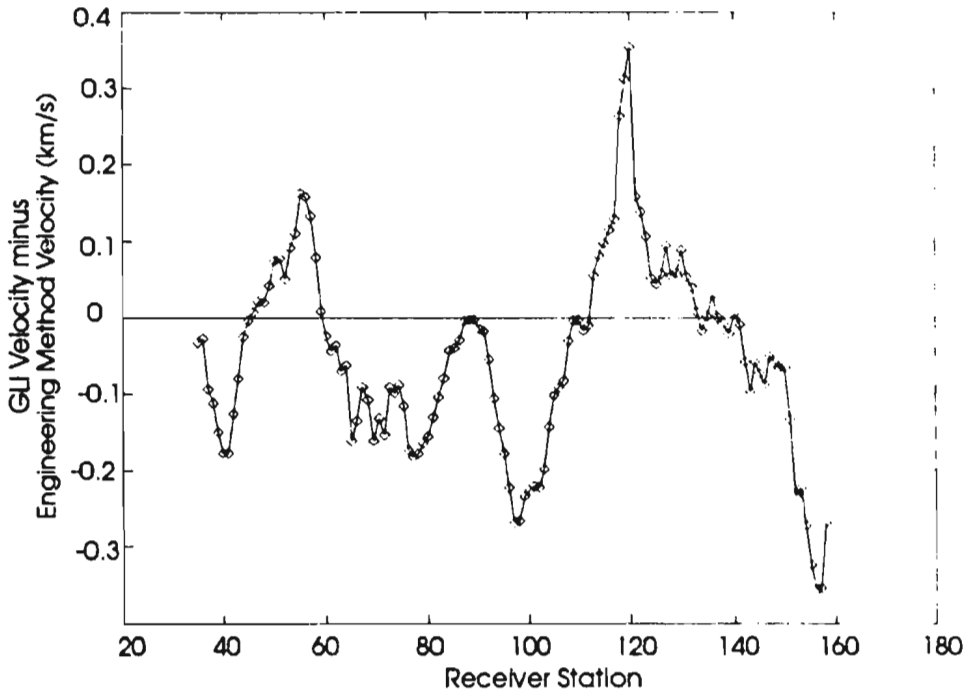

FIG. 34. Difference between bedrock seismic velocity estimates for a portion of the Lithoprobe line 14 derived using Occam's method and summary value smoothing as shown in Fig. 33 (a) and (b).

4.5 Gullbridge Explosives Data

The following is a description of the analysis of the field data from Line 1 at Gullbridge (Fig. 25) that compared static corrections and bedrock velocities obtained using GLI and the engineering technique. The reprocessing of the seismic reflection sections was not considered useful, however, considering the similarity of the static corrections obtained by both methods. The static corrections applied in the processing sequence did not produce any clear reflective features in the section. This was most likely due to the necessity in the field to run the seismic recording and field processing computers from a generator after the failure of an inverter during the early stages of the experiment, causing much of the data to be contaminated by 60 Hz noise (Wright et al., 1993). However, important comparisons can be made between the techniques based on the magnitudes of the static corrections and the pattern of lateral variations in velocity of shallow bedrock obtained.

4.5.1 Procedures

GLI models and procedures

As with the previous analysis of the Buchans explosive data (Section 4.3.1), the procedure was to obtain static corrections from the damped least-squares inversion of a two-layer model (weathering layer and bedrock) and then obtain a refined model for the

bedrock using Occam's method. The main difference in the procedure for the Gullbridge data was that, because of the larger number of equations and parameters (due to the relatively greater length of the seismic line and increased number of channels), the data were divided up into smaller, overlapping sections. An overlap of 50 stations was used to compensate for the poorer resolution of the model towards the ends of the sub-sections.

Statics

The initial model for the damped least-squares inversion is shown below:

WEATHERING LAYER	
NO. OF CELLS	ONE PER RECEIVER STATION
INITIAL VELOCITY	0.5 km/s
THICKNESS (constant)	2.0 m
BEDROCK LAYER	
CELL WIDTH	90 m
INITIAL VELOCITY	5.0 km/s

The width of the bedrock cells was chosen to incorporate approximately the same number of receivers as the Buchans data analysis (i.e. 12 receivers per cell). Their initial velocity was chosen based on previous analysis with the engineering technique which indicated an average around 5.0 km/s for the bedrock velocity. Equivalent shot and receiver statics were used for the GLI technique because this assumption reduced the number of parameters and thus the running time for the procedure.

The data used in the inversion consisted of first-break times recorded at shot-receiver offsets greater than 30 m. The line was divided into 5 smaller overlapping sections for the inversion. A final solution for the entire line was produced by piecing together the 5 smaller sub-sections and discarding the least resolved cells in the region of overlap.

The least-squares procedure was carried out for each section and used a damping parameter of $\beta = 150$ with a reduction factor of 0.5 per iteration. The procedure was terminated if the number of iterations exceeded 15 or if the perturbations to the model slownesses fell below 0.001 s/km.

Bedrock model analysis using Occam's method

For the subtraction of the weathering times, a weathering velocity of 1.0 km/s was assumed, based on an average calculated from the direct arrivals. The bedrock model was modified so that instead of the 90 m wide cells, the boundaries were located halfway between each receiver station. An initial velocity of 5.0 km/s was used for each

cell.

Three different smoothing parameters were tested for the inversion of these data and in each case, different methods were used to divide up the data into manageable portions. This is shown in the table below:

μ (smoothing parameter)	No. of Overlapping sections	Offset Limits
1000	3	> 30 m
500	Entire line	200-400 m
100	3	200-400 m

The purpose of these tests were to see how the smoothing parameter compares with the solution using the engineering technique and how restricting the range of offsets can improve the efficiency of the procedure and reduce the running time.

Engineering procedure

The following procedure was used by Wright and Nguuri (1994) in their analysis of these data. No advantage was found using the GRM over the reciprocal method for these data due to the small offset distance x.

Statics

The time-depth terms were used to estimate separate shot and receiver static

corrections. The first-break times for offsets greater than 30 m were smoothed by the method of summary values using a constant sliding window of length 108-128 m. This was done to estimate the time corrections required in the reciprocal method to accommodate deviations from straight-line geometry and to fine-tune the statics.

Because of the survey geometry and smaller ratio of receiver offset to weathering depth than Buchans, a more rigorous analysis was possible for estimating variations in weathering velocity (Wright, 1994a). However, the solution for statics that was compared with the GLI-derived solution was one that assumed a constant overburden velocity of 1.0 km/s. It was thought that a fairer comparison could be made between the methods if identical models for the weathering layer velocity were assumed.

Bedrock velocities

The first-break times were re-smoothed using after the subtraction of the weathering times and resulted in a velocity profile that had much smaller errors but did not resolve any obvious new geological features.

4.5.2 Comparison of Results for Gullbridge

Statics

The static corrections in both cases assumed a datum at 135 m A.S.L. (Fig. 35 and Fig. 36). The solutions for statics along line 1 have short- to medium-wavelength variations of up to 14 ms corresponding to a full cycle for a signal of dominant frequency

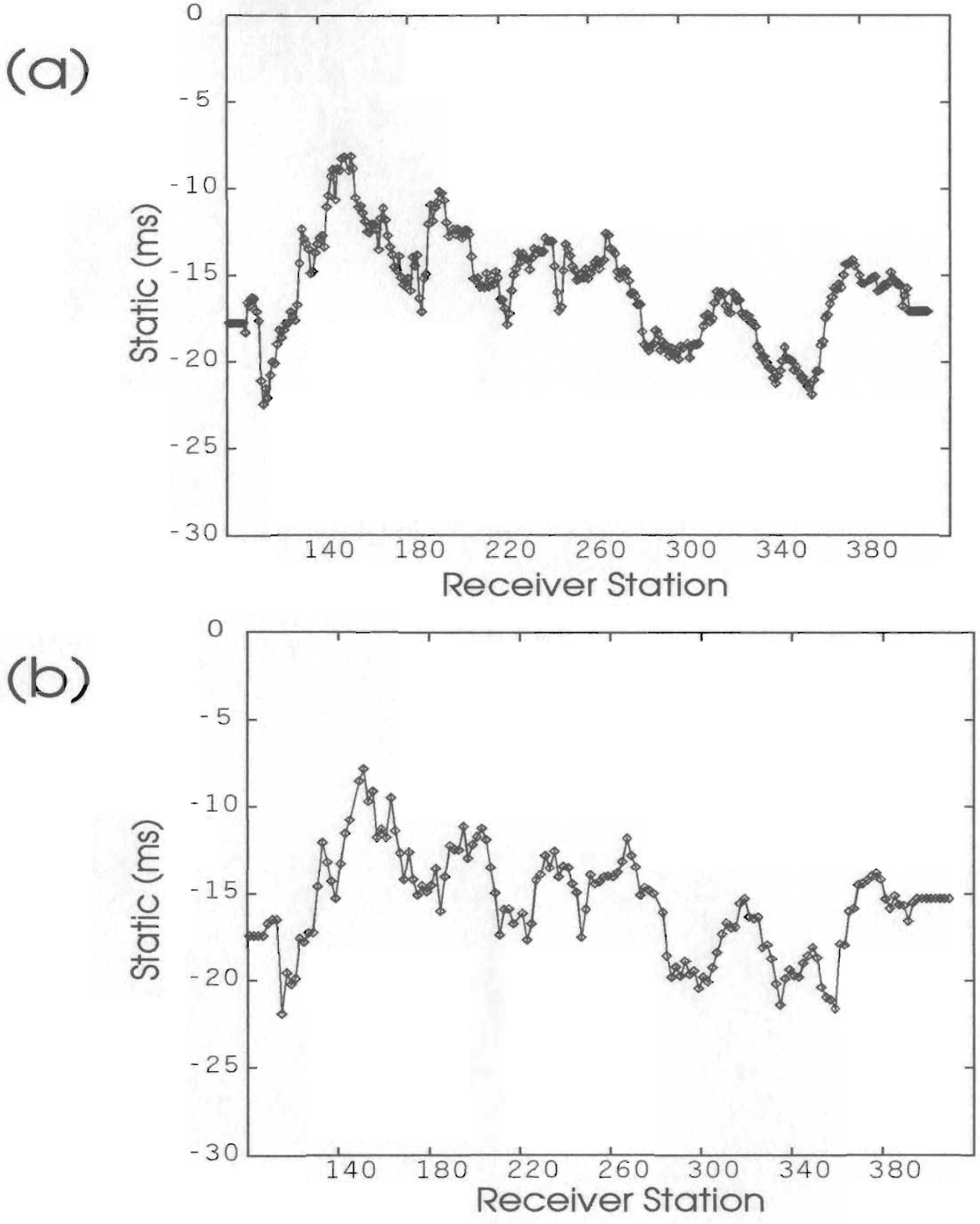

FIG. 35. (After Wright et. al., 1993) (a) Receiver and (b) shot static corrections for Gullbridge line 1 derived using the reciprocal method assuming a weathering velocity of 1.0 km/s. The datum corrected to is 135 m A.S.L.

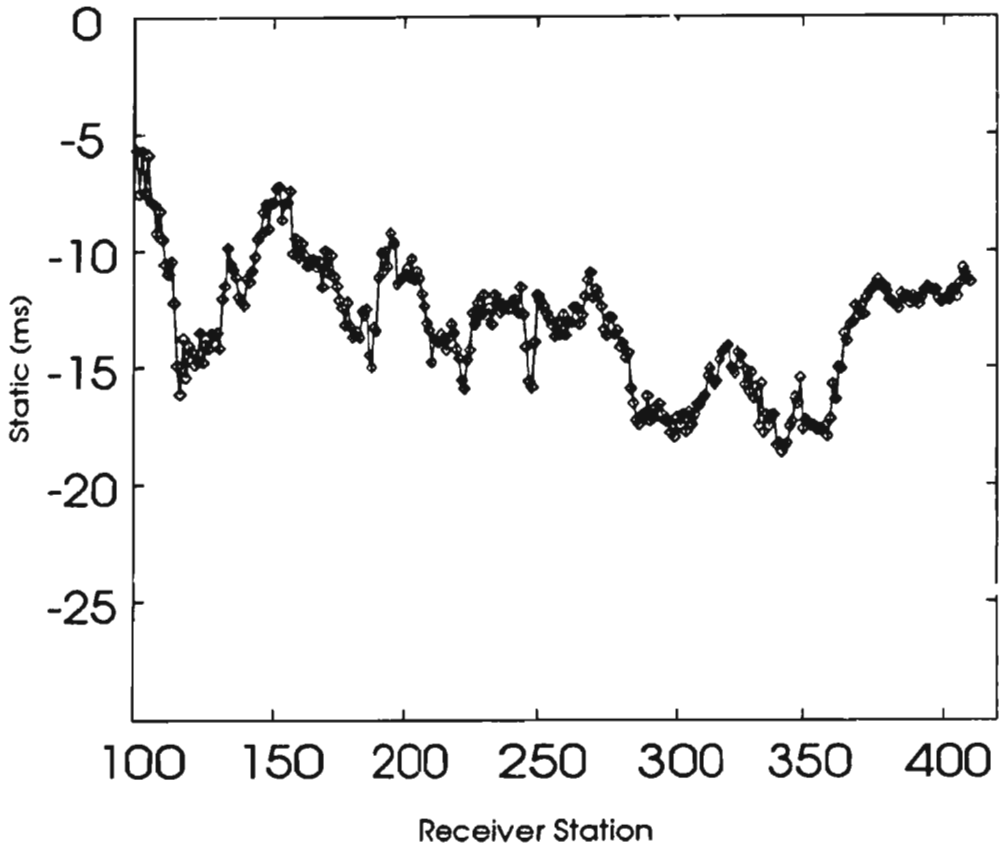

FIG. 36. Static corrections for Gullbridge line 1 derived by the damped least- squares technique and assuming equivalent shot/receiver statics. The datum corrected to is 135 m A.S.L.

of around 80 Hz.

TABLE 6. Breakdown of Gullbridge line 1 into five separate overlapping models: number of equations, parameters and standard deviation for residuals after 15 iterations using damped least squares.

Station Limits	Shot Limits	No. of Equations	No. of Parameters	Standard Deviation for Residuals (ms)
101-205	1-52	2905	115	2.14826
150-255	26-76	2962	111	1.19232
200-310	49-102	3460	121	1.35694
250-350	74-122	2788	116	1.88049
300-410	98-157	3308	111	1.66249

Bedrock velocities

The weathering times were subtracted from the first arrival times to simulate placing the shots and receivers on the bedrock surface. Occam's method was used to obtain a smoother model describing the bedrock velocity variations. As discussed in the previous section, a larger number of equations relative to other data sets required breaking up the data into manageable portions to reduce computational time.

For the initial inversion, a smoothing parameter of $\mu = 1000$ and all first arrival times corresponding to offsets greater than 30 m were used. Line 1 was split into three

overlapping sections (Table 7 below).

TABLE 7. Breakdown of Gullbridge line 1 into three separate overlapping models: number of equations, parameters and standard deviation of residuals after 10 iterations using Occam's inversion with $\mu = 1000$.

Station Limits	Shot Limits	Number of Equations	Number of Unknowns	Standard Deviation for Residuals (ms)
101-250	1-73	4687	150	1.863
200-350	51-122	4653	151	2.436
300-410	103-152	3301	109	2.074

The initial model had a bedrock cell below every receiver station with a velocity of 5.0 km/s and the procedure was stopped after 15 iterations. The three overlapping sections were combined after the inversions were completed; the best resolved bedrock cells (based on the number of raypaths sampling each cell) were selected for the combined model in the region of overlap.

This solution for seismic velocity along the entire line (Fig. 37) has velocities ranging from 2.7 to 5.5 km/s. The main features of the profile are: i) a distinct velocity low less than 4.5 km/s close to station 210; ii) other smaller amplitude velocity lows at stations 300 and 140; and iii) a dramatic decrease in seismic velocity between stations 320 and 360 from 5.5 km/s to 2.7 km/s. If the extreme drop in velocity beyond station 320 is ignored, the average velocity for the bedrock along the line is approximately 5.0 km/s.

Many of the features observed in the velocity profile obtained using Occam's

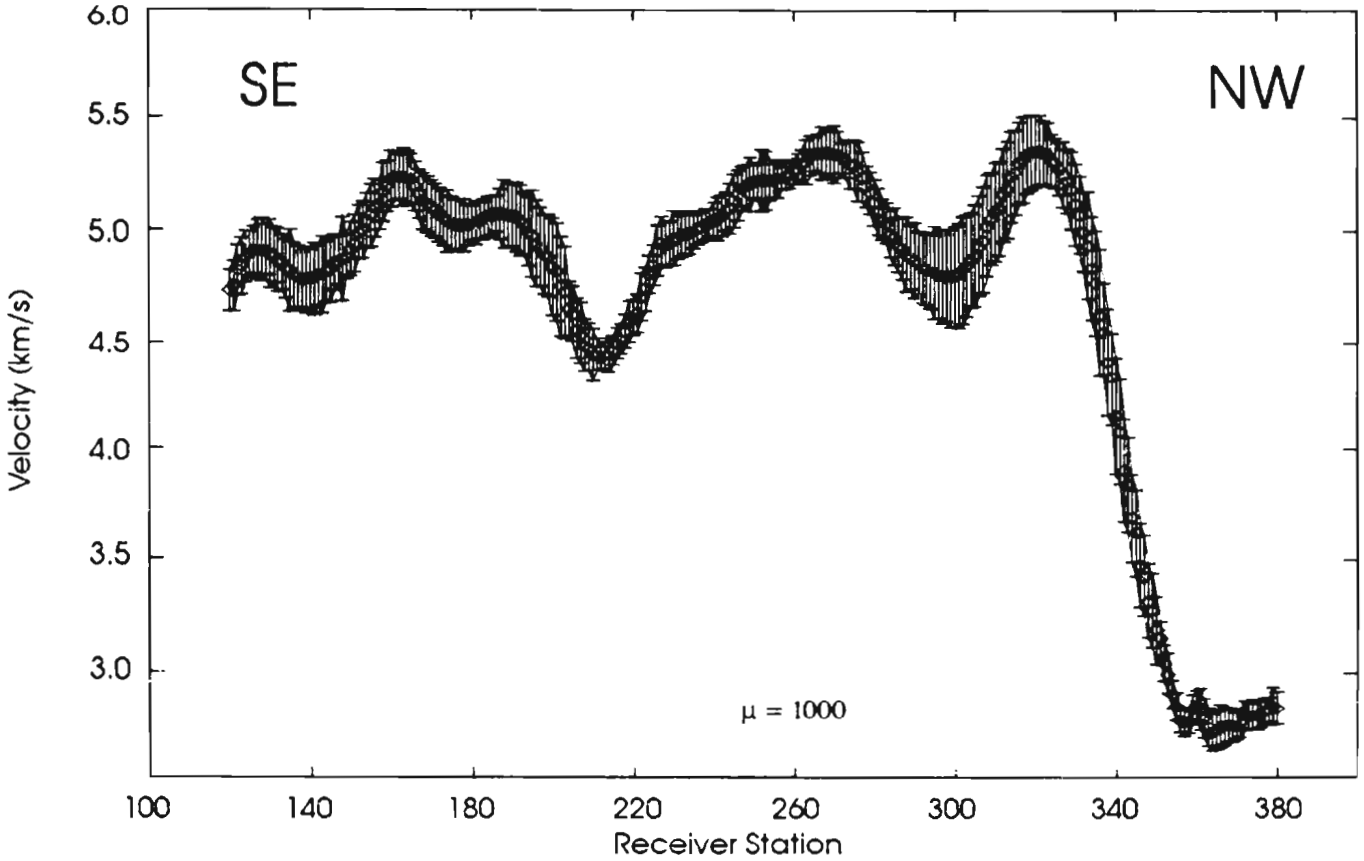

FIG 37 Seismic velocities in bedrock for Gullbridge line 1 estimated using Occam's method with smoothing parameter μ = 1000 Measured velocity values - - 95 % confidence limits are shown

method with $\mu = 1000$ are present in the engineering method solution (Fig. 38 after Wright et al., 1993). The interpretation of this latter velocity profile (Wright et al., 1993) is that the two prominent minima in velocity are clearly associated with the two thrust faults of the Gullbridge Imbricate System that the line crosses (labelled F1 and F2 in Figs. 25 and 38). The signature of fault F2 is present in the Occam's profile using $\mu = 1000$ but fault F1 is not as clearly imaged in this profile. In general, it appears that many smaller-scale variations in velocity present in the reciprocal method solution have been smoothed out of the profile obtained using Occam's method with a smoothing parameter $\mu = 1000$. The lower seismic velocities between stations 288 and 300 observed in both profiles may be due to the presence of more felsic rocks of the Gullbridge Bimodal Unit (Wright, 1994a).

The enormous decrease in seismic velocity at the western end of the line that occurs across the extensional South Brook Fault (F3 on Figs. 25 and 38) forming the boundary between the Lower Ordovician Roberts Arm Group and the Silurian Springdale Group is the dominant feature in both profiles. Seismic velocities lower than 3.0 km/s in Palaeozoic rocks are reported only rarely (Wright, 1994a) and the extremely low velocity values in these rocks are unusual. West of this fault boundary the rocks of the Springdale Group are covered by a peat bog and mine tailings. One possible explanation for these extremely low velocities may be that some infiltration and severe chemical alteration of the upper bedrock surface has occurred due to the downward migration of corrosive fluids. Further work would be required to investigate this hypothesis however.

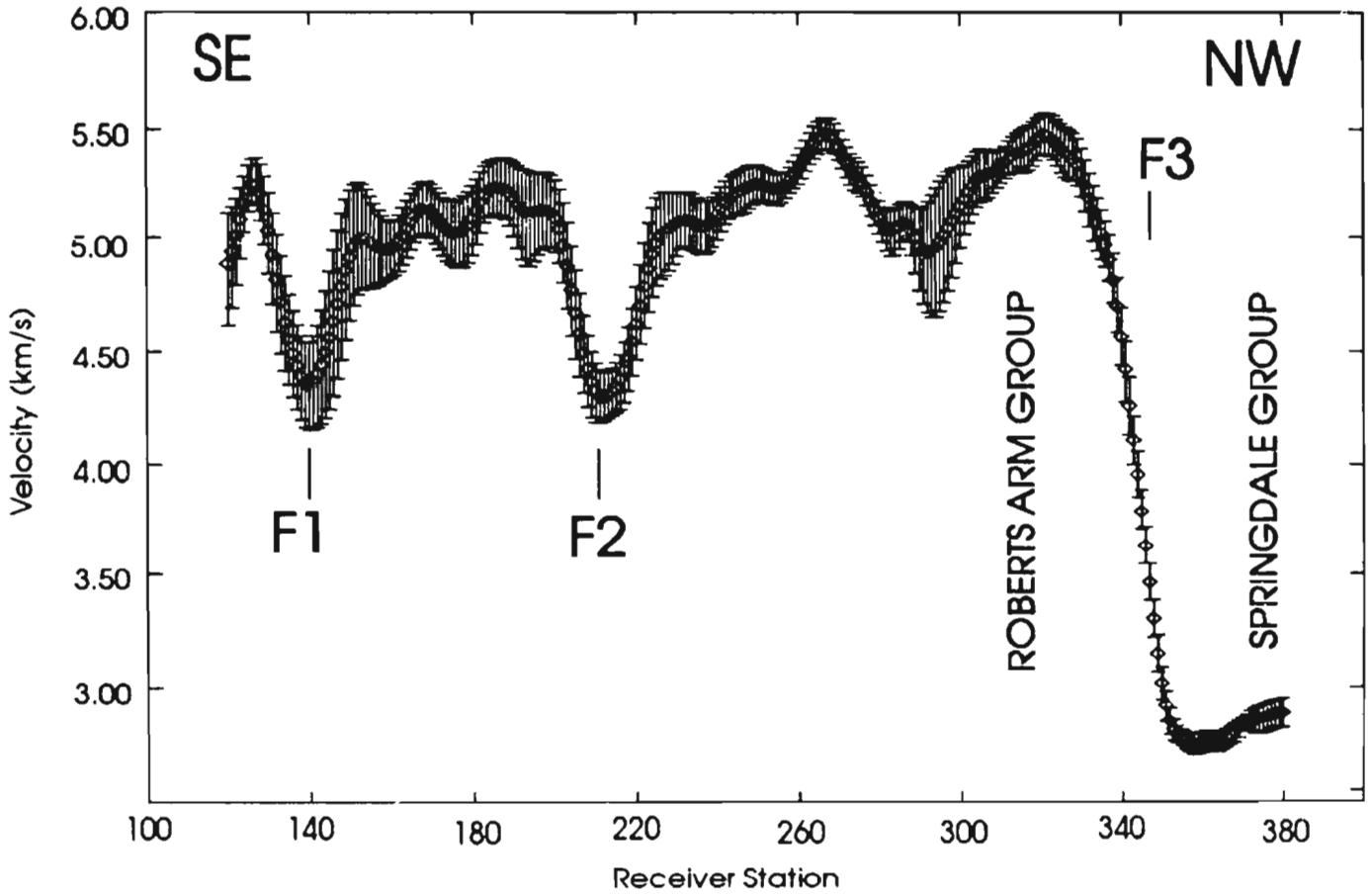

FIG. 38 (After Wright et al., 1993) Seismic velocities in bedrock for Gulbridge line 1 estimated using the method of summary values with a sliding window of length 108-128 m and reciprocal time corrections applied. Measured velocity values +/- 95% confidence limits are shown. F1, F2 and F3 denote faults shown in Fig. 25

Comparison of GLI applied first-break times within a window of shot-receiver offsets with the engineering method

Another approach to the inversion of the bedrock velocity model was to invert the data using GLI and first arrival times from a limited window of shot-receiver offsets. The purpose of this approach was to reduce the computational time of the inversion and see how well the velocities could be resolved with a reduced number of observations used in the inversion procedure. Smoothing parameters $\mu=500$ and $\mu=100$ were tested and an offset window of 200-400 m was used to select first arrival times for the inversion procedure.

In the case $\mu=100$, the line was split into 3 portions as was done for $\mu=1000$ (Table 8). For these inversions only 10 iterations were required to get a fit to the data comparable with the fit obtained by $\mu=1000$. It is important to note however that this fit is measured by the standard deviation on the residuals for the limited shot-receiver offsets only.

TABLE 8. Breakdown of Gullbridge line 1 into three separate overlapping models: number of equations, parameters and standard deviation of residuals after 10 iterations using Occam's inversion with $\mu = 100$ and shot-receiver offsets of 200-400 m.

Station Limits	Shot Limits	Number of Equations	Number of Unknowns	Standard Deviation for Residuals (ms) (*)
101-250	1-73	1315	150	1.802
200-350	51-122	1451	151	1.366
300-410	103-152	881	111	1.387

(*) Estimated for the data within window of offsets 200-400 m.

For $\mu = 500$ an identical window of offsets for first-break data was used but the entire line was inverted in one procedure (Table 9):

TABLE 9. Gullbridge line 1 model - Number of equations, parameters and standard deviation of residuals after 10 iterations using Occam's inversion with $\mu = 500$ and shot-receiver offsets of 200-400 m.

Station Limits	Shot Limits	Number of Equations	Number of Unknowns	Standard Deviation for Residuals (ms) (*)
101-410	1-152	2985	308	1.599

(*) Estimated for the data within window of offsets 200-400 m.

The solutions for $\mu = 500$ and $\mu = 100$ (Figs. 39 and 40) disp'ay many of the same features as the previous inversion with $\mu = 1000$; velocity minima below 4.5 km/s appear to correspond to the locations of faults F1, F2, and F3 (Fig. 38). The velocity low

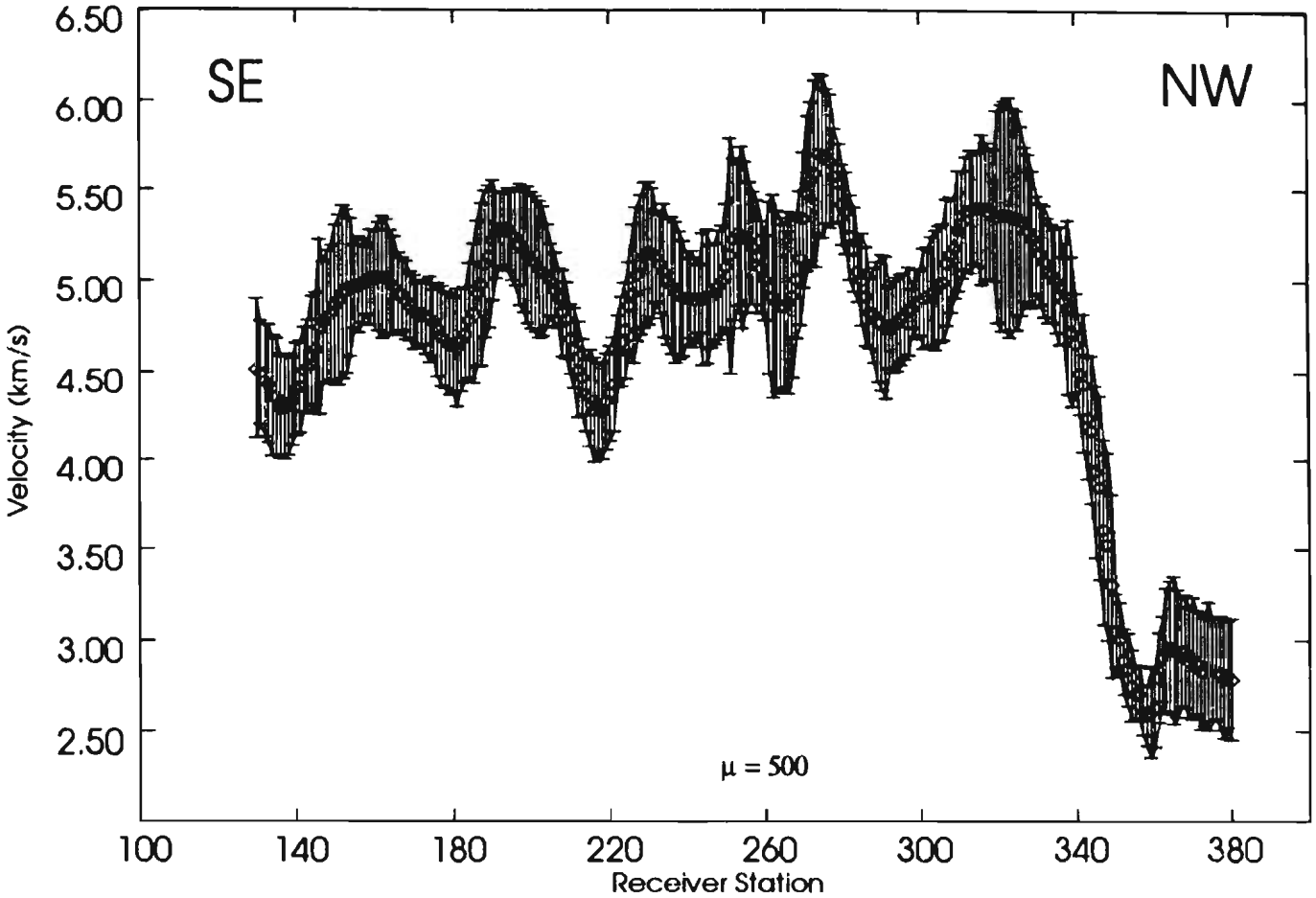

FIG. 39. Seismic velocities in bedrock for Gullbridge line 1 derived using Occam's method with smoothing parameter equal to 500. The entire line was inverted over 10 iterations and only first breaks corresponding to offsets 200 to 400 m were used.

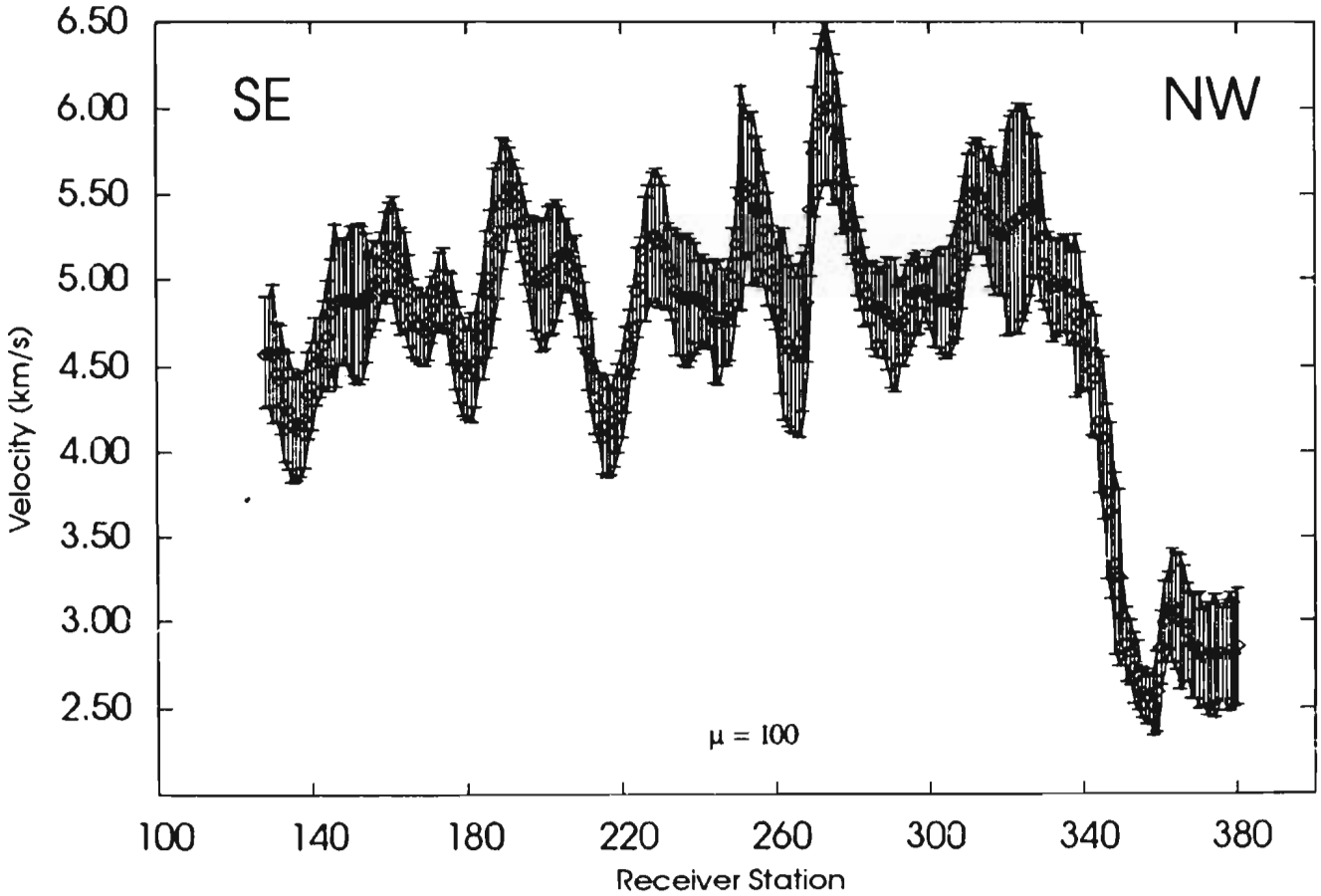

FIG. 40 As for Fig. 39 but with a smoothing parameter of 100. The data was split into 3 overlapping panels for the inversion and only first breaks corresponding to offsets 200 to 400 m were used in the inversion.

corresponding to the location of fault F1 close to station 140 in these profiles is more indicative of a fault than the profile created using a smoothing parameter of $\mu = 1000$. The features displayed by the profile for $\mu = 100$ (Fig. 40) however are more difficult to interpret because of the more rapid variations in the velocity when the amount of smoothing is small.

It is apparent that the 95% confidence limits on the velocity values are larger for the profiles obtained using Occam's inversion with a limited offset window of 200-400 m compared with the inversion using $\mu = 1000$. This is due to the increased scatter of the residuals when using the midpoint method to estimate these 95% confidence limits over a more limited range of values.

4.6 Summary of Results and Conclusions for Analysis of Field Data

For the analysis of field data from two explosives surveys and one Vibroseis survey, the following is a summary of the important results:

i) The comparison of a seismic section (Buchans explosive data) processed with statics derived from GLI versus the reciprocal method showed that there was no significant difference in the overall quality and resolution of the major reflectors. Although there were some differences in the magnitudes of the statics solutions in the mid- to long-wavelength range, the processing appeared to show that, as expected, the most important

effect was the short-wavelength correction within the CMP stack.

ii) Occam's method and summary value smoothing appeared to produce bedrock velocity profiles that displayed the same important features that were interpreted as being due to the presence of faulting or shear zones. The amount of smoothing applied in both cases was subjective and in some cases there were differences between the solutions that were attributed to differences in the amount of smoothing applied. The resolution of the bedrock velocities at Buchans appeared to be poorer for the Vibroseis data than the explosives survey for both techniques due to the lower frequencies generated by the Vibroseis source (40-125 Hz vibrator sweep versus the 250 Hz highest frequency recorded by the explosives data at Buchans), poorer picks due to difficulty in picking Vibroseis data, and powerline noise towards the east end of the line.

CHAPTER 5

5.0 DISCUSSION

The most significant aspect of the research has been the use of a variant of the GLI technique known as Occam's method to derive lateral variations in shallow bedrock seismic velocity. It was found that velocity curves could be obtained using Occam's method that displayed features that were similar to those observed when using the engineering technique on the same data. This type of analysis has been shown here to be a useful tool for interpreting the geology and/or competence of the bedrock beneath the weathering layer for exploration and engineering purposes.

Two important questions are raised in relation to this work. First, what specific properties of the bedrock are responsible for the variations in velocity observed? Secondly, what factors determine the degree to which we can resolve these features in bedrock?

Relation of physical properties to variation in seismic velocity

In answer to the first question, the association of faults or shear zones with local minima in seismic velocity is one aspect of the problem that has been studied in the past (Green, 1980; Wright, 1982; Wright and Huang, 1984; Wright, 1994a,b). It appears that the most important cause of velocity variations in the near-surface bedrock is a change in the density of fractures at scales ranging from microcracks to large fractures

close to the fault or shear zones (Wright, 1994b). Compressional velocity is affected by fracturing because there is a change in the elastic moduli of the material due to lateral displacement of particles as the seismic wave arrives at a planar crack (Nelson, 1984). These effects have been observed in more controlled borehole experiments (e.g. Wright and Huang, 1984) where a close correlation was established between seismic velocity and fracture density from core logging.

For the data looked at here, both Occam's method and smoothing of forward and reverse travel times have been shown to be useful tools for identifying faults and brittle shear zones. Faults inferred from surface geological mapping close to the seismic line and borehole information are generally associated with local minima in seismic velocities. The evidence for associating these velocity minima with real geological features is also strengthened by the fact that these minima have been identified using two independent techniques of bedrock velocity analysis.

The interpretation of lithologies based on P-wave velocity may be more speculative due to the comparatively smaller effect on the velocity compared with fracturing close to fault zones. For example, at Gullbridge the velocity variations attributed to interbedded felsic material in the Gullbridge Bimodal Unit (Wright, 1994a) are relatively smaller in amplitude compared with the velocity minima associated with the fault zones. At Buchans and Gullbridge however there is also some physical basis for an association of the velocities with lithologies based on abundant borehole information and surface geological mapping close to the seismic lines.

Resolution of velocities from refraction analysis

In answer to the second question, there are many factors which may have affected the resolution of the bedrock velocities. These can be listed in 3 general categories (not listed in any order of importance):

i) Acquisition parameters.

ii) Signal-to-noise ratio.

iii) Amount of smoothing.

Acquisition parameters

The best example of how the resolution of the bedrock velocities depends on the data acquisition is shown by comparing the velocity profiles obtained from the Vibroseis data versus the explosives data. The main cause of the relatively poorer resolution of the velocities for the Vibroseis data is the increased difficulty in picking the first-breaks due to the presence of correlation sidelobes, an artifact of the Vibroseis cross correlation, which may have caused relatively larger errors due to cycle skipping. The Vibroseis picks thus have a larger standard deviation about their mean than the explosives picks, and result in larger errors on the velocity estimates.

In all cases, two in-line sources were used to emphasize the amplitude of the reflected signals generated and reduce ground roll. This may result in greater uncertainties in the first-break times and thus less precision in the bedrock velocities due

to interference of the wavelets and a more complex waveform being recorded. The phase spectrum of the recorded signal probably has a large effect on the uncertainty in the first-breaks. A zero phase wavelet is ideal and would produce a peak that would be easily identified, but in general this is not a realistic situation for real data. The complexity of the phase of the wavelet may make it difficult to pick first-breaks especially with noisy data.

Signal to Noise Ratio

The amount of noise that is present during the survey is probably one of the most significant factors affecting the resolution of the bedrock velocities. Picking the first-breaks for the explosives data is done by choosing the first zero crossing of the P-wave arrival but this can be made increasingly difficult at higher noise levels. This was demonstrated at Gullbridge where increased noise levels due to the generator used to run the recording equipment resulted in serious limitations on the number of first-breaks that could be picked with confidence, especially in the immediate vicinity of the recording truck. This resulted in a lower precision of the velocities than would have been expected without this source of noise. For Vibroseis data, high noise levels will increase the uncertainty of picking the highest peak of the trace attributed to the refracted first arrival. This was best demonstrated for the Vibroseis survey at Buchans where electromagnetic noise from a powerline was picked up by the geophone spread resulting in increased uncertainty in picking the first-break times.

An attempt to filter out the noise (post-acquisition) at Gullbridge was made using a notch filter centred at 60 Hz applied to all shot gathers (Wright et al., 1993). This procedure had limited success however because of the presence of harmonics of 60 Hz noise and the fact that the dominant frequency was not always at 60 Hz and was observed at 52 Hz at larger distances from the generator. There are other procedures involving estimation of the noise spectrum based on the pre-first arrival portion of the trace and using this to remove the noise that may be more effective (Per. Comm. Jim Wright, 1994). This may be a way of increasing the number of pickable first-breaks from data with similar noise problems such as encountered at Buchans and Gullbridge.

Amount of Smoothing

Finally, the amount of smoothing applied to the velocity profile has important consequences for the resolution of shallow bedrock velocities. For example, the use of a number of different smoothing parameters for the Buchans explosives data inverted with Occam's method illustrated how oversmoothing could remove important features of the bedrock and undersmoothing could increase the higher frequency noise in the velocity profiles making interpretation difficult. Optimal smoothing was not attempted here because it is a cumbersome and tedious procedure, but may have advantages in reducing the ambiguity involved with deciding how much smoothing to apply.

Future work

The robustness of the SVD method in the inversion procedure is offset by the computing time required to do the decomposition. A typical run with over 300 equations and 100-200 unknowns takes approximately 5 to 7 hours to complete on the CONVEX™ C1 Supercomputer. This can be rather impractical for routine processing of long seismic lines (e.g. Gullbridge line 1) and in this respect the engineering technique is preferable to use because of its shorter run time. Further work would be required to speed up the inversion procedure; for example, Wiggins et al. (1976) uses the Gauss-Seidel method to invert a large number of equations to determine residual statics.

Future work on using refracted arrivals to derive near-surface information may improve the efficiency and usefulness of such an analysis. Improvements in first-break picking software (especially for Vibroseis data) and computing speed may be important in improving the efficiency with which refraction statics can be calculated. The use of directional geophones to measure direct arrivals may remove the uncertainty of weathering velocity determination (Farrell and Euwema, 1987). Further investigation of more efficient ways to do optimal smoothing for both GLI and summary value smoothing may reduce the subjectivity of the amount of smoothing to apply to the data. Finally, the comparison of these techniques should be extended to the case of diving wave models to see which is more effective in deriving a near-surface model.

CHAPTER 6

6.0 CONCLUSIONS

The GLI technique used here to estimate static corrections and for bedrock velocity analysis produces results that are very similar to engineering seismic refraction techniques. For the stacked seismic sections shown here there was no significant improvement in the appearance of the section processed with the GLI-derived statics compared with a section processed with the engineering method statics. The interpretation of the bedrock geology at both Buchans and Gullbridge based on seismic velocity variations obtained using Occam's method indicated the presence of shear zones and/or faults that correlated well with the geology interpreted adjacent to the seismic lines and with the interpretation of the engineering method solutions.

The application of refraction statics corrections to seismic data collected for mineral exploration purposes is an important processing step because of the low amplitude or discontinuous character of the reflections; residual static routines do not perform well in regions of poor reflectivity. The enhancement of reflections using refraction statics techniques has been shown here; for example, the significant improvement in the resolution of the reflectors at depth compared with applying field statics only was apparent for the Buchans Primaflex survey.

Further analysis of the first-break data after obtaining static corrections for bedrock velocity variations may provide additional useful information on the location of zones of faulting, shearing and/or lithological variations beneath the weathering layer

which may be used as an aid to geological mapping in the region. The locations of faults below glacial overburden at Buchans and Gullbridge have been inferred from the analysis of drill hole cores or surface geological mapping and the presence of these faults is evident in the seismic velocity profiles (Wright, 1994a). The additional information that this type of analysis of refraction data can provide may be useful and may become more routine in the future with the availability of better software for first-break picking and refraction analysis.

REFERENCES

Alter, B., 1985. In situ velocity estimates for shallow crystalline rocks in the Adirondack Mountains, New York and the Laramie Range, Wyoming. Bulletin of the Seismological Society of America, **75**: 1363-1369.

Aki, K. and Richards, P. 1980. Quantitative Seismology - Theory and Methods. Vol. 2, W. H. Freeman Co., San Francisco.

Bahorich, M.S., Coruh, C., Robinson, E.S. and Costain, J.K. 1982. Static corrections on the southeastern Piedmont of the United States. Geophysics, **47**: 1540-1549.

Bolt, B.A. 1978. Summary value smoothing of physical time series with unequal intervals. Journal of Computational Physics, **29**: 357-369.

Brocher, T.M. 1981. Shallow velocity structure of the Rio Grande rift north of Socorro, New Mexico: a reinterpretation. Journal of Geophysical Research, **86**: 4960-4970.

Constable, S., Parker, R., and Constable, C. 1987. Occam's inversion: a practical algorithm for generating smooth models from electromagnetic sounding data. Geophysics, **52**: 289-300.

De Armorim, W.N. Hubral, P. and Tygel, M. 1987. Computing field statics with the help of seismic tomography. Geophysical Prospecting, **35**: 907-917.

Docherty, P. 1992. Solving for the thickness and velocity of the weathering layer using 2-D refraction tomography. Geophysics, **57**: 1307-1318.

Dongarra, J.J., Bunch, J.R., Moler, C.B., and Stewart, G.W. 1979. LINPACK user's guide, SIAM Publications, Philadelphia.

Farrell, R.C. and Euwema, R.N. 1984. Refraction statics. Proceedings of the IEEE, **72**: 1316-1329.

Gersztenkorn, A., Bednar, J.B., and Lines, L.R. 1986. Robust iterative inversion for the one-dimensional acoustic wave equation. Geophysics, **51**: 357-368.

Golub, G.H. and Reinsch, C. 1970. Singular Value Decomposition and Least Squares Solutions : Handbook for Automatic Computation, II, Linear Algebra, eds. J. Wilkinson and C. Reinsch. Springer-Verlag, Berlin, Heidelberg, New York.

Graybill, F.A. 1969. Introduction to Matrices with Applications in Statistics. Wadsworth Publishing Co. Inc., Belmont.

Green, A.G. 1980. Delineation of geological contacts by seismic refraction with application to the fault zone between the Thompson Nickel Belt and the Churchill Tectonic Province. Canadian Journal of Earth Sciences, **17**: 1141-1151.

Hagedoorn, J.G. 1959. The plus-minus method of seismic refraction interpretation. Geophysical Prospecting, **7**: 158-182.

Hampson, D. and Russell, B. 1984. First-break interpretation using generalized linear inversion. Journal of the Canadian Society of Exploration Geophysicists, **20**: 40-54.

Hawkins, L.R. 1961. The reciprocal method of routine shallow seismic refraction investigation. Geophysics, **26**: 806-819.

Herman, G. 1980. Image Reconstruction from Projections. Academic Press Inc., New York.

Lanczos, C. 1961. Linear Differential Operators. Van Nostrand, Princeton, pp.665-679.

Leven, J.H. and Taylor, F.J. 1989. Cumulative difference statics: method and application. Exploration Geophysics, **20**: 365-370.

Lines, L.R. and Treitel, S. 1984. Tutorial: A review of least-squares inversion and its application to geophysical problems. Geophysical Prospecting, **32**: 159-186.

Mayrand, L., Green, A.G., and Milkereit, B. 1987. A quantitative approach to bedrock velocity and precision: the LITHOPROBE Vancouver Island Experiment. Journal of Geophysical Research, **92**: 4837-4845.

Neary, G.N. 1981. Mining history in the Buchans area. *In* The Buchans Orebodies: Fifty Years of Geology and Mining, Part 1: Text. *Edited by* E.A. Swanson, D.F. Strong and J.G. Thurlow. Geological Association of Canada, Special Paper 22, Geological Association of Canada, Toronto, pp. 1-64.

Nelson, R.G. 1984. Seismic reflection and mineral prospecting. Exploration Geophysics, **15**: 229-250.

Olsen, K.B. 1989. A stable and flexible procedure for the inverse modelling of seismic

first arrivals. Geophysical Prospecting, **37**: 455-465.

Paige, C. and Saunders, M. 1982. LSQR: An algorithm for sparse linear equations and sparse least squares. Assn. Comp. Math. Trans. on Mathematical Software, **8**: 43-71.

Palmer, D. 1981. An introduction to the generalised reciprocal method of seismic refraction interpretation. Geophysics, **46**: 1508-1518.

Pope, A.J. and Calon, T.J. 1990. A stratigraphic and structural analysis of the Gullbridge property, central Newfoundland, Centre for Earth Resources Research, Department of Earth Sciences, Memorial University of Newfoundland, St. John's. 81 pp.

Scales, J. 1987. Tomographic inversion via the conjugate gradient method, Geophysics, **52**: 179-185.

Scales, J.A., Docherty, P., and Gersztenkorn, A. 1990, Regularization of nonlinear inverse problems: imaging the near-surface weathering layer. Inverse Problems, **6**: 115-131.

Spencer, C., Thurlow, G., Wright, J., White, D., Carroll, P., Milkereit, B. and Reed, L. 1993. A Vibroseis reflection seismic survey at the Buchans Mine in central Newfoundland. Geophysics, **58**: 154-166.

Thurlow, J.G., Spencer, C.P., Boerner, D.E., Reed, L.E., and Wright, J.A. 1992. Geological interpretation of a high resolution reflection seismic survey at the Buchans Mine, Newfoundland. Canadian Journal of Earth Sciences, **29**: 2022-2037.

Treitel, S., Lines, L. and Ruckgaber, G. 1994. Geophysical Inversion and Applications. short course notes (SEG continuing education program), Memorial University of Newfoundland. 142 pp.

Upadhyay, H.D. and Smitheringale, W.G. 1972. Geology of the Gullbridge copper deposit, Newfoundland: Volcanogenic sulphides in cordierite-anthophyllite rocks. Canadian Journal of Earth Sciences, **9**: 1061-1073.

White, D.J. 1989. Two-dimensional seismic refraction tomography. Geophysical Journal, **97**: 223-245.

Williams, H. and Piasecki, M.A.J. 1990. The Cold Spring Melange and a possible model for Dunnage-Gander zone interaction in central Newfoundland. Canadian Journal of Earth Sciences, **27**: 1126-1134.

Wiggins, R.A., Larner, K.L., and Wisecup, R.D. 1976. Residual statics analysis as a general linear inverse problem. Geophysics, **41**: 922-938.

Wright, C. 1982. Seismological studies in a rock body at Chalk River, Ontario, and their relation to fractures. Canadian Journal of Earth Sciences, **19**: 1535-1547.

Wright, C. 1994 a. Variations in overburden and bedrock seismic velocities at Buchans and Gullbridge, Newfoundland; applications to near-surface geology and mineral exploration. Submitted to Canadian Journal of Earth Sciences.

Wright, C. 1994 b. The estimation of P wave velocities in shallow bedrock from refracted arrivals on seismic reflection profiles: an aid to lithological and structural interpretation. Submitted to Exploration Geophysics.

Wright, C. and Huang, C. 1984. A method of determining a preferred P-wave velocity profile in a borehole using surface explosions. Geophysics, **49**: 1041-1050.

Wright, C. and Nguuri, T. 1994. Seismic refraction data from reflection surveys in areas of weak reflections : application to static corrections and resolution of bedrock velocities. Submitted to Geophysical Prospecting.

Wright, C., Muirhead, K.J. and Dixon, A.E. 1985. The P wave velocity structure near the base of the mantle. Journal of Geophysical Research, **90**: 623-634.

Wright, C., Nguuri, T., Hoffe, B., Wright, J.A. and Shields, G. 1993. A seismic reflection survey at the Gullbridge Copper Mine, Newfoundland. Centre for Earth Resources Research, Department of Earth Sciences, Memorial University of Newfoundland, St. John's. 17 pp. and 14 figures.

Wright, C., Wright, J.A. and Hall, J. 1994. Seismic reflection techniques for base metal exploration in eastern Canada: examples from Buchans, Newfoundland. Journal of Applied Geophysics, **32**: 105-116.

Appendix A: Fortran Programs